XXI International Conference of Young Geologists
Niedzica, Poland
2020

Abstract Book
&
Introduction to the Pieniny Klippen Belt

XXIst International Conference of Young Geologists
HERĽANY 2020

BOOK OF ABSTRACTS

XXIst International Conference of Young Geologists
HERĽANY 2020

BOOK OF ABSTRACTS

Niedzica, Poland
05-07.11.2020

MINERALPRESS
KRAKÓW

Wydanie pierwsze

ISBN 978-83-933330-2-8

Edycja:
Peter Kiss
Maria Młynarska
Marína Molčan-Matejová
Bartosz Puzio
Karolina Rybka
Projekt logo:
Tomáš Potočný
Projekt okładki:
Maria Młynarska

Wydawnictwo Mineralogiczne MINERALPRESS
30-065 Kraków, ul. Goetla 39
tel. +48 604 427 198
www.mineralpress.com.pl

SCIENTIFIC BOARD

dr hab. inż. Maciej Manecki, prof. AGH
Faculty of Geology, Geophysics and Environmental Protection
AGH University of Science and Technology, Poland

doc. RNDr. Marianna Kováčová, PhD.
Faculty of Natural Sciences
Commenius University in Bratislava, Slovakia

doc. Mgr. Julián Kondela, PhD.
Faculty of Mining, Ecology, Process Control and Geotechnologies
Technical University of Košice, Slovakia

ORGANIZING COMMITTEE

AGH University of Science and Technology
Faculty of Geology, Geophysics and Environmental Protection
Anna Koteja
Maria Młynarska
Bartosz Puzio
Karolina Rybka
Grzegorz Ziemniak

Comenius University in Bratislava
Faculty of Natural Sciences / Geological Club
Péter Kiss
Martin Maľa
Marína Molčan Matejová
Tomáš Potočný

Technical University of Košice
Faculty of Mining, Ecology, Process Control and Geotechnologies
Igor Ďuriška

Organizer

FUNDACJA dla AGH

Fundacja dla AGH (Poland)

Honorary Patronage

AGH

Prof. dr hab. inż. Tadeusz Słomka

Rector of AGH University of Science and Technology (Poland)

Scientific partners and sponsors

AGH WGGiOŚ MENTE ET MALLEO GEO 1991 KLUB Kraków

The International Conference of Young Geologists*”Herľany”* is organized annually by the Faculty of Geology, Geophysics and Environmental Protection, AGH University of Science and Technology in Kraków Poland, Faculty of Natural Sciences, Comenius University of Bratislava, Slovakia and Faculty of Mining, Ecology, Process Control and Geotechnologies, Technical University of Košice, Slovakia.

The aim of the conference is to support undergraduate and PhD students, who want to share their scientific work related to any field of geology. The conference is a place to present the results and achievments, receive feedback from professionals and expand the international collaboration in a friendly atmosphere. It’s a great start for students presenting their research for the first time.

The XXIth ICYG *“Herľany 2020”* will be hosted at Hotel** Pieniny in Niedzica, Poland. It is organized by the Department of Mineralogy, Petrography and Geochemistry, Faculty of Geology, Geophysics and Environmental Protection, AGH University of Science and Technology in Kraków under the supervision of dr. inż. Maciej Manecki, prof. AGH, in collaboration with friends from Technical University of Košice and Geological Club, Comenius University of Bratislava and University of Wrocław.

Two first days of the conference will be commited to oral presentations, and started with a keynote speeches by prof. Juraj Majzlan from Institute of Geosciences, Friedrich-Schiller University, Jena, Germany and dr inż. Michał Krobicki, AGH University of Science and Technology, Kraków, Poland. The third day is devoted to the field trip - excursion in Pieniny Klippen Belt.

The best presentation delivered by a student in english will by awarded based on the Scientific Committee decision. The award by Geological Club Bratislava is named after Docent Rudolf Mock (1943-1996), a specialist in conodonts, professor of Comenius University and a founder of Geological Club. A supervision on the high level of the presentations will by provided by dr hab. inż. Maciej Manecki (AGH), doc. Julián Kondela (F-BERG TU, Košice), RNDr. Marianna Kováčová (Comenius University in Bratislava).

REVIEWERS

We would like to thank all the reviewers that contributed in increasing the level of the conference abstracts. We appreciate all the valuable comments.

Tomasz Bajda
AGH University of Science and Technology, Kraków, Poland

Krzysztof Dudek
AGH University of Science and Technology, Kraków, Poland

Magdalena Dumańska-Słowik
AGH University of Science and Technology, Kraków, Poland

Silvio Ferrero
University of Potsdam, Potsdam-Golm, Germany

Ashley Gumsley
University of Silesia, Katowice, Poland

Barbora Hudcová
Czech University of Life Sciences, Prague, Czech Republic

Matúš Hyžný
Comenius University of Bratislava, Bratislava, Slovakia

Peter Joniak
Comenius University of Bratislava, Bratislava, Slovakia

Iwona Klonowska
AGH University of Science and Technology, Kraków, Poland

Waldemar Korzeniowski
AGH University of Science and Technology, Kraków, Poland

Karolina Kośmińska
AGH University of Science and Technology, Kraków, Poland

Maciej Manecki
AGH University of Science and Technology, Kraków, Poland

Jakub Matusik
AGH University of Science and Technology, Kraków, Poland

Miriam Nývltová Fišáková
Charles University, Prague, Czech Republic

Dušan Plašienka
Comenius University of Bratislava, Bratislava, Slovakia

Jaroslav Pršek
AGH University of Science and Technology, Kraków, Poland

John Rakovan
Miami University, Oxford, OH, USA

Grzegorz Rzepa
AGH University of Science and Technology, Kraków, Poland

Ján Schlögl
Comenius University of Bratislava, Bratislava, Slovakia

Anna Świerczewska
AGH University of Science and Technology, Kraków, Poland

Justyna Topolska
AGH University of Science and Technology, Kraków, Poland

Katarzyna Walczak
AGH University of Science and Technology, Kraków, Poland

Marek Wendorff
AGH University of Science and Technology, Kraków, Poland

Geoturystyka 2 (13) 2008: 3-18

Geological history of the Pieniny Klippen Belt and Middle Jurassic black shales as one of the oldest deposits of this region – stratigraphical position and palaeoenvironmental significance

Geologiczna historia pienińskiego pasa skałkowego a środkowojurajskie czarne łupki jako jedne z najstarszych utworów regionu – stratygraficzna pozycja i paleośrodowiskowe znaczenie

Michał Krobicki & Jan Golonka

AGH University of Science and Technology, Faculty of Geology, Geophysics and Environmental Protection, Al. Mickiewicza 30, 30-059 Kraków

e-mail: krobicki@geol.agh.edu.pl, jan_golonka@yahoo.com

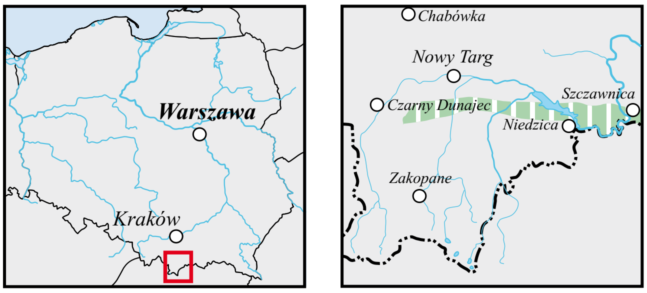

Abstract: *The main aim of this paper is presentation both general history of the Pieniny Klippen Belt and two famous sites in this region: Dunajec River Gorge and Homole Gorge. According to such general introduction the authors explain also paleogeographical position of the Pieniny Klippen Belt Basin within Mesozoic Tethyan Ocean, and especially stratigraphical position and paleoenvironmental conditions of Middle Jurassic black shales and their significance in geodynamic reconstruction of this basin. Both the Dunajec River Gorge, one of the most popular geotouristic object within Pieniny Mts, and Homole Gorge, one of the best place to geological study of the Pieniny Klippen Belt, are most attractive natural phenomena of this geological region.*

Key words: *southern Poland, Carpathians, Pieniny Mts, Pieniny Klippen Belt, black shales, Mesozoic history*

Treść: *Głównym celem niniejszej pracy jest próba prezentacji zarówno generalnej historii pienińskiego pasa skałkowego jak i dwóch słynnych miejsc tego regionu: przełomu Dunajca i wąwozu Homole. W nawiązaniu do takiego generalnego wprowadzenia autorzy przedstawiają również paleogeograficzną pozycję basenu pienińskiego pasa skałkowego w obrębie mezozoicznego oceanu Tetydy, a szczególnie stratygraficzną pozycję i paleośrodowiskowe warunki powstawania środkowojurajskich czarnych łupków oraz ich znaczenie w geodynamicznych rekonstrukcjach tego basenu. Zarówno spływ Dunajcem, jeden z najbardziej popularnych obiektów geoturystycznych w Pieninach, jak i wąwóz Homole, jedno z najlepszych miejsc do studiowania geologii pienińskiej, są najbardziej atrakcyjnymi obiektami przyrodniczymi w tym regionie geologicznym.*

Słowa kluczowe: *południowa Polska, Karpaty, Pieniny, pieniński pas skałkowy, czarne łupki, mezozoik*

Introduction

The Outer Carpathians and Pieniny Klippen Belt realm form the northernmost part of the Polish Carpathians. The Outer (Flysch) Carpathians are composed of Jurassic to Early Miocene flysch sequences (Ślączka, 1996; Oszczypko, 2004, 2006a, b; Oszczypko *et al.*, 2005, 2006). These deposits were folded and overthrust during the Miocene times (Alpine orogeny), forming north-verging nappes detached from their original basement (Ślączka, 1996). All Outer Carpathians nappes are thrusting over the East European Platform covered by Miocene deposits of the Carpathian Foredeep (Figs 1, 2). These nappes have allochthonous character. The deposits included in the nappes originated in basins situated outside their present location. The Pieniny Klippen Belt (PKB) is situated at the boundary between Outer Flysch Carpathians and Inner Carpathians forming strongly tectonized terrain about 600 km long and 1-20 km wide, which stretches from Vienna to the West up to Romania to the East (Fig. 1). Present

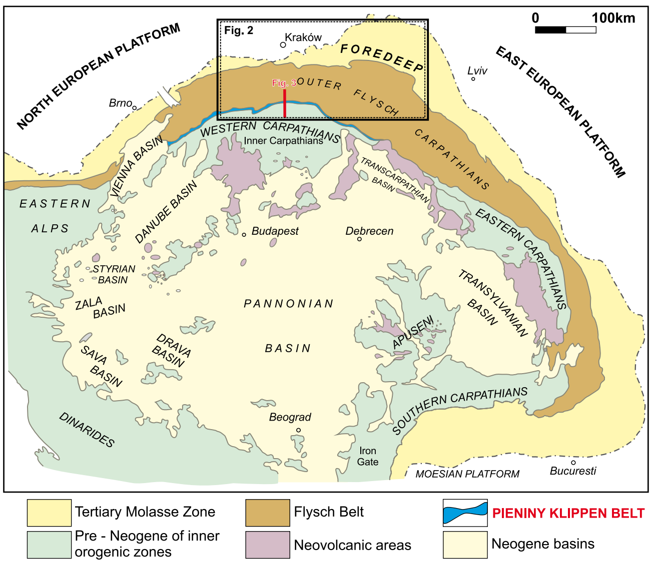

Fig. 1. Tectonic sketch map of the Alpine-Carpathian-Pannonian-Dinaride basin system (modified after Kováč, 1998; Plašienka *et al.*, 2000) • Szkic tektoniczny regionu alpejsko-karpacko-panońsko-dynarydzkiego (zmodyfikowano według Kováč, 1998; Plašienka *et al.*, 2000)

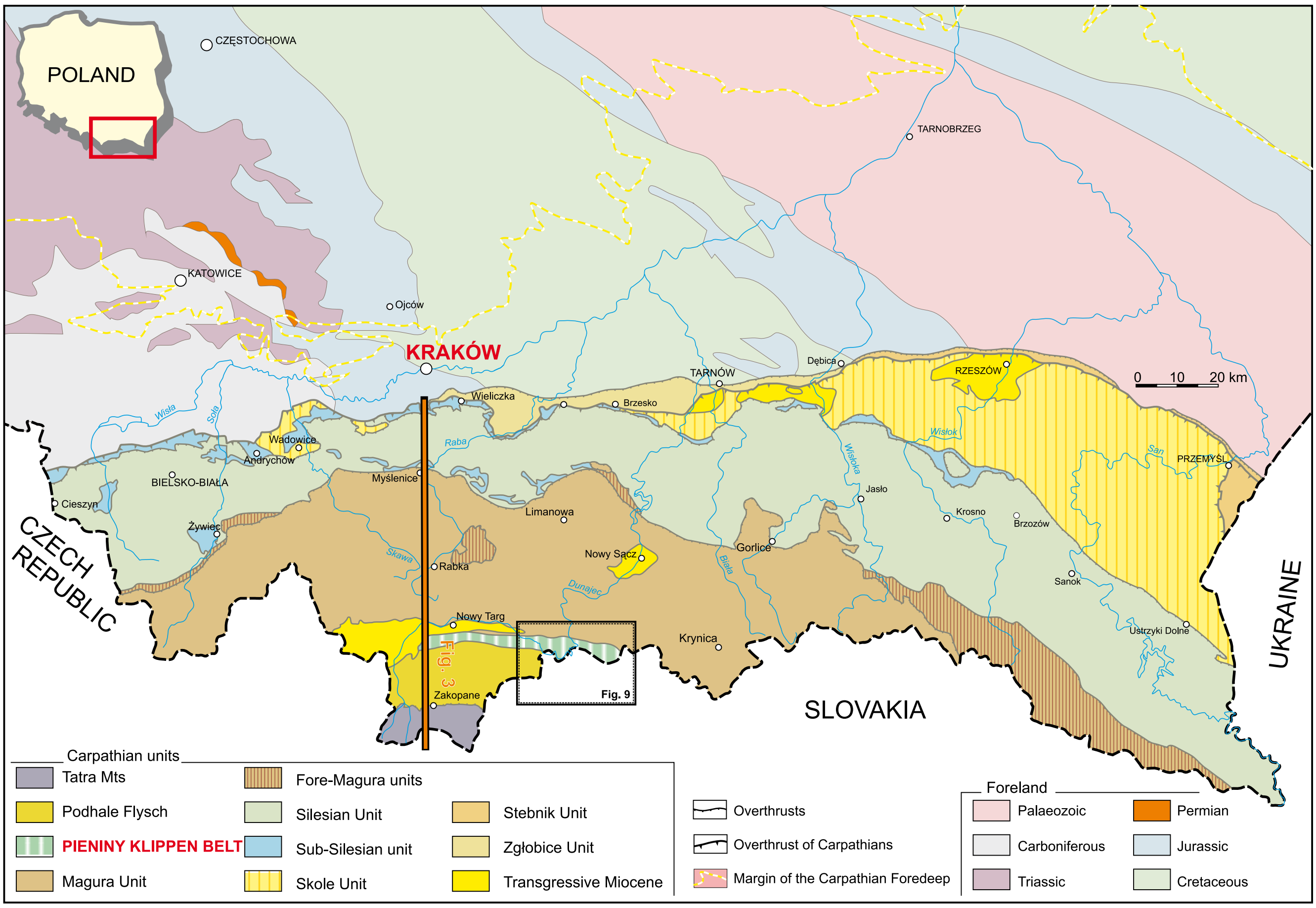

Fig. 2. Geological map of the Polish Carpathians, Carpathian Foredeep and Foreland (after Żytko *et al.*, 1989; Golonka *et al.*, 2006; simplified) with location both of the field trip (rectangle – Fig. 5) and of general cross-section across Carpathians (Fig. 3) • Mapa geologiczna polskich Karpat, Zapadliska Przedkarpackiego i ich przedpola (wg Żytko *et al.*, 1989; Golonka *et al.*, 2006; uproszczono) z lokalizacją zarówno wycieczki terenowej (prostokąt – Fig. 5) jak i generalnego przekroju przez Karpaty (Fig. 3)

day confines of the PKB are strictly tectonic. They may be characterized as (sub)vertical faults and shear zones (Fig. 3), along which a strong reduction of space of the original sedimentary basins took place (Birkenmajer, 1986; Golonka & Krobicki, 2006; Krobicki & Golonka, 2006). The PKB tectonic components of different age, strike-slip, thrust as well as toe-thrusts and olistostromes were mixed together, giving the present-day melange character of the PKB, where individual tectonic units are hard to distinguish.

General history of the Pieniny Klippen Belt Basin

Palinspastic reconstruction of the PKB Basin indicates occurrence of submarine ridge during the whole Jurassic and Cretaceous times. This so-called Czorsztyn Ridge, an elongated structure, subdivided Pieniny and Magura basins within the Carpathian part of the northernmost Tethyan Ocean (Figs 4-6) (comp. Golonka, 2004, 2007a, b with references cited therein). Its SW-NE orientation and location within the Tethyan Ocean is interpreted by means of palaeomagnetic data, relationship of sedimentary sequences and paleoclimate (see discussion in Golonka & Krobicki 2001 see also Aubrecht & Túnyi, 2001; Lewandowski *et al.*, 2005; Grabowski *et al.*, 2008). The basins divided by the Czorsztyn Ridge were dominated by a pelagic type of sedimentation. The deepest part of the PKB Basin is well documented by deep water Jurassic-Early Cretaceous deposits (radiolarites and pelagic *Maiolica*-type cherty limestones) (Birkenmajer, 1979, 1986; Golonka & Sikora 1981; Golonka & Krobicki, 2004; Krobicki *et al.*, 2006) of the so-called Branisko and Pieniny successions. The transitional, shallower sequences, which primary occupied slopes between deepest basinal units and the Czorsztyn Ridge are known as Czertezik and Niedzica successions, and the shallowest zone is Czorsztyn Succession which primary occupied SE slope of the Czorsztyn Ridge (Birkenmajer, 1986; Golonka & Krobicki, 2004; Krobicki & Golonka, 2006) (Fig. 7).

The earliest stage of the basin history is enigmatic and documented only by Triassic pebbles in the Cretaceous-Paleogene flysch. These pebbles indicate the possibility of an existence of enigmatic embayment of the Vardar-Transilvanian Ocean which separated the Tisa (Bihor-Apuseni) block from the Moesian Eastern European Platform (Săndulescu 1988; Golonka & Krobicki, 2004). The other interpretation of these pebbles origin involves the rotation of the Inner Carpathian plate (Golonka, 2005). The oldest Jurassic rocks (Hettangian/Sinemurian in age) of the Pieniny Klippen Belt are preserved only in the Slovakian and Ukrainian part of the region. They consist of different clastic deposits with limestone

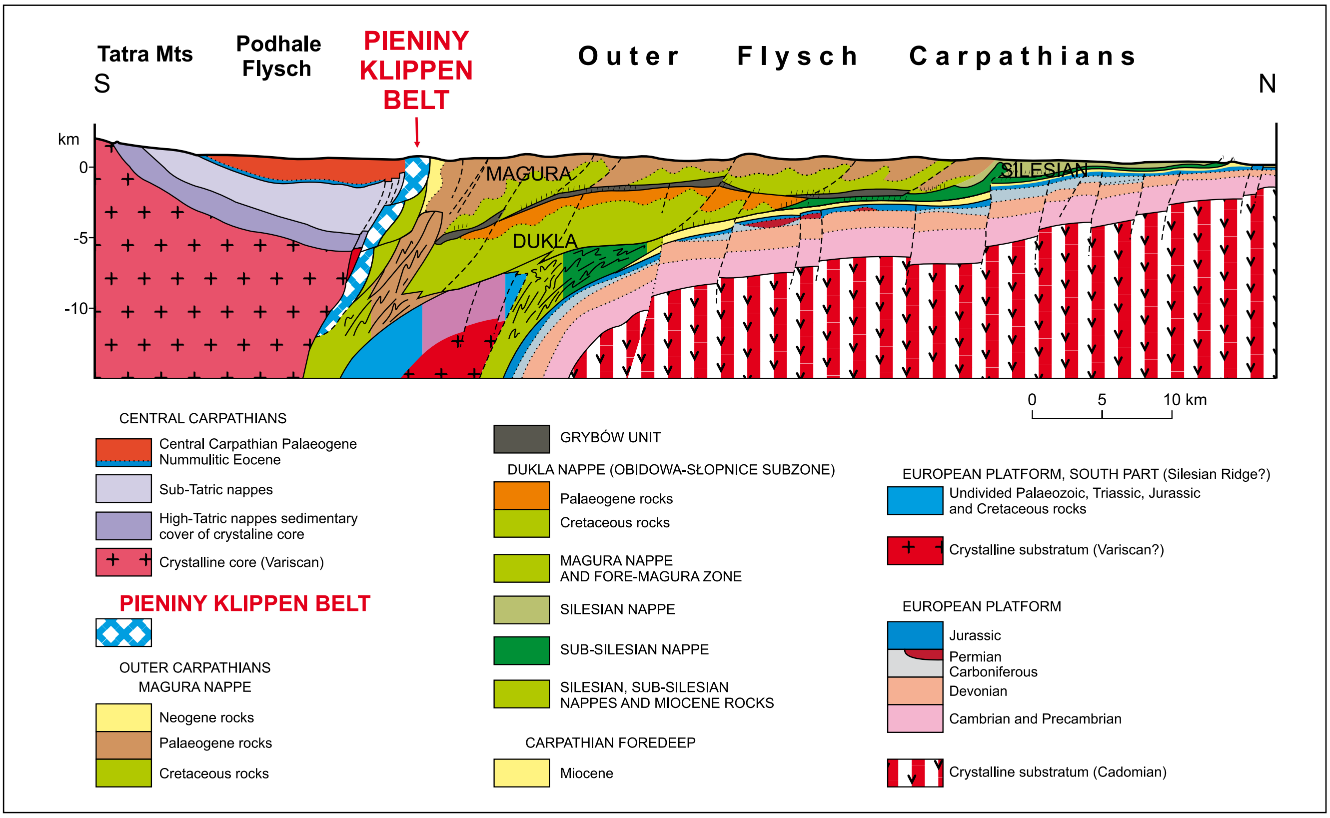

Fig. 3. Generalized cross-section across Polish Carpathians (after Golonka *et al.*, 2006) • Zgeneralizowany przekrój przez polskie Karpaty (wg Golonka *et al.*, 2006)

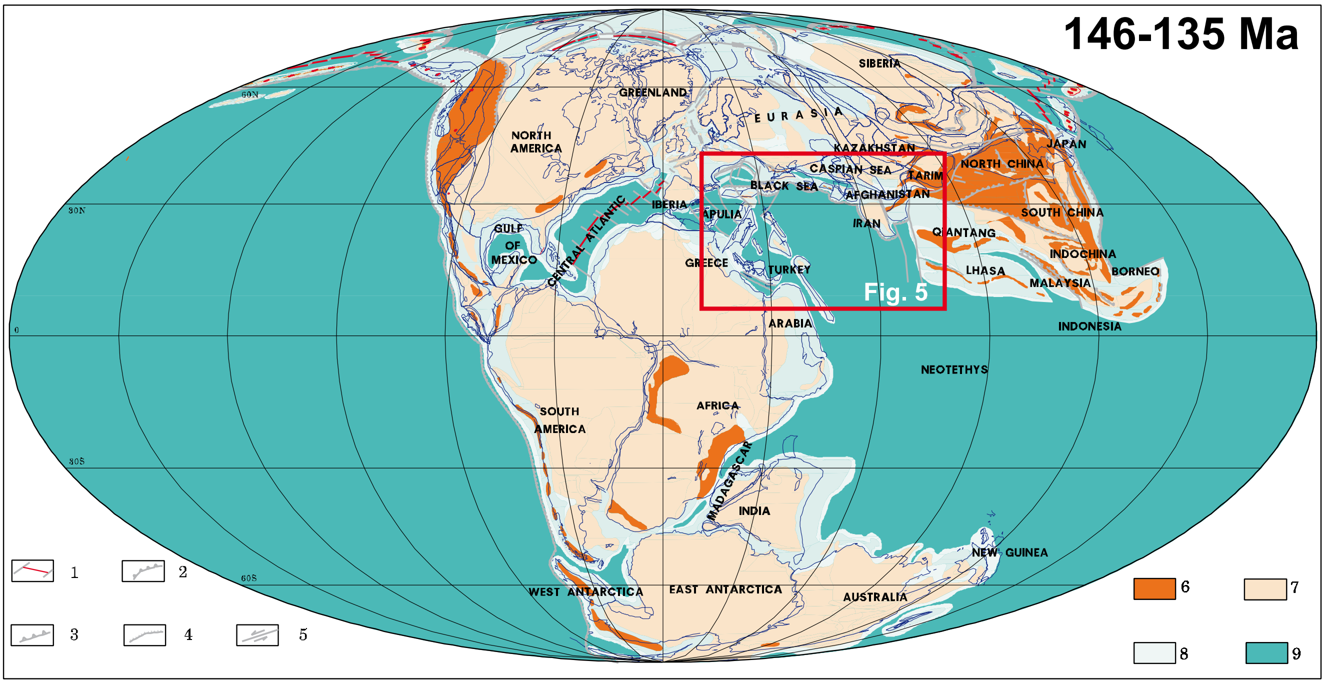

Fig. 4. Global plate tectonic map of latest Jurassic–earliest Cretaceous. Explanations: 1 – oceanic spreading center and transform faults; 2 – subduction zone; 3 – thrust fault; 4 – normal fault; 5 – transform fault; 6 – mountains; 7 – landmass; 8 – shallow sea and slope; 9 – deep ocean basin (from Golonka, 2000; modified) • Globalna mapa tektoniki płyt litosfery w najpóźniejszej jurze – najwcześniejszej kredzie. Objaśnienia: 1 – centra spredingu oceanicznego i uskoki transformujące; 2 – strefa subdukcji; 3 – uskoki nasuwcze; 4 – uskoki normalne; 5 – uskoki transformujące; 6 – góry; 7 – lądy; 8 – płytkie morza i skłon kontynentalny; 9 – głębokie oceany (wg Golonka, 2000; zmienione)

intercalations of *Gresten*-like dark/black facies (Schlögl *et al.*, 2004 with literature). However, Toarcian-Lower Bajocian *Bositra* ("*Posidonia*") black shales with spherosiderites (Skrzypny Shale Formation in local, formal nomenclature, see Birkenmajer, 1977; see Fig. 7), which we will see in Homole Gorge, last stop, as well as dark marls and spotty limestones of widespread Tethyan *Fleckenkalk*/*Fleckenmergel* facies, indicate the oxygen-depleted conditions (Birkenmajer,

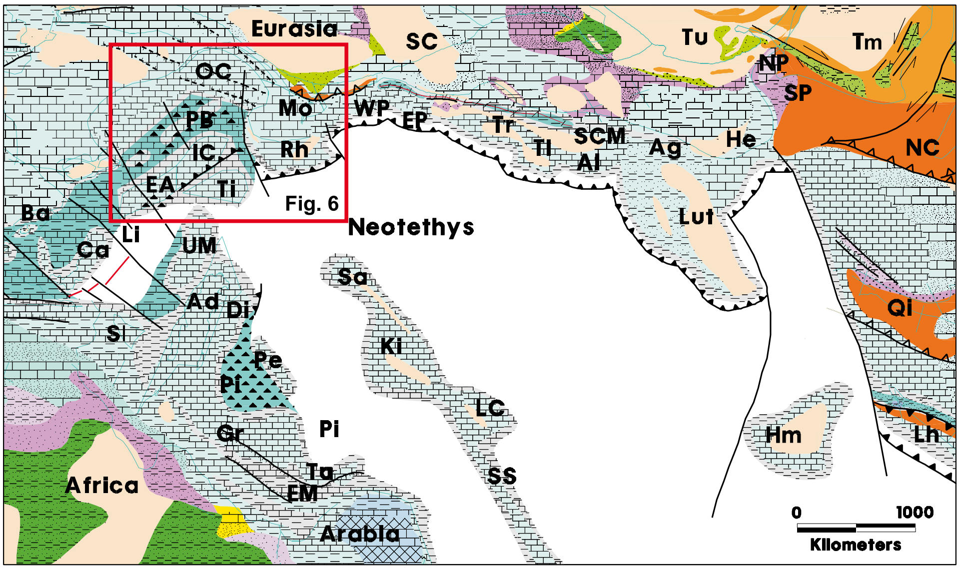

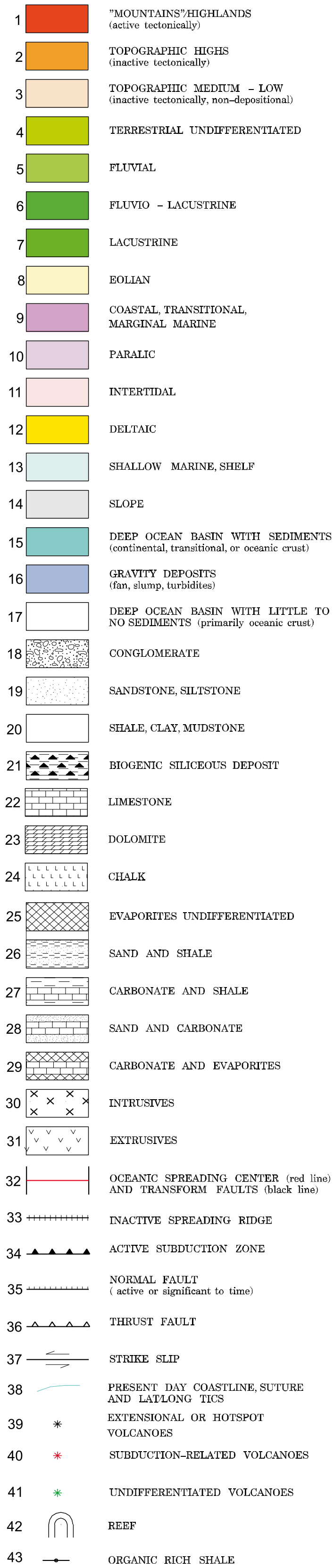

Fig. 5. Plate tectonic, paleoenvironment and lithofacies map of the western Tethys, Central Atlantic and adjacent areas during latest Jurassic–earliest Cretaceous time (after Golonka, 2007a; modified). Abbreviations of oceans and plates names: Ad – Adria (Apulia); Ag – Aghdarband (southern Kopet Dagh); Al – Alborz; Ba – Balearic; Ca – Calabria-Campania; Di – Dinarides; EA –Eastern Alps; EM – Eastern Mediterranean; EP – Eastern Pontides; Gr – Greece; He – Heart; Hm – Helmand; IC – Inner Carpathians; Ki – Kirsehir; LC – Lesser Caucasus; Lh – Lhasa; Li – Ligurian (Piemont) Ocean; Mo – Moesia; NC – North China; NP – North Pamir; OC – Outer Carpathians; PB – Pieniny Klippen Belt Basin; Pe – Pelagonian plate; Pi – Pindos Ocean; Qi – Qiangtang; Rh – Rhodopes; Sa – Sakarya; SC – Scythian; SCM – South Caspian microcontinent; Sl – Sicily; SP – South Pamir; SS – Sanandaj-Sirjan; Ta – Taurus terrane; Ti – Tisa; Tl – Talysh; Tm – Tarim; Tr – Transcaucasus; Tu – Turan; UM – Umbria-Marche; WP – Western Pontides

Mapa tektoniki płyt, paleośrodowiska i litofacji zachodniej Tetydy, przyszłego centralnego Atlantyku i obszarów sąsiednich w najpóźniejszej jurze–najwcześniejszej kredzie (wg Golonka, 2007; zmienione). Objaśnienia skrótów: Ad – Adria (Apulia); Ag – Aghdarband (południowy Kopet Dagh); Al – Alborz; Ba – Baleary; Ca – Kalabria-Kampania; Di – Dynarydy; EA – wschodnie Alpy; EM – wschodni obszar medyterrański; EP – wschodnie Pontydy; Gr – Grecja; He – Heart; Hm – Helmand; IC – Karpaty Wewnętrzne; Ki – Kirsehir; LC – Kaukaz Mniejszy; Lh – Lhasa; Li – ocean liguryjski (piemoncki); Mo – płyta mezyjska; NC – Chiny północne; NP – Pamir północny; OC – Karpaty Zewnętrzne; PB – basen pienińskiego pasa skałkowego; Pe – płyta pelagońska; Pi – ocean Pindos; Qi – Qiangtang; Rh – Rodopy; Sa – Sakarya; SC – płyta scytyjska; SCM – mikrokontynent południowego Morza Kaspijskiego; Sl – Sycylia; SP – Pamir południowy; SS – Sanandaj-Sirjan; Ta – terran Gór Taurus; Ti – płyta Cisy; Tl – Talysh; Tm – Tarim; Tr – obszar transkaukaski; Tu – Turan; UM – Umbria-Marche; WP – Pontides Zachodnie.

Objaśnienia legendy: 1 – góry/wyżyny (aktywne tektonicznie); 2 – wyniesienia nieaktywne tektonicznie; 3 – niziny nieaktywne tektonicznie, bez osadów; 4-17 – środowiska sedymentacji [4 – lądowe nierozdzielne; 5 – rzeczne; 6 – rzeczno-jeziorne; 7 – jeziorne; 8 – eoliczne; 9 – przybrzeżne, przejściowe; 10 – paraliczne; 11 – międzypływowe; 12 – deltowe; 13 – płytkomorskie, szelfowe; 14 – skłonu kontynentalnego; 15 – głębokie oceany z sedymentacją (ze skorupą kontynentalną, przejściową lub oceaniczną); 16 – osady grawitacyjne (loby, spływy, turbidyty); 17 – głębokie oceany bez sedymentacji]; 18 – zlepieniec; 19 – piaskowiec, mułowiec; 20 – iły, łupki, mułowce; 21 – biogeniczne osady krzemionkowe; 22 – wapień; 23 – dolomit; 24 – kreda; 25 – ewaporaty nierozdzielne; 26 – piasek i łupek; 27 – węglany i łupki; 28 – piaski i węglany; 29 – węglany i ewaporaty; 30 – utwory intruzyjne; 31 – utwory ekstruzyjne; 32 – centra spredingu oceanicznego i uskoki transformujące; 33 – nieaktywne grzbiety spredingu; 34 – aktywna subdukcja; 35 – uskok normalny; 36 – nasunięcie; 37 – uskok przesuwczy; 38 – dzisiejsza linia brzegu; 39 – wulkanizm ekstensywny lub gorących plamek; 40 – wulkanizm subdukcyjny; 41 – wulkanizm nieokreślony; 42 – rafa; 43 – łupki bogate w substancję organiczną

1986; Tyszka, 1994, 2001). One of the most rapidly change of sedimentation/paleoenvironments within the PKB basins took place during late Early Bajocian when well-oxygenated multicoloured crinoidal limestones replaced dark and black sedimentation. The origin of the above mentioned Czorsztyn Ridge was connected with this Bajocian postrift geotectonic reorganization (Golonka *et al.*, 2003; Krobicki, 2006). Sedimentation of younger (deposition since latest Bajocian) red nodular *Ammonitico Rosso*-type limestones was an effect of Meso-Cimmerian vertical movements which subsided Czorsztyn Ridge (Birkenmajer, 1986; Krobicki, 2006; Krobicki & Golonka, 2006). In the same time first episode of radiolarite

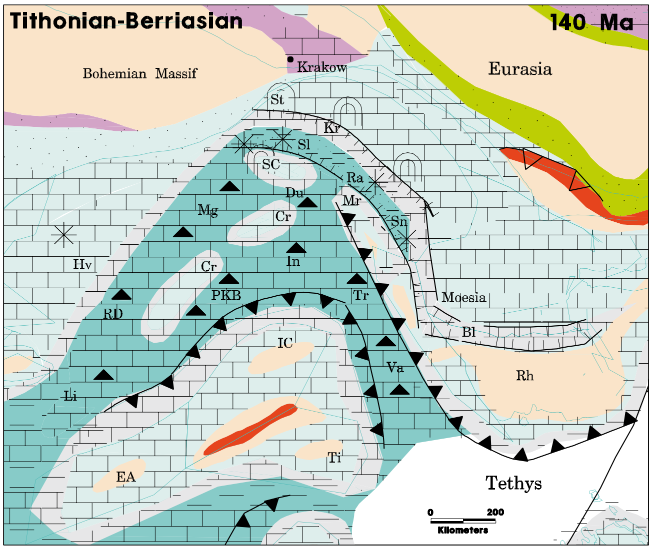

Fig. 6. Paleoenvironment and lithofacies of the circum-Carpathian area during latest Jurassic–earliest Cretaceous; plates position at 140 Ma (modified from Golonka *et al.*, 2006). Abbreviations: Bl – Balkan rift; Cr – Czorsztyn Ridge; Du – Dukla Basin; EA – Eastern Alps; Hv – Helvetic shelf; IC – Inner Carpathians; In – Inačovce-Kričevo zone; Kr – Kruhel Klippe; Li – Ligurian Ocean; Mg – Magura Basin; Mr – Marmarosh Massif; PKB – Pieniny Klippen Belt Basin; Ra – Rakhiv Basin; RD – Rheno Danubian Basin; Rh – Rhodopes; SC – Silesian Ridge (Cordillera); Sl – Silesian Basin; Sn – Sinaia Basin; St – Štramberk Klippe; Ti – Tisa plate; Tr – Transilvanian Ocean; Va – Vardar Ocean. Explanations of colors and symbols – see Fig. 5

Mapa palinspastyczna z typowymi litofacjami obszaru wokół-karpackiego w najpóźniejszej jurze–najwcześniejszej kredzie; pozycja płyt litosfery 140 mln lat temu (wg Golonka *et al.*, 2006; zmodyfikowane) Skróty: Bl – ryft bałkański; Cr – grzbiet czorsztyński; Du – basen dukielski; EA –Alpy Wschodnie; Hv – szelf helwecki; IC – Karpaty Wewnętrzne; In – strefa Inačovce-Kričevo; Kr – Kruhel; Li – ocean liguryjski; Mg – basen magurski; Mr – masyw marmaroski; PKB – basen pienińskiego pasa skałkowego; Ra – basen rachowski, RD – basen renodunajski; Rh – Rodopy; SC – kordyliera śląska, Sl – basen śląski; Sn – basen Sinaia; St – Štramberk; Ti – płyta Cisy; Tr – ocean transylwański; Va – ocean Vardaru. Objaśnienia kolorów i szrafur – patrz Fig. 5

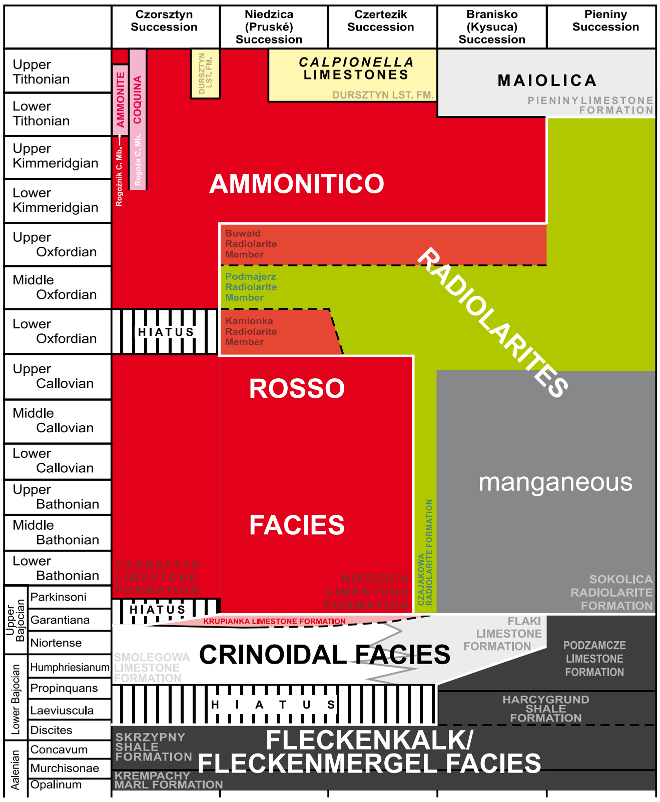

Fig. 7. Stratigraphical correlation between Jurassic lithofacies (lithostratigraphic units) of the Pieniny Klippen Belt successions (after Wierzbowski *et al.*, 2004; supplemented by Krobicki & Wierzbowski, 2004) • Korelacja stratygraficzna jurajskich litofacji (jednostek litostratygraficznych) sukcesji pienińskiego pasa skałkowego (wg Wierzbowski *et al.*, 2004; uzupełnione przez Krobicki & Wierzbowski, 2004)

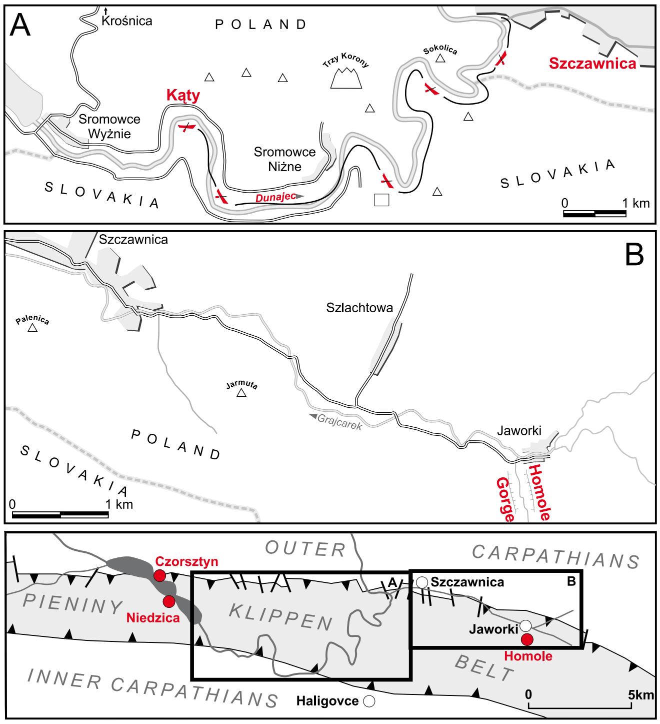

Fig. 8. Polish part of the Pieniny Klippen Belt and location of the Dunajec River Gorge (A) and Homole Gorge (B) • Polska część pienińskiego pasa skałkowego z lokalizacją przełomu Dunajca (A) i Wąwozu Homole (B)

sedimentation took place in the axial, basinal sequences (Birkenmajer, 1977, 1986; Mišík, 1999). This episode marked beginning of the great facial differentiation between deepest and shallowest successions. The main phase of this facial differentiation involving, among the others, mixed siliceous-carbonate sedimentation took place later, mainly during Oxfordian times. Oxfordian radiolarites are typical for transitional (Niedzica and Czertezik) successions and strictly basinal parts of the basin (Branisko and Pieniny successions). Similar compositions of facies are well known in several European Alpine regions (e.g. Betic Cordillera, Southern Alps, Apennine, Karavanke, and Ionian Zone). These regions, together with PKB basins formed the so-called Alpine Tethys (Golonka, 2004). Very intensive Neo-Cimmerian tectonic movements (latest Jurassic – earliest Cretaceous times), which affected the Czorsztyn Ridge are documented by facies diversification, sedimentary-stratigraphic hiatuses, sedimentary breccias, neptunian dykes and/or fauna redeposition. This tectonic activity was caused by formation and

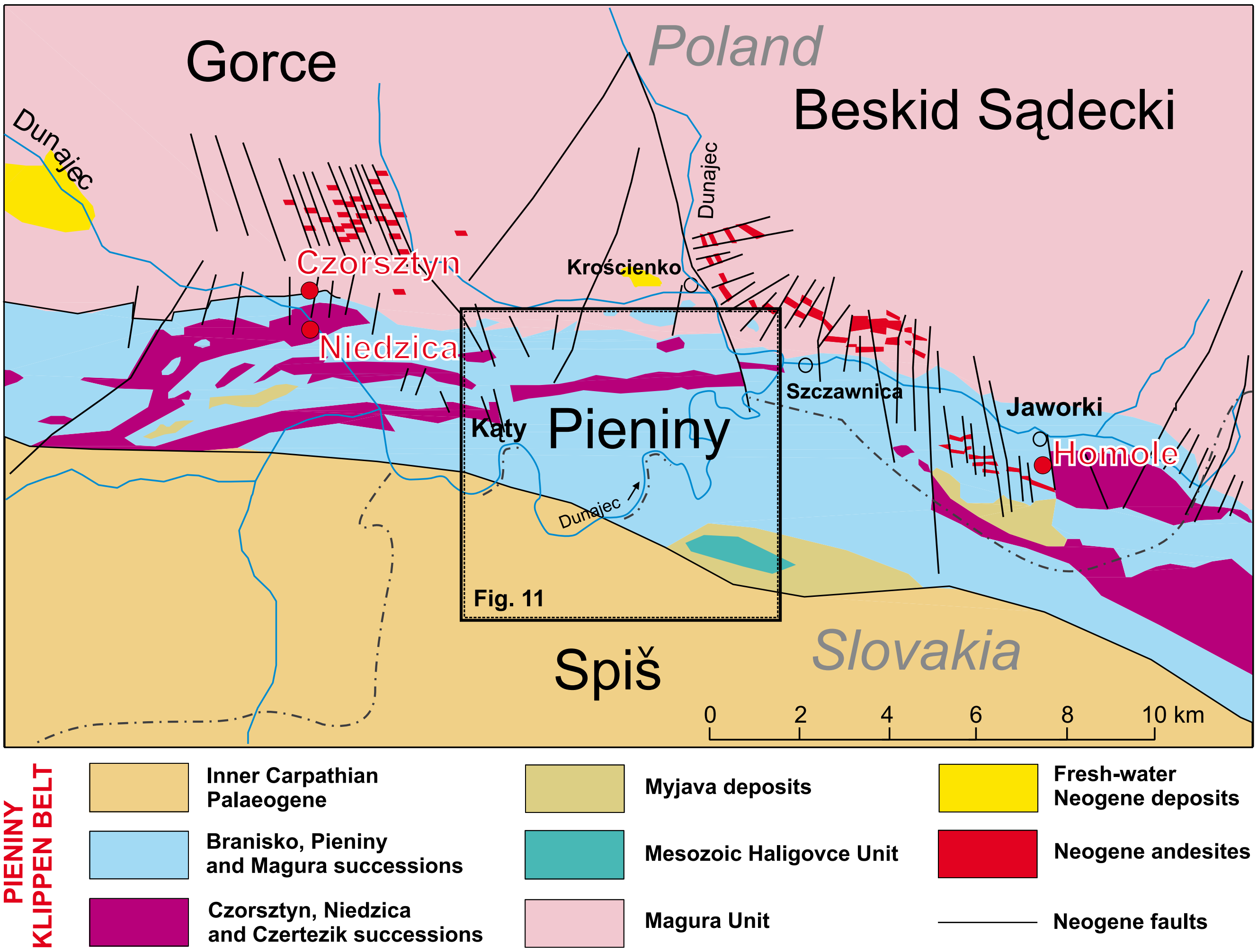

Fig. 9. Geological sketch of the Pieniny Klippen Belt (Polish sektor) and surrounding regions (after Birkenmajer, 1979; simplified) with location of Dunajec River Gorge • Szkic geologiczny polskiej części pienińskiego pasa skałkowego i obszarów otaczających (wg Birkenmajer, 1979; uproszczono) z lokalizacją przełomu Dunajca

Fig. 10. General view to medieval castles over the artificial Czorsztyn Lake – Czorsztyn Castle (A) and Niedzica Castle (B); location – see Fig. 4 • Ogólny widok na średniowieczne zamki nad sztucznym jeziorem czorsztyńskim – zamek w Czorsztynie (A) i zamek w Niedzicy (B); położenie – patrz Fig. 4

Fig. 11. Aerial view of the central Pieniny Mts and Dunajec River Gorge with points of photos: A – Upper Cretaceous red marls of the Scaglia Rossa-type facies (Macelowa Mt); B-E – views to Trzy Korony Mt, Mnichy Mt and Sokolica Mt built by uppermost Jurassic-lowermost Cretaceous Maiolica-type well-bedded limestones, usually strongly tectonic folded (E; hammer for scale), with cherts (see – detail) over Dunajec River Gorge • Zdjęcie lotnicze centralnej części Pienin z przełomem Dunajca z zaznaczeniem miejsc zdjęć: A – czerwone margle górnokredowe facji Scaglia Rossa (Macelowa Góra); B-E – widoki na Trzy Korony, Mnichy i Sokolicę zbudowane z dobrze ułwiconych wapieni najwyższej jury-najniższej kredy, zazwyczaj silnie zaburzone tektonicznie (E; młotek jako skala), z rogowcami (patrz – zbliżenie) facji Maiolica, ponad przełomem Dunajca

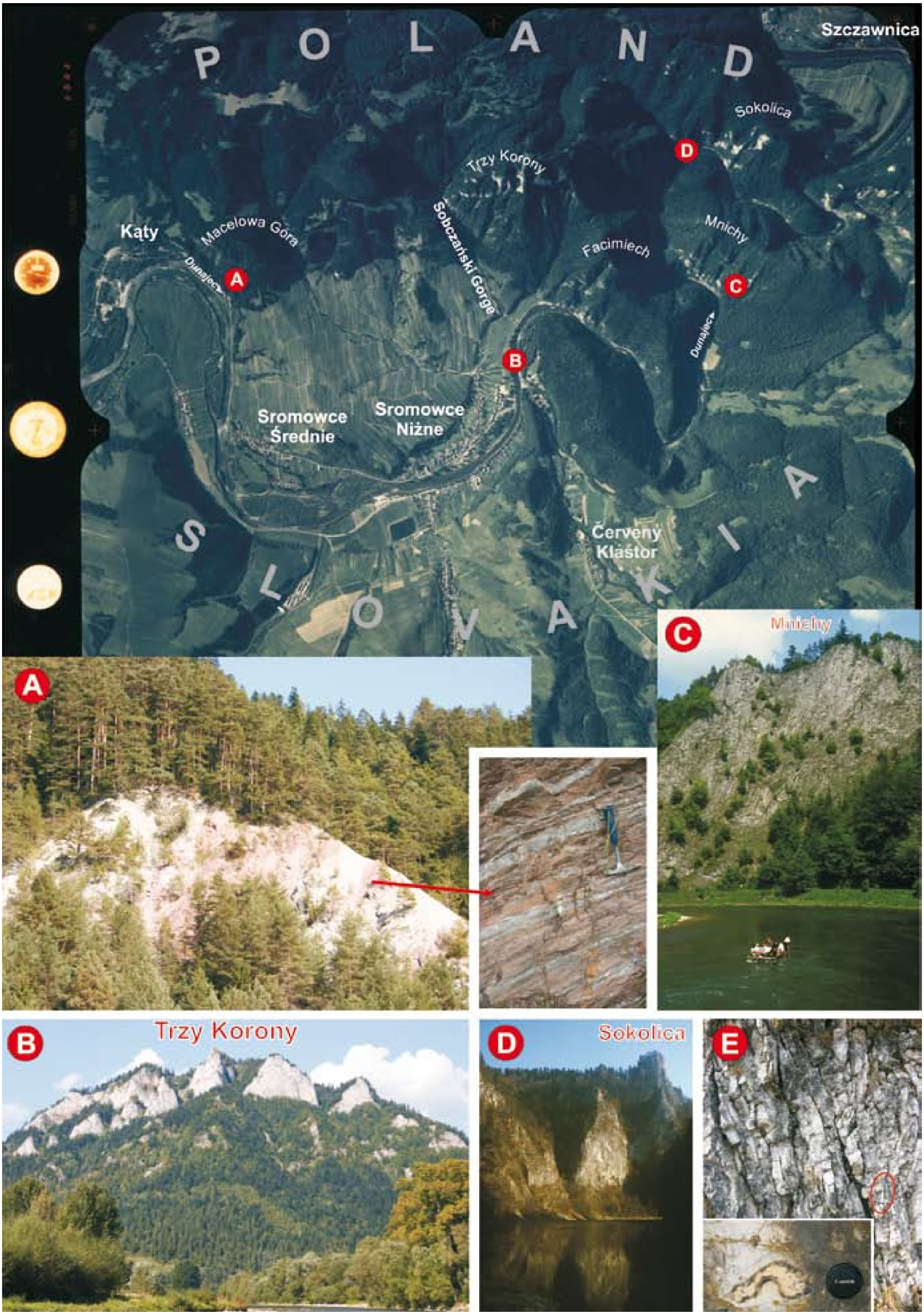
P O L A N D
S L O V A K I A
Szczawnica
Sokolica
Trzy Korony
Sobczański Gorge
Kąty
Macelowa Góra
Dunajec
Facimiech
Mnichy
Sromowce Średnie
Sromowce Niżne
Červeny Klaštor
Dunajec
A
B
C
D
E
Mnichy
Trzy Korony
Sokolica

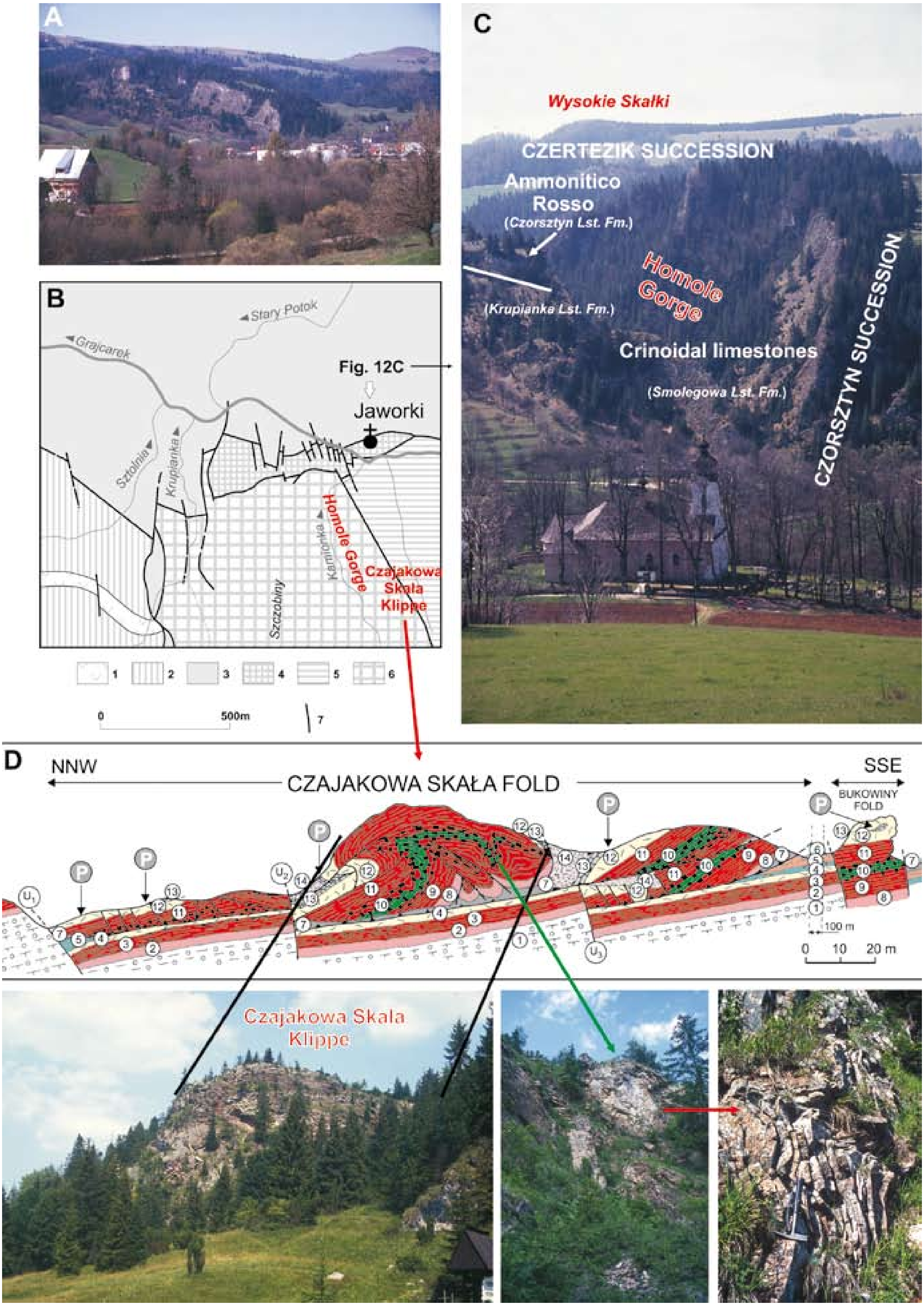
A
C
Wysokie Skałki
CZERTEZIK SUCCESSION
Ammonitico Rosso
(Czorsztyn Lst. Fm.)
(Krupianka Lst. Fm.)
Homole Gorge
Crinoidal limestones
(Smolegowa Lst. Fm.)
CZORSZTYN SUCCESSION
B
Stary Potok
Grajcarek
Fig. 12C
Jaworki
Sztolnia
Krupianka
Homole Gorge
Kamionka
Szczobiny
Czajakowa Skala Klippe
1
2
3
4
5
6
0
500m
7
D
NNW
CZAJAKOWA SKAŁA FOLD
SSE
BUKOWINY FOLD
P
100 m
0
10
20 m
Czajakowa Skala Klippe

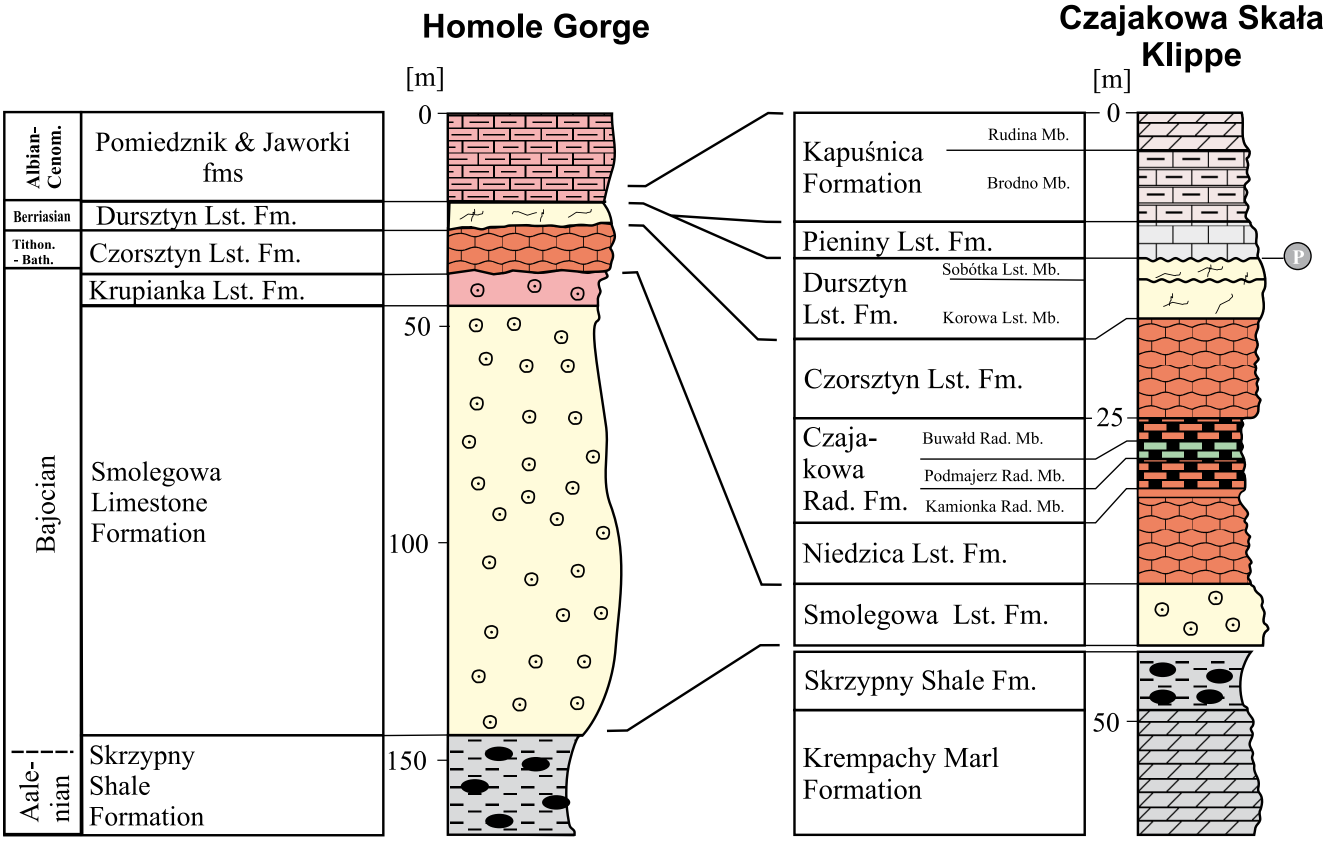

Fig. 13. Lithostratigraphical columns of the Czorsztyn Succession of the Homole Gorge (left) and Niedzica Succession of the Czajakowa Skała klippe (right) (after Birkenmajer, 1977; modified). Explanations of symbols – see the text • Profile litostratygraficzne sukcesji czorsztyńskiej wąwozu Homole (po lewej) i sukcesji niedzickiej Czajakowej Skały (po prawej) (wg Birkenmajer, 1977; zmodyfikowane). Objaśnienia szrafur – patrz tekst

Fig. 12. General panoramic view (A) and geological sketch (B) of vicinity of Jaworki village with more detail view of entrance to Homole Gorge (C) and Czajakowa Skała Klippe and Bukowiny Fold (D) (geology after Birkenmajer, 1970; modified by Jurewicz, 1994). Explanations: B: tectonic sketch of the Homole block, northern part (after Birkenmajer, 1970, 1983); 1 – andesite intrusion (Middle Miocene: Sarmatian); 2 – autochthonous Magura-type Palaeogene; 3 – Grajcarek Unit (Magura Succession); 4 – Czorsztyn Unit (Czorsztyn Succession); 5 – Skalski Stream depression (Niedzica Nappe – Niedzica Succession); 6 – Homole block (Czorsztyn Unit with overthrust Niedzica and Branisko nappes); 7 – strike-slip faults; D: Czorsztyn Succession: 1 – Smolegowa Limestone Fm. (white crinoidal limestones); 2 – Krupianka Limestone Fm. (red crinoidal limestones); 3 – Czorsztyn Limestone Fm. (red nodular Ammonitico Rosso-type limestones); 4 – Dursztyn Limestone Fm. (pink and white Callpionella limestones); 5 – Pomiedznik Formation (marly limestones); 6– Jaworki Formation (variegated marls); Niedzica Succession: 7 – Krempachy Marl and Skrzypny Shale formations (Fleckenmergel-type grey and black spotty marls/shales sometime with spherosiderite concretions – latter formation); 8 – Smolegowa Limestone Fm. (green-red crinoidal limestones); 9 – Niedzica Limestone Fm. (red nodular Ammonitico Rosso-type limestones); 10 – Czajakowa Radiolarite Fm. (red and green radiolarites); 11 – Czorsztyn Limestone Fm. (red nodular Ammonitico Rosso-type limestones); 12 – Dursztyn Limestone Formation (red and white Callpionella limestones); 13 – Pieniny Limestone Fm. (white and grey cherty Maiolica-type limestones); 14 – Kapuśnica Fm. (greenish spotty limestones). P – Location of phosphate deposits on the uppermost surface of the Sobótka Limestone Member of the Dursztyn Limestone Fm. (formal units after Birkenmajer, 1977) • Ogólna panorama (A) i szkic geologiczny (B) okolic wsi Jaworki z bardziej szczegółowym widokiem na wejście do wąwozu Homole (C) oraz na Czajakową Skałę i fałd z Bukowin (D) (geologia wg Birkenmajer, 1970; zmodyfikowane przez Jurewicz, 1994). Objaśnienia: B – szkic tektoniczny bloku Homoli, część północna (wg Birkenmajer, 1970, 1983); 1 – intruzje andezytowe (środkowy miocen: sarmat); 2 – paleogen autochtoniczny typu magurskiego; 3 – jednostka Grajcarka (sukcesja magurska); 4 – jednostka czorsztyńska (sukcesja czorsztyńska); 5 – depresja Skalskiego potoku (płaszczowina niedzicka – sukcesja niedzicka); 6 – blok Homoli (jednostka czorsztyńska z nasunięciem płaszczowiny niedzickiej i braniskiej); 7 – uskoki przesuwcze; D – sukcesja czorsztyńska: 1 – formacja wapienia ze Smolegowej (białe wapienie krynoidowe); 2 – formacja wapienia z Krupniaki (czerwone wapienie krynoidowe); 3 – formacja wapienia czorsztyńskiego (czerwone wapienie bulaste typu Ammonitico Rosso); 4 – formacja wapieni dursztyńskich (różowe i białe wapienie kalpionellowe); 5 – formacja z Pomiedzkina (wapienie margliste); 6 – formacja z Jaworek (margle pstre); sukcesja niedzicka: 7 – formacje margli z Krempachów i łupków ze Skrzypnego (szare i czarne plamiste margle/łupki typu Fleckenmergel niekiedy z konkrecjami sferosyderytów – druga z formacji); 8 – formacja wapienia ze Smolegowej (zielono-czerwone wapienie krynoidowe); 9 – formacja wapienia niedzickiego (czerwone wapienie bulaste typu Ammonitico Rosso); 10 – formacja radiolarytów z Czajakowej (czerwone i zielone radiolaryty); 11 – formacja wapienia czorsztyńskiego (czerwone wapienie bulaste typu Ammonitico Rosso); 12 – formacja wapieni dursztyńskich (różowe i białe wapienie kalpionellowe); 13 – formacja wapienia pienińskiego (białe i szare wapienie rogowcowe typu Maiolica); 14 – formacja z Kapuśnicy (zielonkawe wapienie plamiste). P – lokalizacja utworów sfosfatyzowanych na powierzchni ogniwa wapieni z Sobótki formacji wapieni dursztyńskich (jednostki formalne wg Birkenmajer, 1977)

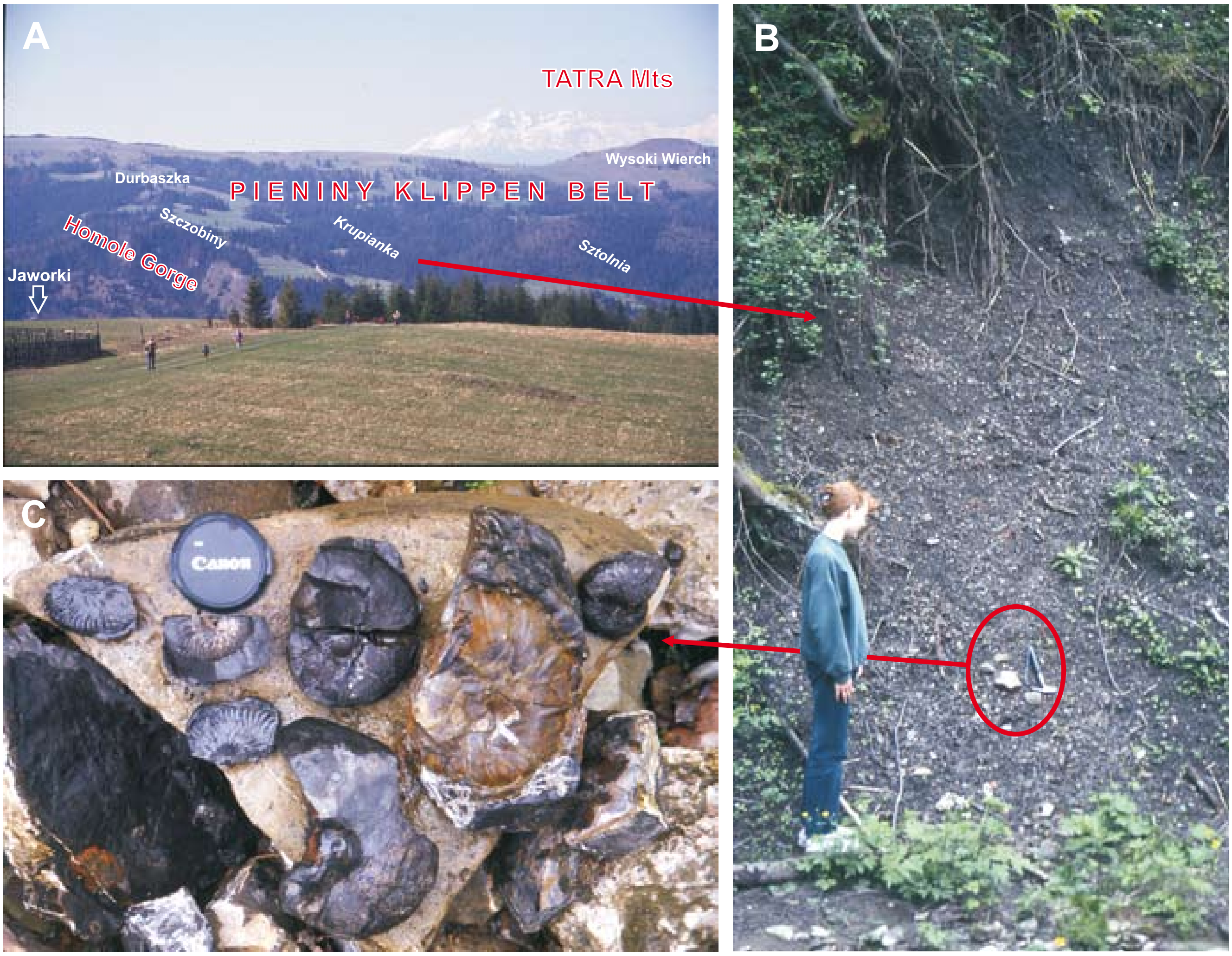

Fig. 14. General, panoramic view on Tatra Mts and Pieniny Klippen Belt regions from vicinity of Jaworki village (A) and location in Krupianka stream of the Middle Jurassic (Aalenian-lowermost Bajocian) black shales with spherosiderites (Skrzypny Shale Formation) (B) sometime full of ammonites (C) • Ogólny, panoramiczny widok na Tatry i pieniński pas skałkowy z okolic wsi Jaworki (A) i lokalizacja w potoku Krupianka środkowojurajskich (aalen-najniższy bajos) czarnych łupków sferosyderytowych formacji łupków ze Skrzypnego (B) czasami obfitych w amonity (C)

destruction of submarine tectonic horsts in the Carpathian basins (Birkenmajer, 1958, 1975, 1986; Michalík & Reháková, 1995; Krobicki, 1996; Krobicki & Słomka, 1999; Golonka *et al*., 2003; Krobicki *et al*., 2006). During latest Jurassic – earliest Cretaceous times (Tithonian-Berriasian) cherty limestones of *Maiolica*-type (=*Biancone*) facies were deposited within deeper successions. It is one of the famous, widespread Tethyan facies well known both from the Alpine and the Apennine regions of the Alpine Tethys (Pszczółkowski, 1987; Wieczorek, 1988). These white-gray, micritic well-bedded calpionellids-bearing limestones build now the highest part of the Pieniny Mts (e.g., Trzy Korony Mt, Sokolica Mt etc). The Late Cretaceous history of the PKB basin is connected with unification of sedimentary regimes within ridge and slope successions (Albian-Coniacian), and deposition of multicoloured green/variegated/red marls full of foraminiferids (the youngest are *Scaglia Rossa*-type pelagic red marls – Birkenmajer, 1986; Bąk, 2000). The syn-orogenic flysch deposits developed in the basinal parts during the last episode of the history of the PKB basin. Then, the Czorsztyn Ridge collided with the Inner Carpathian terranes around the Cretaceous/Paleogene boundary (Birkenmajer, 1986). The post-orogenic subvolcanic activities took place in this region mainly during Miocene times – (Birkenmajer, 2003 with literature cited therein). Now, the PKB is strictly tectonic zone reflecting its Palaeogene-Neogene evolution when (sub) vertical faults and shear zones developed and a strong reduction of space of the original sedimentary basins took place.

Selected most famous geological objects in the Pieniny Klippen Belt and their geotouristic values

Rafting trough Dunajec River Gorge

One of the major geotouristic attraction of the Pieniny Klippen Belt region is the rafting through the Dunajec River Gorge (Golonka & Krobicki, 2007, see also Alexandrowicz & Alexandrowicz, 2004). The rafting trip on the Dunajec River, which starts at Sromowce Kąty harbour (Figs 8, 9), takes geotourist through the Dunajec Gorge to Szczawnica. The Dunajec offers magnificent view of the cliffs sculptured in the Pieniny Mountains by the tectonic activity and river's erosion. It offers also the close view of the outcrops of Jurassic and Cretaceous rocks of the Pieniny Succession and complex tectonics of the PKB.

The Kąty's harbor has good connection with main touristic points in the Pieniny Mts and is easily accessible both from Zakopane (from south) and from Kraków (from north). Kąty are located very close to famous medieval castles (Czorsztyn Castle – Fig. 10A and Niedzica Castle – Fig. 10B), which occupied good accessible and visible places just above artificial Czorsztyn Lake (Figs 8, 9).

The **Macelowa Mt** (Fig. 11) is the first viewpoint along our boat trip. The Oxfordian radiolarites and latest Jurassic-Early Cretaceous gray cherty limestones of the *Maiolica* facies (Pieniny Limestone Formation) of the Pieniny Succession, occupy topmost and middle part of this mountain in completely overturned position. Therefore, the youngest part of this succession occurs in lowest (topographically) position and is represented by the Late Cretaceous *Globotruncana*-bearing marls of the *Scaglia Rossa*-type deposits (Fig. 11A) (Birkenmajer, 1979; Bąk, 2000). In close view we can see red marls and marly limestones with greyish intercalations of calcareous sandstones and siltstones of turbiditic origin connected with distal parts of submarine fans, typical flysch and flyschoidal sedimentation (comp. Mutti & Ricci Lucchi, 1975; Słomka, 1986; Stow, 1986; Mutti & Normark, 1987; Ghibaudo, 1992; Reading & Richards, 1994; Lowe, 1997; Shanmugam, 2000). The red *Globotruncana* marls of the Scaglia Rossa-type facies (in local nomenclature – Macelowa Marl Member of the Jaworki Formation; Birkenmajer, 1977), which we can see now, is the youngest part of this unit. The Jaworki Formation is composed (stratigraphically) by green-variegated-red globotruncanid marls with perfect studied biostratigraphy (Bąk, 2000). Such type of facies is wide known both from Alpine and Apennine geology. The primary seaways between several parts of the Tethyan Ocean, especially the above mentioned Alpine Tethys (Golonka, 2004), which existed during the Late Cretaceous times are very well documented by these facies occurrences. Later, Dunajec River crosses through several vertical strike-slip faults, which separate the Pieniny Klippen Belt from the Central Carpathians Palaeogene Flysch region (precisely – Oligocene in age). At Sromowce Niżne village (Figs 8, 11) the Dunajec River enters again Pieniny Klippen Belt.

The most famous and beautiful peak of the Pieniny Mts – **Trzy Korony Mt** (Three Crowns) (982 m a.s.l.) (Fig. 11B) is good visible at the beginning of the Dunajec River Gorge (Birkenmajer *et al.*, 2001). In local, folk nomenclature, the Trzy Korony peak is known as (from left to right): Kaśka (Kate), Zośka (Sophie) and Kudłata Maryśka (Hairy Mary). The very steep walls of this peak are formed by strongly folded thin-bedded, grey, cherty limestones of the *Maiolica* (=*Biancone*) facies of the Pieniny Limestone Formation (Kimmeridgian-Albian) of the Pieniny Succession.

The origin of the Dunajec River Gorge is connected with young, mainly Neogene history, related to the neotectonic movements. This river have had the mature stage in the latest Miocene–Pliocene time, and manifested by meandering shape. Then, during episode of the uplifting of the Pieniny Mts, such shape of the river have been conserved, when more competent Late Cretaceous marls and marly limestones, softer than Jurassic/Early Cetaceous cherty limestones, which occurred between several tectonic slices, have been easily eroded by the Dunajec River water, during the fault-related uplift. Origin of strongly faulted, usually thin-bedded *Maiolica*-type cherty limestones is connected with this tectonic activity of Alpine orogeny (Fig. 11E). Some of the faults were still active during the Quaternary and were connected with rare earthquakes (Baumgart-Kotarba, 1996, 2001; Zuchiewicz *et al.*, 2002 and references therein). Recently vertical movements reached up to + 0.5 mm per year, according to very detail geodetic measurements (Vanko, 1988; Vass, 1998). Detail description of origin and age of the Dunajec River Gorge, with the review of structural and geomorphological features of the Pieniny Mts and formation of magnificent cliffs of the Gorge, was published by Birkenmajer (2006) (see also – Zuchiewicz, 1982).

The next interesting point on the right bank of the Dunajec River is the medieval **Czerwony Klasztor (Red Monastery**) constructed in 1330, where one of the Camelot's pharmacist (Brother Cyprian – Franciszek Ignacy Jeszke) collected a huge quantity of plants (282 species), both from the Pieniny and Tatra mountains.

The Pieniny Limestone Formation builds steep cliffs along the Dunajec River Gorge, described in more detail by Golonka & Krobicki (2007). One of the most spectacular views along rafting trip is **Mnichy** (**Seven Monks**) (Fig. 11C) and **Sokolica Mt** (**Falcon's Mt**) (Fig. 11D). The name of this mountain is derived from numerous falcons, which used to nest here.

The Sokolica is frequently visited by hikers because of magnificent view of the Tatra Mts and the ancient, 500 years-old pine forest (Tłuczek, 2004). Close to the Szczawnica town, the Dunajec River Gorge ended, just after the last cliff built by thin-bedded cherty limestones. This town is popular spa, famous for its mineral springs, which have been known since the medieval time, but first written remarks came from XVI century.

After rafting on Dunajec River we will go eastward to Jaworki village. The Grajcarek stream valley runs parallel with the Pieniny Klippen Belt, where Jurassic and Lower Cretaceous rocks of the so-called tectonic Grajcarek Unit are exposed (with full development of the Magura (Hulina) Succession. This succession was deposited within the northwestern part of the Carpathian Tethys, separated palaeogeographically by the Czorsztyn Ridge from the other basinal succession (Birkenmajer, 1986; Golonka, 2004; Golonka & Krobicki, 2004). On the northern side this unit is in tectonic contact with the flysch rocks of the Krynica Unit of the Magura Nappe. Several Miocene andesite intrusions cut both tectonic units (Malinów abandoned quarry, Jarmuta and Krupianka hills).

Homole Gorge near Jaworki village

The famous deep **Homole Gorge** is cutting through the rocks of the so-called Homole tectonic block south of the Jaworki village (Figs 8, 9, 12-14). The origin this block is speculative and a subject of scientific debate. There is a variety of opinions, from the autochthonous position within the Czorsztyn ridge (e.g. Birkenmajer, 1986) through the nappe thrust over the other tectonic units (e.g. Książkiewicz, 1977; Golonka & Rączkowski, 1984; Jurewicz, 1997, 2005) to the olistoliths (Cieszkowski & Golonka, 2005, 2006; Cieszkowski *et al*., 2008). In the Homole Gorge up to near 100 m thick section of white crinoidal limestones of the Smolegowa Limestone Formation of the Czorsztyn Succession is exposed (Birkenmajer, 1963, 1977). These limestones are overlain by red crinoidal limestones (of the Krupianka Limestone Formation) and *Ammonitico Rosso*-type nodular limestones of the Czorsztyn Limestone Formation, which reach maximum 20 m in thickness. Both Smolegowa and Krupianka formations are Bajocian (Middle Jurassic) in age whereas condensed nodular limestones of the *Ammonitico Rosso* facies (Czorsztyn Limestone Formation) represent Middle Jurassic to Early Cretaceous. The decrease of sedimentation rate in pelagic sedimentation regime happened during late Middle-Late Jurassic times. This phenomenon is recorded by the deepening-upward sequence of deposits. The famous Pieniny Klippen Belt tectonic fold and thrust structures can be observed in the Czajakowa Skała Klippe in the upper part of the Homole Gorge (Birkenmajer, 1970, 1979) (Fig. 12D). The Niedzica Nappe is there thrust here over the thick Czorsztyn Unit. Several beds representing the red nodular limestones of the *Ammonitico Rosso*-type of the Niedzica Limestone Formation and Czorsztyn Limestone Formation as well as intercalated radiolarites of the Czajakowa Radiolarite Formation are strongly tectonically disturbed, forming the overturned fold (Birkenmajer, 1970; Jurewicz, 1994) (Fig. 12D). The type locality of the Czajakowa Radiolarite Formation occurs within this klippe (Fig. 13). The Czajakowa Skała Klippe also shows a complete sequence of the Jurassic deposits of the Niedzica Succession (Birkenmajer, 1977; Wierzbowski *et al*., 1999). The oldest black and grey marly shales with spherosiderite concretions of the Skrzypny Shale Formation (Birkenmajer, 1977; Tyszka, 1994) are exposed here. These deposits are overlain by yellowish-greyish-red and dark cherry-greenish crinoidal limestones. The contact between black shales and crinoidal limestones is sharp and irregular. The ammonite fauna was found in the lowermost part of the crinoidal limestones of the Smolegowa Limestone Formation. These very precise biostratigraphical data suggest a hiatus between black shales and crinoidal limestones, spanning the Laeviuscula and a part of Propinquans ammonite zones of the Lower Bajocian (Middle Jurassic) (Krobicki & Wierzbowski, 2004; Krobicki, 2006). The small outcrops of these black shales occur below Czajakowa Skała Klippe within local landslide. The best outcrops of these rocks within the Pieniny Klippen Belt in Poland occur in the Krupianka stream, which run the Homole Gorge, westward. Their thickness reach 4-5 metres. The shales contain a lot of spherosiderites and sometimes perfectly preserved ammonites (Fig. 14). The ammonite fauna indicates latest of Aalenian and/or earliest of Bajocian (Middle Jurassic) age of black shales, representing oxygen-depleted facies of the *Fleckenmergel*-type. ❒

This research have been financially supported by AGH grant (11.11.140.447)

Streszczenie

Geologiczna historia pienińskiego pasa skałkowego a środkowojurajskie czarne łupki jako jedne z najstarszych utworów regionu – stratygraficzna pozycja i paleośrodowiskowe znaczenie

Michał Krobicki & Jan Golonka

Karpaty Zewnętrzne (fliszowe) i **pieniński pas skałkowy** tworzą najbardziej północną część polskich Karpat. Te pierwsze są zbudowane przez fliszowe utwory jurajsko-wczesnomioceńskie (Ślączka, 1996; Oszczypko, 2004, 2006a, b; Oszczypko *et al*., 2005, 2006). Utwory te były oderwane od swojego podłoża i fałdowane oraz nasuwane od południa w miocenie (orogeneza alpejska) formując płaszczowiny (Ślączka, 1996). Wszystkie płaszczowiny Karpat Zewnętrznych są nasunięte na platformę wschodnioeuropejską przykrytą utworami miocenu zapadliska przedkarpackiego (Fig. 1, 2). Płaszczowiny są elementem allochtonicznym, a utwory je budujące powstawały w karpackich basenach sedymentacyjnych, daleko na południe od ich dzisiejszego miejsca występowania. Pieniński pas skałkowy (pps) natomiast, znajduje się na granicy Zewnętrznych Karpat Fliszowych i Karpat Wewnętrznych, stanowiąc bardzo silnie stektonizowaną strefę, która dzisiaj ma około 600 km długości i 1-20 km szerokości, biegnąc od okolic Wiednia na zachodzie aż do Rumunii na wschodzie. (Fig. 1). Zarówno północna jak i południowa granica pps są dzisiaj granicami tektonicznymi, mając prawie pionowy przebieg (Fig. 3), wzdłuż których następowało tektoniczne skracanie oryginalnego basenu sedymentacyjnego (Birkenmajer, 1986; Golonka & Krobicki, 2006; Krobicki & Golonka, 2006). W swoim regionalnym charakterze pps jest generalnie strefą melanżu tektonicznego, gdzie poszczególne jednostki tektoniczne są trudne do rozróżnienia.

Palinspastyczna rekonstrukcja basenu pps wskazuje na występowanie podmorskiego grzbietu podczas jego jurajsko-kredowej historii. Jest to tzw. **grzbiet czorsztyński**, który stanowił wydłużoną strefę, rozdzielającą pierwotnie basen magurski (Karpat Zewnętrznych) od basenu pienińskiego w obrębie najbardziej północnej części oceanu Tetydy (Fig. 4-6) (por. Golonka, 2007a, b z literaturą tam cytowaną). Geograficzna orientacja tego grzbietu, z **SW** na **NE**, jest interpretowana na podstawie badań paleomagnetycznych, analizy facjalnej osadów mezozoicznych jak i warunków paleoklimatycznych (patrz dyskusja – Golonka & Krobicki, 2001; oraz Aubrecht & Túnyi, 2001; Lewandowski *et al*., 2005; Grabowski *et al*., 2008). Baseny sedymentacyjne rozdzielone przez grzbiet czorsztyński były zdominowane przez pelagiczny typ sedymentacji. Najgłębsze części basenu pps są dobrze udokumentowane przez jurajsko-wczesnokredowe utwory głębokowodne (radiolaryty i wapienie rogowcowe typu *Maiolica*) (Birkenmajer, 1979, 1986; Golonka & Sikora, 1981; Golonka & Krobicki, 2004; Krobicki et a., 2006) tzw. sukcesji **braniskiej** i **pienińskiej**. Nieco płytsze, przejściowe

sukcesje (**czertezicka** i **niedzicka**) okupowały miejsce odpowiadające skłonowi kontynentalnemu pomiędzy głębszymi partiami basenu a częścią najpłytszą, reprezentowaną przez sukcesję **czorsztyńską**, która zajmowała pierwotnie SE skłon grzbietu czorsztyńskiego (Birkenmajer, 1986; Krobicki & Golonka, 2006).

Najwcześniejsze stadium historii basenu pienińskiego jest enigmatyczne i udokumentowane jedynie egzotykami z fliszowych utworów kredy i paleogenu. Egzotyki te sugerują istnienie hipotetycznej „zatoki" oceanu Vardar-Transylwania, który oddzielał blok Cisy (rejon Bihor-Apuseni) od platform mezyjskiej i wschodnioeuropejskiej (Săndulescu, 1988; Golonka & Krobicki, 2004). Najstarsze utwory jury pps (hetang-synemur) znane są tylko na Słowacji i Ukrainie i reprezentowane są przez zróżnicowane, szaro-czarne utwory klastyczne facji ***gresteńskiej*** z nielicznymi wkładkami czarnych wapieni (Schlögl *et al*., 2004 z literaturą). Natomiast młodsze (toark-dolny bajos) są wapienie i margle plamiste facji ***Fleckenkalk*/*Fleckenmergel*** i czarne łupki sferosyderytowe z małżami *Bositra* („*Posidonia*") (w lokalnej terminologii – formacja łupków ze Skrzypnego; Birkenmajer, 1977), powstałe w okresowo niedotlenionych środowiskach sedymentacji oceanu Tetydy (Birkenmajer, 1986; Tyszka, 1994. 2001). We wczesnym bajosie (jura środkowa) grzbiet czorsztyński ukształtował się jako wyraźny grzbiet śródoceaniczny, z czym związana była równocześnie bardzo gwałtowna zmiana sedymentacji/paleośrodowiska, kiedy dobrze dotlenione, różnokolorowe (białe, żółtawe, różowe, szare, czerwone) **wapienie krynoidowe** zastąpiły szare i czarne niedotlenione utwory wczesnej jury i początków jury środkowej (Krobicki & Wierzbowski, 2004). Te wapienie krynoidowe osadzały się w najpłytszych i przejściowych sukcesjach osadowych (czorsztyńska, niedzicka i czertezicka). Bajoskie wynurzenie grzbietu czorsztyńskiego pomiędzy basenem pienińskim a magurskim było związane z postryftową fazą ewolucji basenu pienińskiego i najprawdopodobniej odpowiada pierwszym epizodom ruchów fazy mezokimeryjskiej orogenezy alpejskiej (Golonka *et al*., 2003; Krobicki, 2006). Nieco później (od najpóźniejszego bajosu) osadziły się czerwone, pelagiczne wapienie bulaste facji ***Ammonitico Rosso***. W tym samym czasie w najgłębszych partiach basenu pps tworzyły się po raz pierwszy **radiolaryty** (Birkenmajer, 1986; Mišík, 1999). Późnojurajska (oksford-kimeryd) historia basenu pienińskiego ukazuje jego najsilniejsze zróżnicowanie facjalne z sedymentacją mieszanych utworów krzemionkowo-wapiennych. Te pierwsze osadzały się w relatywnie płytszych środowiskach sedymentacji (np. sukcesja czorsztyńska), a radiolaryty powstawały w sukcesjach przejściowych i basenowych (Birkenmajer, 1977, 1986; Mišík, 1999). Na przełomie jury i kredy efekt działania neokimeryjskich ruchów tektonicznych, doprowadził do silnego zróżnicowania facjalnego. Formowaniem się i destrukcja podmorskich zrębów tektonicznych jest utożsamiana z dużą aktywnością tektoniczną w basenach karpackich w tym czasie (Birkenmajer, 1958, 1975, 1986; Michalík & Reháková, 1995; Krobicki, 1996; Aubrecht *et al*., 1997; Krobicki & Słomka, 1999; Plašienka, 2002; Golonka *et al*., 2003; Krobicki *et al*., 2006). Równocześnie w głębszych partiach basenu pienińskiego (głównie sukcesja braniska i pienińska) trwała sedymentacja mikrytowych wapieni rogowcowych facji ***Maiolica*** (=*Biancone*). Jest to jedna z najszerzej rozprzestrzenionych litofacji w całej Tetydzie (Pszczółkowski, 1987; Wieczorek, 1988). W polskiej części Pienin te białe, cienkouławicone wapienie budują najwyższe szczyty tych gór (np. Trzy Korony, Sokolica etc.). Pelagiczne margle otwornicowe, początkowo zdominowane przez hedbergelle, dokumentują z kolei albski (najmłodsze piętro wczesnej kredy) etap sedymentacji w basenie (Birkenmajer, 1986). Natomiast późnokredowe utwory pelagiczne, zdominowane są przez czerwone margle globotrunkanowe (najpopularniejszy rodzaj otwornic w tym czasie) facji ***Scaglia Rossa*** (Birkenmajer, 1986; Bąk, 2000).

Jedną z największych **atrakcji geoturystycznych** pienińskiego pasa skałkowego jest **spływ Dunajcem**, opisana ostatnio szczegółowo przez Golonkę & Krobickiego (2007) (patrz również Alexandrowicz & Alexandrowicz, 2004) i z tego powodu tutaj tylko lakonicznie wzmiankowana. Początek spływu ma miejsce na przystani Kąty (Fig. 8, 9) we wsi Sromowce i kończy się w Szczawnicy (ok. 2-2.5 godziny). Dogodne połączenia komunikacyjne tego miejsca umożliwiają łatwe dotarcie tutaj zarówno od północy (Kraków) jak i od południa (Zakopane). Wycieczka ta oferuje nadzwyczajne widoki stromych ścian centralnych Pienin, uformowanych tak zarówno dzięki procesom tektonicznym jak i erozji rzecznej. Przy okazji można odwiedzić niedalekie, średniowieczne zamki w Czorsztynie (Fig. 10A) bądź w Niedzicy (Fig. 10B). Na trasie spływu pierwszym interesującym obiektem geologicznym (geoturystycznym) jest **Macelowa Góra** (Fig. 11), która w odwróconej pozycji tektonicznej ukazuje ciągły profil utworów najwyższej jury-dolnej kredy sukcesji pienińskiej (od górnojurajsko-dolnokredowych wapieni rogowcowych facji *Maiolica* na górze aż po górnokredowe margle globotrunkanowe facji *Scaglia Rossa* na dole). W obrębie tych margli można zaobserwować cienkie (kilka cm) wkładki turbidytowych piaskowców i mułowców, których geneza ściśle nawiązuje do głębokomorskiej sedymentacji typu fliszowego (por. Mutti & Ricci Lucchi, 1975; Słomka, 1986; Stow, 1986; Mutti & Normark, 1987; Ghibaudo, 1992; Reading & Richards, 1994; Lowe, 1997; Shanmugam, 2000). Kolejnymi spektakularnym obiektami na trasie spływu są **Trzy Korony** (982 m n.p.m.) (Fig. 11B) i **Sokolica** (Fig. 11D), najwyższe szczyty centralnych Pienin, prawie w całości zbudowane z cienkoławicowych, silnie tektonicznie zdeformowanych wapieni rogowcowych facji *Maiolica*, również należących do sukcesji pienińskiej. Natomiast, tektoniczno-erozyjna historia Przełomu Dunajca była obiektem zainteresowania już XIX-to wiecznych geologów, lecz nie do końca w szczegółach rozpoznany jest fenomen jego powstania mimo upływu tylu lat od tamtych czasów (zob. Zuchiewicz, 1982; Birkenmajer, 2006). Przełom ten tworzy wiele łusek tektonicznych ponasuwanych na siebie a zbudowanych głównie z twardych, odpornych na erozję wapieni rogowcowych, a przekładających się wielokrotnie (łuski tektoniczne) z mniej odpornymi na wietrzenie i erozję marglami i łupkami, głównie górnej kredy. Bezsprzeczny jest związek budowy geologicznej tego obszaru, a zwłaszcza jego plan strukturalno-tektoniczny, z genezą Przełomu Dunajca, co w świetle najnowszych danych neotektonicznych zyskuje nowe argumenty (Zuchiewicz *et al*., 2002). W historii badań tego frapującego zagadnienia proponowano co najmniej cztery rozwiązania. Najstarszy z nich preferował genezę **epigenetyczną**, uznając, że Dunajec wcinał się w miękkie utwory przykrywające zwartą pokrywą wapienne skałki podłoża. Drugi pogląd skupiał się na **antecedentnej** genezie Przełomu Dunajca, sugerując powolne podnoszenie się górotworu pienińskiego i stopniowe wcinanie się meandrującego pierwotnie pra-Dunajca w podłoże. Pomysł trzeci wskazuje na tektoniczne uwarunkowania powstania przełomu (płynie on obecnie po utworach budujących maksymalną depresję strukturalną) i dlatego został nazwany przełomem **strukturalnym**. Ostatnia z propozycji rozważa możliwość kaptażu systemu rzecznego Białki-Białego Dunajca przez tzw. „Dunajec sądecki", co miało wywołać efekt erozji wstecznej, a przez to Przełom Pieniński można by uznać za przełom **regresyjny**. Bez względu na to, która z propozycji jest prawdziwa, przebieg procesu formowania się przełomu miał miejsce pomiędzy późnym miocenem a plejstocenem jak ostatnio to zreasumował Birkenmajer (2006) w nawiązaniu do najnowszych obserwacji tego fenomenu.

Po spływie Dunajcem udajemy się w kierunku wsi Jaworki, na wschód za Szczawnicę, aby zwiedzić słynny **Wąwóz Homole** (Fig. 8, 9, 12-14). Jest to praktycznie jedyne miejsce w pienińskim pasie skałkowym Polski gdzie wapienna płyta, pochylona nieznacznie pod stosunkowo niewielkim kątem ku północy, jest relatywnie słabo zaburzona tektonicznie. Dlatego w terminologii geologicznej tego obszaru zwykło się używać określenia „tektoniczny blok (płyta) Homoli" (Birkenmajer, 1970, 1979), dla skrótowego zobrazowania jego charakteru strukturalnego. Prawie ze wszystkich stron jest on obcięty licznymi uskokami tektonicznymi, a i w swojej wewnętrznej budowie charakteryzuje się przebiegiem licznych dyslokacji tektonicznych. Są one głównie efektem działania odprężających sił w obrębie tej płyty, która z jednej strony jest erozyjnie podcinana przez okoliczne potoki, a z drugiej strony izolowane w ten sposób bloki wapieni ulegają grawitacyjnemu zapadaniu się w plastyczne podłoże zbudowane z miękkich łupków środkowojurajskich. Główna część wąwozu zbudowana jest ze środkowojurajskich (bajos) białych wapieni krynoidowych tzw. formacji wapienia ze Smolegowej, których miąższość dochodzi tutaj do 100 metrów (Fig. 13). Wapienie te są przykryte niewielkiej miąższości czerwonymi wapieniami krynoidowymi (formacja wapienia z Krupianki) oraz czerwonymi wapieniami bulastymi facji *Ammonitico Rosso* (formacja wapienia czorsztyńskiego). Wszystkie wymienione utwory należą do sukcesji czorsztyńskiej (Birkenmajer, 1970, 1977). Na nie nasunięte są, w postaci spektakularnego fałdu **Czajakowej Skały** obalonego ku północy, utwory sukcesji niedzickiej, które w postaci lokalnej płaszczowiny leżą na poziomej płycie wapiennej bloku Homoli. Sekwencja utworów płaszczowiny niedzickiej jest zbliżona do profilu sukcesji czorsztyńskiej (Fig. 13) z wyjątkiem środkowej jej części z jednej strony [gdzie występują górnojurajskie (oksford) utwory krzemionkowe – radiolaryty, nieobecne w profilu sukcesji czorsztyńskiej] a z drugiej strony wyraźną dysproporcją w miąższości środkowojurajskich wapieni krynoidowych. Profil tej sukcesji rozpoczynają ciemne utwory jury środkowej, występując w grupie Czajakowej Skały, gdzie tworzą spąg nasunięcia płaszczowiny niedzickiej na jednostkę czorsztyńską. Zwłaszcza czarne łupki sferosyderytowe były podatne na takie tektoniczne przemieszczenia, a dzisiaj powodują tworzenie się osuwisk strukturalnych, czego najlepszym przykładem jest polana pod Czajakową Skałą, gdzie łupki te znajdują się w najniższej części jednego z najlepiej widocznych osuwisk. W sukcesji tej wapienie krynoidowe są niewielkiej miąższości a przykryte czerwonymi wapieniami bulastymi. Te drugie dostarczyły bogatej fauny amonitów, na podstawie których precyzyjnie ustalono ich wiek na bajos-oksford (jura środkowa-jura górna). Wapienie te najlepiej odsłaniają się w głównej skałce Czajakowej Skały (Birkenmajer, 1970, 1979; Wierzbowski *et al*., 1999). Radiolaryty stanowią najbardziej charakterystyczny wyróżnik litologiczny dla sukcesji niedzickiej, świetnie widoczny w samym jądrze obalonego fałdu (Birkenmajer, 1970, 1979; Jurewicz, 1994; Golonka & Krobicki, 2001). Formacja ta składa się z trzech ogniw (Birkenmajer, 1977) (w następstwie stratygraficznym): czerwone radiolaryty, zielone radiolaryty i ponownie czerwone radiolaryty formacji radiolarytów z Czajakowej, które tutaj mają swój stratotyp (Fig. 12, 13). Są to cienkoułowicone (od kilku do 20 cm miąższości – por. Fig. 12D) utwory rogowców i wapieni krzemionkowych przeławicanych cienkimi łupkami o grubościach nieprzekraczających 2 cm. Leżące ponad radiolarytami czerwone wapienie bulaste i cienkoułowicone mikrytowe wapienie kalpionellowe są wieku górnojurajsko-dolnokredowego, a ponad nimi niewielkiej miąższości jasnopopielate wapienie mikrytowe z rogowcami, które wieńczą profil utworów dolnej kredy. Wiekowo wapienie te odpowiadają wapieniom rogowcowym formacji wapienia pienińskiego znanym z centralnej części Pienin (patrz wyżej – spektakularne strome szczyty Trzech Koron, Sokolicy, Mnichów) (Fig. 11).

Natomiast najstarsze utwory sukcesji czorsztyńskiej odsłaniające się w południowej części bloku Homoli jak i w korycie sąsiadującego od zachodu potoku Krupianka (Fig. 14), reprezentowane są przez szare lub szarobrunatne margle i wapienie margliste plamiste oraz **czarne łupki ze sferosyderytami** (odpowiednio formacja margli z Krempachów i **formacja łupków ze Skrzypnego**) (aalen-najniższy bajos) (ekwiwalenty facjalne czarnych łupków obserwowanych w osuwisku pod Czajakową Skałą). W odniesieniu do geologii alpejskiej można zaklasyfikować te utwory do szeroko rozprzestrzenionej w całym łańcuchu alpejskim facji *Fleckenkalk*/*Fleckenmergel* (= plamiste wapienie/margle). Paleośrodowiskowo utwory te reprezentują niedotlenione (redukcyjne) warunki środowiska sedymentacji we wczesnym etapie rozwoju basenu pienińskiego.

Literatura (References)

Alexandrowicz, Z. & Alexandrowicz, S.W., 2004. Geoparks – the most valuable landscape parks in southern Poland. *Polish Geological Institute, Special Paper*, 13: 49-56.

Aubrecht, R. & Túnyi, I., 2001. Original orientation of neptunian dykes in the Pieniny Klippen Belt (Western Carpathians): the first results. *Contributions to Geophysics and Geodesy*, 31: 557-578.

Baumgart-Kotarba, M., 1996. On origin and age of the Orava Basin, West Carpathians. *Studia Geomorphologica Carpatho-Balcanica*, 30: 101-116.

Baumgart-Kotarba, M., 2001. Continuous tectonic evolution of the Orava basin from Late Badenian to the present-day. *Geologica Carpathica*, 52: 103-110.

Bąk, K., 2000. Biostratigraphy of deep-water agglutinated Foraminifera in Scaglia Rossa-type deposits of the Pieniny Klippen Belt, Carpathians, Poland. In: Hart, M.B., Kaminski, M.A. & Smart, C.W. (Eds.): *Proceedings of the Fifth International Workshop on Agglutinated Foraminifera*. Grzybowski Foundation Special Publication, 7: 15-41, Kraków.

Birkenmajer, K., 1958. Submarine erosional breaks and Late Jurassic synorogenic movements in the Pieniny Klippen Belt geosyncline. *Bulletin de Academie Polonaise de Science, Sér., sci. chim., géol. & géogr.*, 8: 551-558.

Birkenmajer, K., 1963. Stratigraphy and paleogeography of the Czorsztyn Series (Pieniny Klippen Belt, Carpathians) in Poland. Studia Geologica Polonica, 45: 7–158. *Studia Geologica Polonica*, 45: 7-158. (In Polish, English summary)

Birkenmajer, K., 1970. Pre-Eocene fold structures in the Pieniny Klippen Belt (Carpathians) of Poland. *Studia Geologica Polonica*, 31: 1-77. (In Polish, English summary)

Birkenmajer, K., 1975. Tectonic control of sedimentation at the Jurassica-Cretaceous boundary in the Pieniny Klippen Belt, Carpathians. Colloque sur la limite Jurass.-Crét., Lyon-Neuchâtel (1973). *Mémoire BRGM*: 294-299.

Birkenmajer, K., 1977. Jurassic and Cretaceous lithostratigraphic units of the Pieniny Klippen Belt, Carpathians, Poland. *Studia Geologica Polonica*, 45: 1-158.

Birkenmajer, K., 1979. *Przewodnik geologiczny po pienińskim pasie skałkowym*. Wydawnictwa Geologiczne, 1-237, Warszawa. (In Polish only)

Birkenmajer K., 1983. Strike-slip faults in the northern boundary zone of the Pieniny Klippen Belt, Carpathians. *Studia Geologica Polonica*, **77**: 89-112. (In Polish, English summary)

Birkenmajer, K., 1986. Stages of structural evolution of the Pieniny Klippen Belt, Carpathians. *Studia Geologica Polonica*, 88: 7-32.

Birkenmajer, 2003. Post-collisional Late Middle Miocene (Sarmatian) Pieniny Volcanic Arc, Western Carpathians. *Bulletin of the Polish Academy of Sciences*, *Earth Sciences*, 51, 1: 79-89.

Birkenmajer, K., 2006. Dunajec River Gorge, Pieniny Mts, West Carpathians. *Pieniny – przyroda i człowiek*, 9: 9-22. (In Polish, English summary)

Birkenmajer, K., Bąk, M. & Bąk, K., 2001. Stop C5.3 – Sromowce Niżne – Trzy Korony Mt. In: Birkenmajer, K. & Krobicki, M. (Eds.); *12th meeting of the Association of European Geological Societies; 10-15 September 2001, Kraków: Carpathian palaeogeography and geodynamics: a ultidisciplinary approach; field trip guide*. Polish Geological Institute, Kraków: 146-150.

Cieszkowski, M. & Golonka, J., 2005. Olistolites and olistostromes as geotouristic objects – examples from Northern Carpathians, Poland. In: Doktor, M. & Waśkowska-Oliwa, A. (Eds.) *Geotourism – new dimensions in XXI century tourism and chances for future development*. 2nd International Conference Geotour 2005, 22-24 September, Kraków: 21-23.

Cieszkowski, M. & Golonka, J., 2006. Olistostrom as indicators of the geodynamic process (Northern Carpathians). *Geolines*, 20: 27-28.

Cieszkowski, M., Golonka, J., Krobicki, M., Ślączka A., Oszczypko, N. & Waśkowska-Oliwa, A., 2008. The Northern Carpathians plate tectonic evolutionary stages and origin of olistolites. In: Németh, Z. & Plašienka, D. (eds.) *SlovTec 08, 6th Meeting of the Central European Tectonic Studies Group (CETeG) & 13th Meeting of the Czech Tectonic Studies Group (ČTS)*, 23-26 April 2008, Upohlav, Pieniny Klippen Belt, Slovakia. Proceedings and Excursion Guide: 21-22

Ghibaudo, G., 1992. Subaqueous sediment gravity flow deposits: practical criteria for their field description and classification. *Sedimentology*, 39: 423-454.

Golonka, J., 2000. *Cambrian-Neogene Plate Tectonic Maps*. Wydawnictwa Uniwersytetu Jagiellońskiego, Kraków, 125 pp.

Golonka, J., 2004. Plate tectonic evolution of the southern margin of Eurasia in the Mesozoic and Cenozoic. *Tectonophysics*, 381: 235-273.

Golonka, J., 2005. Mesozoic plate tectonics of the Inner Carpathians – rotational approach. *Geolines*, 19: 42-43.

Golonka, J., 2007a. Late Triassic and Early Jurassic palaeogeography of the world. *Palaeogeography, Palaeoclimatology, Palaeoecology*, 244, 1-4: 297-307.

Golonka, J., 2007b. Phanerozoic paleoenvironment and paleolithofacies maps. Mesozoic. *Kwartalnik AGH*, *Geologia*, 33, 2: 211-264.

Golonka, J. & Krobicki, M., 2001. Upwelling regime in the Carpathian Tethys: a Jurassic-Cretaceous palaeogeographic and palaeoclimatic perspective. *Geological Quarterly*, 45: 15-32.

Golonka, J. & Krobicki, M., 2004. Jurassic paleogeography of the Pieniny and Outer Carpathian basins. *Rivista Italiana di Paleontologica Stratigrafica*, 110: 5-14.

Golonka, J. & Krobicki, M., 2006. Field trip A – From Tethyan to Platform Facies. Outer Carpathians. In: Wierzbowski, A., Aubrecht., R., Golonka, J., Gutowski, J., Krobicki, M., Matyja, B.A, Pieńkowski, G. & Uchman, A. (eds.). *Jurassic of Poland and adjacent Slovakian Carpathians. Field trip guidebook. 7th International Congress on the Jurassic System*, 6-18 September 2006, Kraków, Poland. pp. 11-15.

Golonka, J. & Krobicki, M., 2007. Dunajec River rafting as one of the most important geotouristic object of the future trans-bordering PIENINY Geopark. *Geoturystyka*, 3 (10): 29-44.

Golonka, J. & Rączkowski, W., 1984. Arkusz Piwniczna; Detailed Geological Map of Poland; Geological Institute – Publishing House Wydawnictwa Geologiczne. 85 p. Warszawa.

Golonka, J. & Sikora, W., 1981. Microfacies of the Jurassic and Lower Cretaceous sedimentarily thinned deposits of the Pieniny Klippen Belt in Poland. *Biuletyn Instytutu Geologicznego*, 31: 7-37. (In Polish, English summary)

Golonka, J., Krobicki, M., Oszczypko, N., Ślączka, A. & Słomka, T., 2003. Geodynamic evolution and paleogeography of the Polish Carpathians and adjacent areas during Neo-Cimmerian and preceding events (latest Triassic-earliest Cretaceous). In. McCann, T. & Saintot, A. (Eds) *Tracing Tectonic Deformation Using the Sedimentary Record*. Geological Society, Special Publication, London, 208: 138-158.

Golonka, J., Gahagan, L., Krobicki, M., Marko, F., Oszczypko, N. & Ślączka, A., 2006. Plate-tectonic evolution and paleogeography of the Circum-Carpathian region. In: Golonka, J. & Picha, F.J. (eds), The Carpathians and their foreland: Geology and hydrocarbon resources. *American Association of Petroleum Geologists*, *Memoire*, 84: 11-46.

Grabowski, J., Krobicki, M. & Sobień, K., 2008. New palaeomagnetic results from the Polish part of the Pieniny Klippen Belt, Carpathians – evidence for the palaeogeographic position of the Czorsztyn Ridge in the Mesozoic. *Geological Quarterly*, 52 (1): 31-44.

Jurewicz, E., 1994. Structural analysis of the Pieniny Klippen Belt at Jaworki, Carpathians, Poland. *Studia Geologica Polonica*, 7-87. (In Polish, English summary)

Jurewicz, E., 1997. The contact between the Pieniny Klippen Belt and Magura Unit (the Małe Pieniny Mts.). *Geological Quarterly*, 41, 3: 315-326.

Jurewicz, E., 2005. Geodynamic evolution of the Tatra Mts. and the Pieniny Klippen Belt (Western Carpathians): problems and comments. *Acta Geologica Polonica*, 3: 295-338.

Kováč, M., Nagymarosy, A., Oszczypko, N., Ślączka, A., Csontos, L., Marunteanu, M., Matenco, L. & Márton. M., 1998. Palinspastic reconstruction of the Carpathian-Pannonian region during the Miocene, In: Rakús, M. (Ed.), *Geodynamic development of the Western Carpathians*. Geological Survey of Slovac Republic, Bratislava: 189–217.

Krobicki, M., 1996. Neo-Cimmerian uplift of intraoceanic Czorsztyn pelagic swell (Pieniny Klippen Belt, Polish Carpathians) indicated by the change of brachiopod assemblages. In: Riccardi A.C. (Ed.): Advances in Jurassic Research. *GeoResearch Forum*, 1-2: 255-264, Zurich.

Krobicki, M., 2006. Field trip A – From Tethyan to Platform Facies. Outer Carpathians. Stop A5 – Falsztyn – Czorsztyn Succession (Aalenian-Bajocian). In: Wierzbowski, A., Aubrecht., R., Golonka, J., Gutowski, J., Krobicki, M., Matyja, B.A, Pieńkowski, G. & Uchman, A. (eds.). *Jurassic of Poland and adjacent Slovakian Carpathians. Field trip guidebook. 7th International Congress on the Jurassic System, 6-18 September 2006, Kraków, Poland*. pp. 39-41.

Krobicki, M. & Golonka, J., 2006. Pieniny Klippen Belt. In: Wierzbowski, A., Aubrecht, R., Golonka, J., Gutowski, J., Krobicki, M., Maryja, B.A, Pieńkowski, G. & Uchman, A. (Eds.). *Jurassic of Poland and adjacent Slovakian Carpathians. Field trip guidebook. 7th International Congress on the Jurassic System*, 6-18 September 2006, Kraków, Poland. pp. 15-22.

Krobicki, M., Poprawa, P. & Golonka, J., 2006. Early Jurassic – Late Cretaceous evolution of the Pieniny Klippen Basin indicated by tectonic subsidence analysis. In: Oszczypko, N., Uchman, A. & Malata, E. (eds), *Palaeotectonic evolution of the Outer Carpathian and Pieniny Klippen Belt Basins*. Instytut Nauk Geologicznych UJ: 165-178. Kraków. (In Polish only)

Krobicki, M. & Słomka, T., 1999. Berriasian submarine mass movements as results of tectonic activity in the Carpathians basins. *Geologica Carpathica*, 50, 42-44.

Krobicki, M. & Wierzbowski, A., 2004. Stratigraphic position of the Bajocian crinoidal limestones and their palaeogeographic significance in evolution of the Pieniny Klippen Basin. *Tomy Jurajskie*, 2: 69-82. (In Polish, English summary)

Książkiewicz, M., 1977. The Tectonics of the Carpathians. In: Geology of Poland, Volume 4. Tectonics (ed. Pożaryski, W.), 476-699.Wydawnictwa Geologiczne, Warszawa.

Lewandowski, M., Krobicki, M., Matyja., B.A. & Wierzbowski, A., 2005. Palaeogeographic evolution of the Pieniny Klippen Basin using stratigraphic and palaeomagnetic data from the Veliky Kamenets section (Carpathians, Ukraine). *Palaeogeography, Palaeoclimatology, Palaeoecology*, 216: 53-72.

Lowe, D.R., 1997. Reinterpretation of depositional processes in a classic flysch sequence (Pennsylvanian Jackfork Group), Ouachita Mountains, Arkansas and Oklahoma: discussion: *American Association of Petroleum Geology Bulletin*, 81, 3: 460-465.

Mišík, M., 1999. Contribution to the lithology and paleogeography of radiolarites in the Western Carpathians. *Mineralia Slovaca*, 31: 491-506.

Michalík, J. & Reháková, D., 1995. Sedimentary records of Early Cretaceous tectonic activity in the Alpine-Carpathian region. *Slovak Geological Magazine*, 2: 159-164.

Mutti, E. & Normark, W.R., 1987. Comparing examples of modern and ancient turbidite systems: problems and concepts. In: Legget, J. K. & Zuffa, G.G. (Eds), *Marine Clastic Sedimentology, concepts and case studies*: Graham & Trotman, London, 1-38.

Mutti, E. & Ricci Lucchi, F., 1975. Turbidite facies and facies associations. In: Mutti, E. *et al*., (Eds): Examples of turbidite facies associations from selected formations of the Northern Apennines. Field Trip A11, IX Int. Sedimentol. Congr., Nice, 21-36.

Oszczypko, N., 2004. The structural position and tectonosedimentary evolution of the Polish Outer Carpathians. *Przegląd Geologiczny*, 52, 8/2: 780-791.

Oszczypko, N., 2006a. Late Jurassic-Miocene evolution of the Outer Carpathian fold-and-thrust belt and its foredeep basin (Western Carpathians, Poland). *Geological Quarterly*, 50, 1: 169-194.

Oszczypko, N., 2006b. Position of the Polish Outer Carpathians in the Alpine arc and their stages of development. In: Oszczypko, N., Uchman, A. & Malata, E. (eds), *Palaeotectonic evolution of the Outer Carpathian and Pieniny Klippen Belt Basins* (Rozwój paleotektoniczny basenów Karpat Zewnętrznych i pienińskiego pasa skałkowego). Instytut Nauk Geologicznych UJ: 9-18. Kraków. (In Polish, English summary)

Oszczypko, N. & Oszczypko-Clowes, M., 2006. Evolution of the Magura Basin. In: Oszczypko, N., Uchman, A. & Malata, E. (eds), *Palaeotectonic evolution of the Outer Carpathian and Pieniny Klippen Belt Basins* (Rozwój paleotektoniczny basenów Karpat Zewnętrznych i pienińskiego pasa skałkowego). Instytut Nauk Geologicznych UJ: 133-164. Kraków. (In Polish, English summary)

Oszczypko, N., Oszczypko-Clowes, M., Golonka, J. & Marko, F., 2005. Oligocene-Lower Miocene sequences of the Pieniny Klippen Belt and adjacent Magura Nappe between Jarabina and the Poprad River (East Slovakia and South Poland): their tectonic position and palaeogeographic implications. *Geological Quarterly*, 49 (4): 379-402.

Plašienka, D., 2002. Early stages of tectonic evolution of the Pieniny Klippen Belt. *GeoLines*, 14: 75-78.

Plašienka, D., Grecula, P., Putiš, M., Kováč, M. & Hovorka, D. 2000. Evolution and structure of the Western Carpathians: an overview. In: Grecula, P., Hovorka, D. & Putiš, M. (eds.), *Geological evolution of the Western Carpathians*, Geocomplex. Bratislava, pp. 1-24.

Pszczółkowski, 1987. Paleogeography and paleotectonic evolution of Cuba and adjoining areas during the Jurassic-Early Cretaceous. *Annales Societatis Geologorum Poloniae*, 57: 27-142.

Reading, H.G. & Richards. M., 1994. Turbidite systems in deep-water basin margins classified by grain size and feeder system. *American Association of Petroleum Geology Bulletin*, 78, 5: 792-822.

Săndulescu, M., 1988. Cenozoic Tectonic History of the Carpathians, In: Royden L. & Horváth F. (Eds.): The Pannonian Basin: A study in basin evolution. *American Association of Petroleum Geology*, *Memoire*, 45: 17-25, Tulsa.

Schlögl, J., Rakús, M., Krobicki, M., Matyja, B.A., Wierzbowski, A., Aubrecht, R., Sitár, V. & Józsa, Š., 2004. Beňatina Klippe – lithostratigraphy, biostratigraphy, palaeontology of the Jurassic and Lower Cretaceous deposits (Pieniny Klippen Belt, Western Carpathians, Slovakia). *Slovak Geological Magazine*, 10, 4: 241-262.

Shanmugam, G., 2000. 50 years of turbidite paradigm (1950s-1990s): deep-water processes and facies models – a critical perspective. *Marine Petroleum Geology*, 17: 285-342.

Słomka, T., 1986. Statistical approach to study of flysch sedimentation – Kimmeridgian-Hauterivian Cieszyn Beds, Polish Outer Carpathians. *Annales Societatis Geologorum Poloniae*, 56: 227-336. (In Polish, English summary)

Stow, D.A.V., 1986. Deep clastic seas. In: Reading, H.G., (Ed.), *Sedimentary environments and facies*, Blackwell Scientific, Oxford, 399-444.

Ślączka, A., 1996. Oil and gas in the northern Carpathians. In: Wessely, G. & Liebl, W., (Eds.): Oil and gas in Alpidic thrustbelts and basins of Central and Eastern Europe, *Eur. Ass. Geosci. Engin., Sp. Publ*., 5: 187-195. Geological Society, London.

Tłuczek, D., 2004. *Pozycja geologiczna paleogeńskich wapieni organogenicznych oraz zlepieńców i piaskowców organodetrytycznych rejonu Lipnika (Pieniny na południe od Szczawnicy-kartowanie detaliczne, mikrofacje, aspekt geoturystyczny).* Unpublished Mr. Thesis. Archiwum ING UJ., 129 pp. (In Polish only)

Tyszka, J., 1994. Response of Middle Jurassic benthic foraminiferal morphogroups to disoxic/oxic conditions in the Pieniny Klippen Basin, Polish Carpathians. *Palaeogeography, Palaeoclimatology, Palaeoecology*, 110: 55-81.

Tyszka, J., 2001. Microfossil assemblages as bathymetric indicators of the Toarcian/Aalenian „Fleckenmergel"-facies in the Carpathian Pieniny Klippen Belt. *Geologica Carpathica*, 52: 147-158.

Vanko, J., 1988. Mapa recentných vertikálnych pohybov Západných Karpát na Slovensku ore epochu 1952-1977. *Geodetický a kartografický obzor, Bratislava*, 34/76: 216-222. (In Slovak only)

Vass, D., 1998. Neogene geodynamic development of the Carpathian arc and associated basins. In: Rakús, M., (Ed.) *Geodynamic development of the Western Carpathians*. Geological Survey of Slovac Republic, Bratislava, Dionýz Štúr Publishers: 155-158.

Wieczorek, J., 1988. Maiolica – A unique facies of the Western Tethys. *Annales Societatis Geologorum Poloniae*, 58: 255-276.

Wierzbowski, A., Jaworska, M. & Krobicki, M., 1999. Jurassic (Upper Bajocian-lowest Oxfordian) ammonitico rosso facies in the Pieniny Klippen Belt, Carpathians, Poland: its fauna, age, microfacies and sedimentary environment. *Studia Geologica Polonica*, 115: 7-74.

Wierzbowski, A., Aubrecht, R., Krobicki, M., Matyja, B.A. & Schlögl, J., 2004. Stratigraphy and palaeogeographic position of the Jurassic Czertezik Succession, Pieniny Klippen Belt (Western Carpathians) of Poland and Eastern Slovakia. *Annales Societatis Geologorum Poloniae*, 74: 237-256.

Zuchiewicz, W., 1982. Geneza przełomu Dunajca przez Pieniny. Wszechświat, 83 (10-11): 169-173. (In Polish only)

Zuchiewicz, W., Tokarski, A.K., Jarosiński, M. & Márton, E., 2002. Late Miocene to present day structural development of the Polish segment of the Outer Carpathians. *EGU Stephen Mueller Special Publication Series*, 3: 185-202.

Żytko, K., Zając, R., Gucik, S., Ryłko, W., Oszczypko, N., Garlicka, I., Nemčok, J., Eliáš, M., Menčik, E. & Stránik, Z., 1989. Map of the tectonic elements of the Western Outer Carpathians and their foreland. In: Poprawa, D. & Nemčok, J. (eds.), *Geological Atlas of the Western Outer Carpathians and their Foreland*. Państwowy Instytut Geologiczny, Warszawa/GUDŠ Bratislava/Uug Praha.

How do metastable secondary minerals form?

JURAJ MAJZLAN[1]
keynote speech

1- Institute of Geosciences, Friedrich-Schiller University, Burgweg 11, 07749 Jena, Germany; Juraj.Majzlan@uni-jena.de

Thermodynamic measurements, done in our and other groups, show that many secondary minerals, typical for oxidation zones of ore deposits, are metastable. Why and how do they form and persist? Which chemical systems are particularly rich in such metastable phases? Is there systematics as to which phases form initially and which ones later?

Field studies show that metastable minerals form not only directly from aqueous solutions. Initial precipitation of metastable phases and their conversion to the stable ones is described by the Ostwald's step rule. Thermodynamic data show that there is a tendency, but no rule, that structurally more complex phases are also thermodynamically more stable. The Ostwald's step rule could then state that the initial, metastable phases are structurally simple, easily assembled from aqueous solutions, nanoparticles, gels, disordered solids, or clusters. There is no need to postulate that the initial phase must bear some structural similarity to the precursor. Calculation of saturation indices for mine drainage solutions show that they are mostly or always supersaturated with respect to the stable phases and the aqueous concentrations are sufficient to precipitate metastable minerals. It seems, however, that more complex precursors, such as nanoparticles, gels, X-ray amorphous solids, or clusters, cause often the formation of metastable minerals. In our work, we encounter often gelatinous substances with copper, manganese or tungsten that slowly convert to metastable minerals, in processes that resemble the synthetic sol-gel chemistry. Another possibility is the crystallization of various metastable minerals from solid, homogeneous 'resins' that are X-ray amorphous. Minerals typical for near-surface environments may be stabilized or destabilized by their surface energy at high specific surface areas. For example, ferrihydrite is often described as a metastable phase but can be shown to be stable with respect to hematite in the nanometer regime.

Refinement of tectonostratigraphy within the West Ny-Firesland terrane of Svalbard based on detrital zircon provenance and metaigneous rock dating

JAKUB BAZARNIK[1], JAROSŁAW MAJKA[2,3], WILLIAM C. MCCLELLAND[4] KAROLINA KOŚMIŃSKA[3], KARSTEN PIEPJOHN[5] , SYNNØVE ELVEVOLD[6] and JUSTIN V. STRAUSS[7]

1 – Polish Geological Institute – National Research Institute, Carpathian Branch; Skrzatów 1, 31-560 Kraków, Poland; jakub.bazarnik@pgi.gov.pl;
2 – Department of Earth Sciences, Uppsala University, Villavägen 16, 752-36 Uppsala, Sweden;
3 – Faculty of Geology, Geophysics and Environmental Protection, AGH-UST, Mickiewicza 30, 30-059 Kraków, Poland;
4 – Department of Earth and Environmental Sciences, University of Iowa, Iowa 52242, Iowa City, USA;
5 – Bundesanstalt fur Geowissenschaften und Rohstoffe, Stilleweg 2, 30655 Hanover, Germany;
6 – Norwegian Polar Institute, Fram Centre, N-9296 Tromsø, Norway;
7 – Department of Earth Sciences, Dartmouth College, HB6105 Fairchild Hall, Hanover, NH 03755, USA

On the Ny-Friesland peninsula, the northern-most area of Spitsbergen, a major tectonic boundary between two major tectonic units of Svalbard's Eastern Basement Province has been described (e.g. Witt-Nilsson et al., 1998, Gee and Tebenkov, 2004). The West Ny-Friesland terrane is composed of metasedimentary and metaigneous rocks of the Atomfjella Complex and separated from the Nordaustlandet terrane by the Mosselhavøya Thrust. The Nordaustlandet terrane is composed of metamorphic rocks of the Mosselhalvøya Group and younger sedimentary cover.

The U-Pb zircon dating of metaigneous rocks using SHRIMP IIe/MC ion microprobe in the Micro-Analyses Laboratory, PGI-NRI in Warszawa, Poland, showed three main age populations. The age ca. 1.75 Ga is very common and was already noticed by previous authors (Johansson et al., 1995; Larionov et al., 1995; Johansson & Gee, 1999), while the ages of ca. 2.0 Ga and 1.38 Ga (Bazarnik et al., 2019) are somewhat unexpected. The detrital zircon provenance analyses were performed in the Arizona Laserchron Laboratory in Tucson, USA. The obtained detrital zircon spectra of the Mosselhalvøya Group and the Rittervatnet Unit of the Atomfjella Complex revealed many similarities in prominent peaks and broad spectra of lesser peaks and suggest comparable ca. 1.0 Ga depositional age. The age ca. 450 Ma reflects Caledonian peak metamorphism, whereas ca. 420 Ma marks the timing of major shearing. Additionally, the peak P-T conditions of metamorphism are similar in both units.

The presented results show that the Mosselhalvøya Group is a part of the metamorphic complex of the West Ny-Friesland terrane and the Mosselhalvøya Thrust has only local meaning. In light of this research, it can be concluded that the boundary between the two major terranes is located along the eastern margin of the Mosselhalvøya Group. Moreover, the obtained ages of metaigneous rocks are unique for the Svalbard archipelago and more similar to those reported from the crystalline basement of Northeast Greenland (e.g. Kalsbeek et al., 1999, 2008; Upton et al., 2005). This, in fact, suggests proximity of the West Ny-Friesland terrane to Northeast Greenland during pre-Caledonian time.

Acknowledgement: This research was supported by National Science Centre of Poland (grant no. 2015/19/N/ST10/02646) and the internal project of the Polish Geological Institute-NRI (61.2899.1601.00.0).

References:

Bazarnik, J., Majka, J., McClelland, W.C., Strauss, J.V., Kośmińska, K., Piepjohn, K., Elvevold, S., Czupyt, Z. & Mikuš, T. 2019. U-Pb zircon dating of metaigneous rocks from the Nordbreen Nappe of Svalbard's NyFriesland suggests their affinity to Northeast Greenland. Terra Nova, 31, 6, 518-526.

Gee, D.G. & Tebenkov, A.M. 2004. Svalbard: a fragment of the Laurentian margin. In: The Neoproterozoic Timanide Orogen of Eastern Baltica (D.G. Gee and V. Pease, eds). Geological Society of London, Memoir, 30, 191-206.

Johansson, Å. & Gee, D.G. 1999. The late Palaeoproterozoic Eskolabreen granitoids of southern Ny Friesland, Svalbard Caledonides – geochemistry, age and origin. Geol. Fören. Stockholm Förh., 121, 113-126.

Johansson, Å., Gee, D.G., Björklund, L. & Witt-Nilsson, P. 1995. Isotope studies of granitoids from the Bangenhuken Formation, Ny Friesland Caledonides, Svalbard. Geological Magazine, 132, 303-320.

Kalsbeek, F., Higgins, A.K., Jepsen, H.F., Frei, R., & Nutman, A.P. 2008. Granites and granites in the East Greenland Caledonides. In: The Greenland Caledonides: Evolution of the Northeast Margin of Laurentia (A.K. Higgins, J.A. Gilotti and M.P. Smith, eds). Geological Society of America Memoir, 202, 227-249.

Kalsbeek, F., Nutman, A.P., Escher, J.C., Friderichsen, J.D., Hull, J.M., Jones, K.A. & Pedersen, S.A.S. 1999. Geochronology of granitic and supracrustal rocks from the northern part of the East Greenland Caledonides: ion microprobe U–Pb zircon ages. Geology of Greenland Survey Bulletin, 184, 31-48.

Larionov, A.N., Johansson, Å., Tebenkov, A.M. & Sirotkin, A.N. 1995. U-Pb Zircon ages from the Eskolabreen Formation, southern Ny Friesland, Svalbard. Norsk Geologisk Tidsskrift, 75, 247-257.

Upton, B.G.J., Rämö, O.T., Heaman, L.M., Blichert-Toft, J., Kalsbeek, F., Barry, T.L. & Jepsen, H.F. 2005. The Mesoproterozoic Zig-Zag Dal basalts and associated intrusions of eastern North Greenland: mantle plume–lithosphere interaction. Contribution to Mineralogy and Petrology, 149, 40-56.

Witt-Nilsson, P., Gee, D.G. & Hellman, F.J. 1998. Tectonostratigraphy of the Caledonian Atomfjella Antiform of northern Ny Friesland, Svalbard. Norsk Geologisk Tidskrift, 78, 67-80.

Methane Emissions and Hard Coal Production in Budryk and Pniówek Mines in the Upper Silesian Coal (Poland)

MARCIN DREGER[1]

1 – University of Silesia, Faculty of Natural Sciences, Institute of Earth Sciences, Będzińska 60 str. Sosnowiec, Poland, e-mail: marcin.dreger@interia.pl

The research is focused on the variability of hard coal output and methane emission into coal workings and the atmosphere from the two most methane endangered coal mines in Poland – Budryk and Pniówek that are both operated by the Jastrzębie Coal Company. Hard coal production is much more complicated every year. Shallow-lying and easily extracted coal reserves have been mostly depleted. Reaching deeper coal seams is burdened by working in higher temperatures and methane threat that forces improvements of underground ventilation system to keep underground atmosphere free of methane and as cool as possible. Hard coal output has been decreasing every year in the Upper Silesia Coal Basin (USCB) – the biggest coal basin in Poland, due to economic changes in the country and natural hazards accompanying extraction at higher depths. During the year of research (2018), Polish mines extracted 63.4 million Mg of hard coal, which was two times less than twenty years ago (1998) (WUG, 2019). Methane emissions are one of the most dangerous hazards in Polish underground coal mining. During the year of research (2018), the absolute methane emission from all coal mines in the Upper Silesian Coal Basin exceeded 917 million m^3 of CH_4. Methane migrates into coal workings during extraction works and from overlying and underlying coal seams. Unfortunately, CH_4 is extremely flammable gas (with concentrations 5-15% CH_4 and >12% O_2) (Budryk, 1961). Single spark or open fire can ignite the gas and cause a catastrophic explosion. The Budryk mine is one of the youngest mines in Poland and one of the most prone to methane-associated risks. In 2016, the total CH_4 emission exceeded 140 million of m^3 (Fig.1a). This huge increase in methane emissions in coal workings is correlated with increased coal production and depth of exploitation (mining factors). The natural factors are presence of continuous, impermeable Miocene cover and high methane content in coal seams, which were deposited deeper in the geological past (Krause, 2019). On the other hand, in Pniówek mine (Fig.1b), the methane emission was largest at the beginning of the 1986-1991 research period. In the following years, emissions decreased to less than 140 million m^3, which are still one of the largest amounts emitted in the entire Upper Silesian Coal Basin.

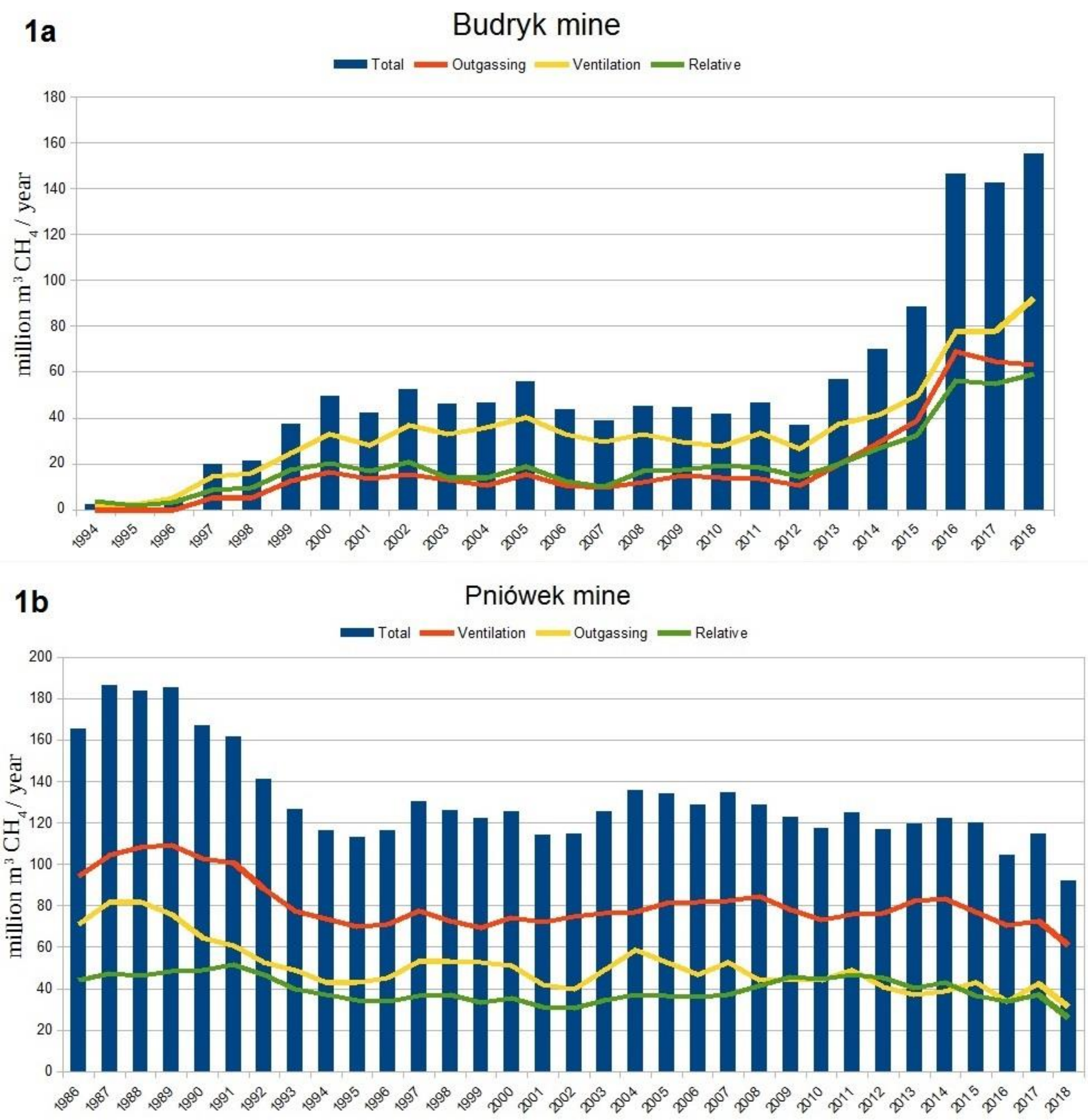

Figure 1. The methane emission in Budryk and Pniówek mines.

Acknowledgement: The author is grateful to the employees of Central Mining Institute in Katowice and authorities of Budryk and Pniówek coal mines for their kind cooperation and leads during data collection for the research.

References:

Budryk W. 1961. Wentylacja kopalń Wyd. Górniczo-Hutnicze, Katowice

Krause E., 2019. Zagrożenie metanowe w kopalniach węgla kamiennego. Wyd. GIG Katowice

WUG (State Mining Authority in Katowice) Statystyki Wypadków, available online June 2019 [http://www.wug.gov.pl/bhp/statystyki_wypadkow]

Ca-Al LDH obtained via transformation of limestone powder and aluminium can for Cr(VI) removal in single-element system and in the presence of competitive anion

JUSTYNA HAŁABUZA[1], KAROLINA RYBKA[1]

1 – Department of Mineralogy, Petrography and Geochemistry, Faculty of Geology, Geophysics and Environmental Protection, AGH University of Science and Technology, al. Mickiewicza 30, 30-059, Cracow, Poland, justynahalabuza126@gmail.com; krybka@agh.edu.pl

Layered Double Hydroxides (LDH) are a large class of materials with general formula $[M^{II}_{1-x}M^{III}_{x}\ OH_2]^{x+}\ [A^{n-}]_{x/n} \cdot y\ H_2O$ that are built of layers comprising divalent (Ca, Mg, Mn, Fe, Co, Ni, Cu, Zn) and trivalent (Al, Li, Fe) metal cations, and easily exchangeable anions (Cl^-, Br^-, NO_3^-, CO_3^{2-}, SO_4^{2-}, SeO_4^{2-}) in the interlayer space. Their most interesting properties are high anion exchangeability, compositional flexibility and biocompatibility. Those materialscan be applied as adsorbents in wastewater treatment, but also utilized in catalysis, separation, biomedicine, drug delivery and other environmental applications (Mishra *et al.*, 2018). Their synthesis can be easily carried out under laboratory conditions. However, many past studies have focused on using metal precursors different from the chemical reagents (e.g. minerals, wastes, brine water) in order to lower the price of the final material. The aim of the project is to investigate the affinity of Ca-Al LDH towards Cr(VI), in a single element system, and in the presence of a competitive chloride anion. Hexavalent chromium anions are frequent component of the wastewater derived from the tannery industry, for instance, in the Podhale region of Poland (Nowobilska-Luberda *et al.*, 2013). The increased concentration of this anion in the water may cause cancer and inflammation of stomach and intestines.

Materials were synthesized by a co-precipitation method with a constantly controlled pH set to 10.5 using aqueous solution of 5 M NaOH. A limestone powder (LP) was used as a source of Ca^{2+}, and aluminum can (AC) was used as a source of Al^{3+}. Prior to the synthesis, LP was dissolved in pure HCl, and AC was dissolved in 3 M NaOH. Afterwards, the Ca^{2+} solution was added dropwise to the Al^{3+} solution. The obtained precipitate was aged for 24h, washed with redistilled water and dried at 60˚C. The influence of ageing time was investigated by probing the precipitate and characterizing materials right after the synthesis and at intervals of 1h and 24h of ageing. Obtained materials were analyzed by the X-ray diffraction (XRD), scanning electron microscopy (SEM) and Fourier Transformed Infrared Spectroscopy (FTIR). The adsorption experiments were performed at adsorbent dose equal to 5 g/L. The aqueous solutions of $K_2Cr_2O_7$ and NaCl were used as a source of Cr(VI) and Cl^-, respectively. The single-element adsorption experiment was performed at Cr(VI) concentration ranged from 0.04 to 20 mM/L. The adsorption experiment with the competitive chloride anion was performed at Cr(VI) concentration equal to 20 mM and Cl^- concentration equal to 0.1 M. Concentration of Cr(VI) was determined by the 1,5-Diphenylcarbazide colorimetric method for both experiments.

Diffractograms of synthesized material showed an instant precipitation of the LDH phase with other admixtures: portlandite $Ca(OH)_2$ and hydrophilite $CaCl_2$. After 1 h of ageing, peaks for portlandite and hydrophilite were of lower intensity and no peaks for portlandite were observed after 24 h of ageing. The FTIR spectra showed that water (1630 cm^{-1}) and hydrocarbonates HCO_3^- (1410 cm^{-1}) were present in the structure. Moreover, the LDH lattice vibrations in the position of 533 and 422 cm^{-1} were observed. The SEM observations showed the morphology of the materials: hexagonal plates up to 1 μm in diameter of LDH and nanometrical crystals of hydrophilite and portlandite. The adsorption experiments showed that all materials effectively removed Cr(VI) from all the solutions. Sorption efficiency was increasing with the increasing Cr(VI) concentration and reached 1600 mmol/kg. The pH value increased significantly from 4.6 before adsorption to 11.6 afterwards. Competitive anion increased the removal of Cr(VI) up to 3000 mmol/kg. The XRD patterns of materials after adsorption experiment in single-element system revealed that LDH dissolved since characteristic peaks of this phase were no longer observable. Moreover, characteristic reflections of other Ca-, Al- bearing phases were noticed which indicated the recrystallization of LDH. However, the XRD pattern of LDH after adsorption of Cr(VI) in the presence of Cl^- revealed that the structure of LDH remained unchanged, but reflections of a new Ca-, Al- phases were also observed.

The results showed that the transformation of LP and AC into Ca-Al LDH is possible. Moreover, they are good scavengers of Cr(VI). However, their stability and sorption efficiency is even better in presence of chlorides.

Acknowledgement: We are grateful to dr hab. inż Maciej Manecki, prof AGH for scientific support and performing SEM analysis. Some of the analyses were financed by the decision of the Dean of the Faculty of Geology, Geophysics and Environmental Protecion, no. 1/KW/XII/2019.

References:

Mishra, G., Dash, B., Pandey, S. 2018. Layered double hydroxides: A brief review from fundamentals to application as evolving biomaterials. *Applied Clay Science*, 153, 172–186. doi:10.1016/j.clay.2017.12.021

Nowobilska-Luberda, A., Nowobilska, E., Satora, S. 2013. Chromium ions in wastewater and bottom sediments in the Podhale Area. *Acta Scientiarum Polonorum, Formatio Circumiectus*, 12, 2, 73–82.

Microorganisms in the age of Dinosaurs

JAN HINKELMAN[1]

1 – Institute of Zoology, Slovak Academy of Sciences, Dúbravská cesta 9, 845 06 Bratislava, Slovakia jan.hinkelman@savba.sk

Microorganisms in Myanmar amber are rare with only 20 genera and 21 species of protozoa (Poinar 2008, 2009, 2010, 2016; Poinar and Poinar 2004; Poinar and Vega 2019; Ross 2019), one species of alphaproteobacteria (Poinar, 2014) and pathogens (Poinar and Poinar, 2005) described so far. Poinar and Telford (2005) documented a parasitic protozoan (Plasmodiidae) from the abdominal cavity of a female biting midge (Diptera: Ceratopogonidae). Similarly, parasitic flagellates were documented in a sand fly (Diptera). Both parasites were associated with numerous sporozoites, characteristic of malaria parasites, suggesting that these flies served as vectors for this disease (Poinar and Poinar 2004; Poinar and Telford 2005; Poinar 2008). Poinar (2009) described two cockroaches from Myanmar amber with protists preserved in their abdominal cavity. These protists are related to mutualistic flagellates that occur in extant *Cryptocercus* cockroaches and lower termites (Poinar, 2009) and evidence an already established endosymbiotic relationships during Early Cretaceous. Gregarines, gut inhabiting parasitic microorganisms, were also recorded from Myanmar amber (Poinar, 2010) as well as Eccrinales (Mesomycetozoea) (Poinar, 2016) and cellular slime-mold (association of unrelated, free-living, single-celled eukaryotes) (Poinar and Vega, 2019).

Bacteria in Myanmar amber are rare, with one record of Rickettsial-like (Rickettsiaceae) bacterial cells found within the body cavity of a larval tick (Poinar, 2014). Its shape and size closely resemble extant members of Rickettsiaceae found in ticks. Evidence of pathogens within Myanmar amber has been found in the form of lytoplasmic polyedrosis virus and trypanosomid infection in an adult bitting midge (Poinar and Poinar 2005) and DWV-Iflavirus recorded from a cockroach (Vršanský et al., 2019). Nuclear polyedrosis virus was also detected in a sand fly (Poinar and Poinar, 2005).

Symbiotic protozoan bacteria and other microorganisms are generally rare in amber. Such microorganism assemblages or „microcenoses" can be valuable in determining their ecology as well as their evolution.

References

Poinar, G.O. 2009. Early Cretaceous protist flagellates (Parabasalia: Hypermastigia: Oxymonada) of cockroaches (Insecta: Blattaria) in Burmese amber. *Cretaceous Research* 30, 1066–1072.

Poinar, G.O. 2008. *Leptoconops nosopheris* sp. n. (Diptera: Ceratopogonidae) and *Paleotrypanosoma burmanicus* gen. n., sp. n. (Kinetoplastida: Trypanosomatidae), a biting midge - trypanosome vector association from the Early Cretaceous. *Memórias do Instituto Oswaldo Cruz*, 103, 468–471.

Poinar, G.O. 2010. Gregarine infections in insects. In: Fossil Behavior Compendium (Boucot and Poinar, eds.) 54–56 (CRC Press, Boca Raton).

Poinar, G.O. 2014. Rickettsial-like cells in the Cretaceous tick, *Cornupalpatum burmanicum* (Ixodida: Ixodidae). *Cretaceous Research* 52, 623–627.

Poinar, G.O. 2016. What fossils reveal about the Protozoa progenitors, geographic provinces, and early hosts of malarial organisms. *American Entomologist*, 62, 22–25.

Poinar, G.O. & Vega F.E. 2019. Mid-Cretaceous cellular slime mold (Eukarya: Dictyostelia?) in Burmese amber. *Historical Biology*

Book of abstracts. ISBN 978-83-933330-2-8

Poinar, G.O. & Poinar, R. 2004. *Paleoleishmania proterus* n. gen., n. sp., (Trypanosomatidae: Kinetoplastida) from Cretaceous Burmese amber. *Protist*, 155, 305–10.
Poinar, G.O. & Telford, S.R. 2005. *Paleohaemoproteus burmacis* gen. n., sp. n. (Haemospororida: Plasmodiidae) from an Early Cretaceous biting midge (Diptera: Ceratopogonidae). *Parasitology*, 131, 79–84.
Poinar, G.O. & Poinar R. 2005. Fossil evidence of insect pathogens. *Journal of Invertebrate Pathology* 98, 243-250.
Ross, A.J. 2019. Burmese (Myanmar) amber taxa, on-line checklist v.2019.1. http://www.nms.ac.uk/explore/stories/natural-world/burmese-amber Accessed 25 May 2019
Vršanský, P. et al. 2019. Pathogenic DWV infection symptoms in a Cretaceous cockroach. *Palaeontographica Abteilung A Palaeozool-Stratigr* 314, 1–10.

Rare earth elements distribution vs. crystallographic orientation in fluorapatite

MACIEJ JARANOWSKI[1,2], BARTOSZ BUDZYŃ[2], GRZEGORZ RZEPA[1], GABRIELA A. KOZUB-BUDZYŃ[1], ZBIGNIEW SAWŁOWICZ[3]

1 – AGH University of Science and Technology, Faculty of Geology, Geophysics and Environmental Protection, al. Mickiewicza 30, PL–30059 Kraków, Poland; m.d.jaranowski@gmail.com; gprzepa@cyf-kr.edu.pl; lato@agh.edu.pl
2 – Institute of Geological Sciences, Polish Academy of Sciences, Research Centre in Kraków, Senacka 1,PL–31002 Kraków, Poland; ndbudzyn@cyf-kr.edu.pl
3 – Institute of Geological Sciences, Jagiellonian University, Gronostajowa 3a, PL–30387 Kraków, Poland; zbigniew.sawlowicz@uj.edu.pl

The Ca phosphate apatite [$Ca_5(PO_4)_3(F,Cl,OH)$], a solid solution of fluorapatite, chlorapatite and hydroxyapatite, is a common accessory mineral in igneous and metamorphic rocks and one of the main hosts of rare earth elements (REE). Its atomic framework allows substitutions of variety of components and causes extreme diversions in its chemical composition (Pan and Fleet, 2002; Hughes and Rakovan, 2015). Apatite is broadly used as a thermochronometer using various isotopic systems offering a wide range of closure temperatures (Chew and Spikings, 2015). The complexity of apatite provides opportunity to investigate metasomatic processes and composition of the fluids (Harlov, 2015). Particularly interesting for current work is the differential distribution of REE with respect to crystallographic orientation in apatite crystal, which has been previously reported in fluorapatites from Llallagua, Bolivia and Golconda Mine, Minas Gerais, Brasil (Rakovan and Reeder, 1996).
In this study we investigate distribution of the REE in three crystals of fluorapatite from Panasqueira mine, Covilha, Castelo Branco (Portugal), Yates mine, Otter Lake, Quebec (Canada) and Cerro de Mercado mine, Durango (Mexico). These fluorapatites were selected based on the large size and gem-quality of the crystals (2–4.3 cm in size), different environments of their crystallization and expected moderate to high concentrations of REE.
The fluorapatite crystals were cut using slow rotating diamond saw to expose sections parallel and perpendicular to the *c*-axis. The internal textures were preliminarily imaged using CITL (UK) "cold cathode" cathodoluminescence (CL) device, model CLmk3A coupled to an optical microscope with attached Nikon Eclipse 50i camera. The backscattered electrons (BSE) imaging and chemical analyzes of apatite were performed using a JEOL SuperProbe JXA-8230 electron microprobe equipped with five wavelength dispersive spectrometers. Two different setups were used: (1) 15 kV, 5 nA, 8 μm spot size for analyzes focused on light elements (primarily volatiles); and (2) 15 kV, 40 nA and 5 μm spot size for complete compositional analyzes of fluorapatite. The EPMA measurements were performed in traverses parallel and perpendicular to *c*-axis. Qualitative analyzes of volatiles (CO_3, OH, H_2O) were conducted using a Thermo Scientific DXR Raman Microscope with a 900 grooves/mm grating, a CCD detector, and an Olympus 10× objective (with a spot size of ca. 2.1 μm). A 532 nm diode laser with a maximum power of 10 mW was the excitation source.
The CL and BSE imaging revealed growth zonation and irregular zones adjacent to cracks or inclusions in the Panasqueira fluorapatite. The Otter Lake fluorapatite demonstrates weak growth zoning, distinct subsector zoning, and irregular zones along cracks and inclusions of secondary phases. The Durango fluorapatite displays weak growth zoning. Preliminary EPMA

Book of abstracts. ISBN 978-83-933330-2-8

measurements reveal significant compositional differences between investigated fluorapatites. The Durango fluorapatite (1.01–1.80 REE_2O_3 wt.%) is compositionally homogeneous with slight decrease of Ce, Y, Si and Na contents in the outermost rim. In contrast, the Panasqueira fluorapatite, with lesser amounts of REE (0.04–1.14 REE_2O_3 wt.%), demonstrates significant increase of Ce, Y, Na and Si in the rims along traverses perpendicular to *c*-axis. Furthermore, the Panasqueira fluorapatite also demonstrates significant zoning in Sr and Mn, which partially correlate with variations in Ca distribution. The highest concentrations of REE occur in the Otter Lake fluorapatite, i.e. 1.12–2.44 wt.% REE_2O_3. Distribution of Ce, La, Y, Si and Na in the Otter Lake crystal demonstrates increase in the rims, with notable increase of Y content in the rim across central section of the crystal (perpendicular to *c*-axis). Micro-Raman spectroscopy results indicate presence of OH and CO_3 in the investigated fluorapatites.
In summary, a diverse distribution of Y and LREE that partially depends on the crystallographic orientation was determined in the Panasqueira and Otter Lake fluorapatites. Future works will involve LA-ICP-MS trace elements analysis to evaluate relative relations of LREE vs. HREE distribution with respect to crystallographic orientation.

Acknowledgements: The fluorapatite crystals were purchased from Dan Weinrich (Weinrich Minerals, Inc., Grover, Missouri, USA). This work was partially supported by the ING PAN Research Funds (project "Orogen"; to B.B.).

References:

Chew, D.M. & Spikings, R.A. 2015. Geochronology and thermochronology using apatite: time and temperature, lower crust to surface. *Elements*, 11, 3, 189–194.

Harlov, D.E. 2015. Apatite: a fingerprint for metasomatic processes. *Elements*, 11, 3, 171–176.

Hughes, J.M. & Rakovan, J.F. 2015. Structurally robust, chemically diverse: apatite and apatite supergroup minerals. *Elements*, 11, 3, 165–170.

Pan, Y. & Fleet, M.E. 2002. Compositions of the Apatite-Group Minerals: Substitution Mechanisms and Controlling Factors. *Reviews in Mineralogy and Geochemistry*, 48, 1, 13–49.

Rakovan, J. & Reeder, R.J. 1996. Intracrystalline rare earth element distributions in apatite: Surface structural influences on incorporation during growth. *Geochimica et Cosmochimica Acta*, 60, 22, 4435–4445.

A step towards better reconstruction of smelting temperatures: the case of historical Cu-slags from the Old Copper Basin, Poland

KATARZYNA KĄDZIOŁKA[1], ANNA PIETRANIK[1], JAKUB KIERCZAK[1], ANNA POTYSZ[1], TOMASZ STOLARCZYK[2]

1 – Institute of Geological Sciences, University of Wroclaw, Pl. Maksa Borna, 50-204 Wrocław, Poland, katarzyna.kadziolka2@uwr.edu.pl, anna.pietranik@uwr.edu,pl, jakub.kierczak@uwr.edu.pl, anna.potysz@uwr.edu.pl
2 – Museum of Copper, Partyzantów 3, 59-220 Legnica, Poland, archeologia@muzeum-miedzi.art.pl

Historical smelting is often preserved only in the form of pollution present in the area (e.g. Kierczak *et. al.*, 2013), as well as in the form of slags. For archaeometallurgical research, slags constitute a valuable research material containing information about the ore and pyrometallurgical process (Ettler *et. al.*, 2009; Kierczak and Pietranik, 2011). The process changed over the years, especially concerning types of furnaces. It resulted in the evolution of smelting parameters, in particular of the temperature, a crucial factor controlling the efficiency of metal separation from ore. Currently, heat in the furnace is properly supervised, but it has been that way only for the last 50-100 years. The recognition detailed temperatures for historical smelting allows to globally track the development of technology and when applied to common smelting remains, such as slags, it becomes a powerful tool for archaeometallurgy. However, current methods of temperature estimations are highly imprecise, not considering complexity of chemical composition (Manasse and Mellini, 2002; Costagliola et. al., 2008) and the lack of equilibrium during cooling (Álvarez-Valero et. al., 2009). We conducted detailed geochemical study of slags from the Old Copper Basin in order to establish reliable tool for future thermochemical research.

The Old Copper Basin is located in southwestern Poland, in the western part of Sudety Mountains, Kaczawskie Foothills region, south-eastern margin of the North Sudetic Basin. In the 20th century, the area was named the Old Copper Basin (OCB) in reference to Cu-mineralization and its historical mining. The exploitation of Cu-ore shales and marls of the Zechstein Kupferschiefer formation has been conducted on a small scale for several centuries since the beginning of the 16th century. Similarly, metal smelting was established repeatedly but was most successful in 19th century with Stilles Glück smelter, working in Leszczyna with a mine of the same name (Site 1A). Four sites were selected for this study, two related to the smelters activity and of a known age (Site 1A (19th century), Site 2A (oldest – 18th century)) and two located in a close proximity but of unknown ages (1B, 2B).

We applied numerus chemical and mineral phase diagrams, Px-WR geothermometry, thermodynamical modelling with MELTS software and experimental thermal XRD to recognize the temperature of slag creation (Kądziołka et. al., 2019). A statistically important difference was noted for samples from Site 1B which presented smelting (liquidus) temperatures nearly 200°C higher than the remaining set. This reflects differences in chemistry, especially in total SiO_2 (lower) and CaO (higher) concentration resulting from more effective pyrometallurgical processes. Slags from Sites 1A and 2B presented slightly lower smelting temperatures (1210°C) than older slags from Site 2A (1225°C). The implication is that two main smelters – Stilles Glück (Site 1A, 2B) and Kondratów smelter (2A) led similar smelting processes with no distinct technological predominance despite the age difference.

With an example of slags from the OCB we were able to estimate smelting (liquidus), steady-state crystallization and near-solidus temperatures, presenting almost a full thermal history of slags form selected sites. We discovered that the age of analysed materials was ambiguously associated with temperature. Our research provides the following insights regarding temperature reconstructions: (1) commonly used methods such as chemical and mineral phase diagrams usually fail to provide reliable liquidus temperature estimations as slags represent chemically complex systems crystallizing in disequilibrium conditions, (2) application of thermodynamical modelling allows to achieve statistically reliable and detailed liquidus temperatures as all major elements, redox conditions and atmospheric pressure are included in calculations, (3) attention should be paid to both bulk and glass chemical composition as they may record various temperatures where bulk composition is the closest to the initial melt composition and constitutes a base for reconstruction of liquidus temperature. Glass composition, however, provides melts composition on the initial stage of crystallization. (4) various geothermometers allow to investigate following stages of crystallization and analyse cooling conditions of slag samples.

Acknowledgement: This research was supported by the Polish Ministry of Sciences and Higher Education within Diamentowy Grant (decision: DI2015 023345) with funds for science in 2016-2018.

References:

Álvarez-Valero, A.M., Pérez-López, R., Nieto, J.M. 2009. Prediction of the environmental impact of modern slags: A petrological and chemical comparative study with Roman age slags. *American Mineralogist* 94, 1417–1427.

Ettler, V., Červinka, R., Johan, Z. 2009. Mineralogy of medieval slags from lead and silver smelting (Bohutín, Příbram district, Czech Republic): towards estimation of historical smelting conditions. *Archaeometry*, 51, 6, 987–1007.

Kądziołka, K., Pietranik, A., Kierczak, J., Potysz, A., Stolarczyk, T., 2019. Towards better reconstruction of smelting temperatures: methodological review and the case of historical K-rich Cu-slags from the Old Copper Basin, Poland. *Journal of Archaeological Science,* in press.

Kierczak, J. & Pietranik, A. 2011. Mineralogy and composition of historical Cu slags from the Rudawy Janowickie Mountains, Southwestern Poland. *Canadian Mineralogist* 49, 1281–1269.

Kierczak, J., Potysz, A., Pietranik, A., Tyszka, R., Modelska, M., Néel, C., Ettler, V., Mihaljevič, M. 2013. Environmental impact of the historical Cu smelting in the Rudawy Janowickie Mountains (southwestern Poland). *Journal of Geochemical Exploration* 124, 183–194.

Manasse, A. & Mellini, M. 2002. Chemical and textural characterisation of medieval slags from the Massa Marittima smelting sites (Tuscany, Italy). *Journal of Cultural Heritage* 3, 187–198.

Apatite challenge – synthesis of Ca–mimetites

AGNIESZKA KAMIŃSKA[1], PIOTR MOSUREK[1], SAMANTA PROKOP[2] and BARTOSZ PUZIO[1]

1 - *AGH University of Science and Technology, Department of Mineralogy, Petrography and Geochemistry; Kraków, Poland; agnieszka.d.kaminska@gmail.com*
2 - *AGH University of Science and Technology, Faculty of Metal Engineering and Industrial Computer Science; Kraków, Poland*

The crystallographic properties of apatites allow a number of isomorphic substitutions (Pan and Fleet, 2002). This controls its thermodynamic stability (Puzio et al., 2018) which determines their various applications, for example as the environmentally inert catalysts (Masaoka and Kyono, 2006) or as the metal sequestration agents in water treatment and contaminated soil remediation (Ma et al., 1993; Cotter–Howells, 1996; Chen et al., 1997; Bajda, 2010). There is thus a need for better understanding of phases that govern the mobility of As, F, Br and I in the environment. Mimetite is a mineral which belongs to the apatite supergroup. The members of this subgroup can precipitate from Pb–As contaminated waters (Inegbenebor et al., 1989; Flis et al., 2011). Such processes are of considerable interest to mineralogists and environmental geochemists. Although the crystal structure of mimetite group minerals is well known, their Ca members are poorly studied. Therefore this research was conducted (1) to synthesize five analogs of calcium arsenates: svabite - $Ca_5(AsO_4)_3F$, johnbaumite - $Ca_5(AsO_4)_3OH$, turneaureite - $Ca_5(AsO_4)_3Cl$, and two other phases which existence in nature is not confirmed: $Ca_5(AsO_4)_3Br$ and $Ca_5(AsO_4)_3I$; (2) to determine the effects of halogen substitution on the structural parameters of Ca-As bearing apatites; (3) to determine the regularity of characteristic bands shifting in IR and Raman spectra for phases in question. These new findings will serve as important source of basic knowledge for future research including thermodynamic studies, water treatment procedures and management of As-bearing hazardous materials and wastes.

A series of As substituted Ca-apatites was prepared using aqueous precipitation method (Baker et al., 1966). The synthesis of pure johnbaumite and turneaureite analogs was performed by dropwise addition of aqueous solutions of $Pb(NO_3)_2$ and $Na_2HAsO_4{\cdot}7H_2O$. The Pb/As and As/X (where X: Cl) molar ratios in the mixed solutions were maintained at 1.67 and 3.00, respectively. The johnbaumite and turneaureite were synthesized at ambient conditions: pH 11.5, T=75°C and pH 4.5, T=25°C respectively under air atmosphere. The solutions (prepared with re-distilled water) were added at a rate of 2 mL/min, and the pH was maintained constant using 1 M solution of NH_4OH or HNO_3. After the completion of synthesis, the suspensions were aged for 72 h, then centrifuged, and washed with re-distilled water. The turneaureite was also synthesized by modified flux-melt methods (Narasaraju et al., 1982; Weil et al., 2009). Stoichiometric mixture of synthetic johnbaumite and $CaCl_2$ was placed in ceramic crucible and heat-treated in a muffle furnace to 870°C, held at this temperature for 8 h. Then the furnace was switched off and the crucible was removed at room temperature. The samples were analyzed by powder X-ray diffraction (PXRD), Fourier-transformed infrared spectroscopy (FTIR), Raman spectroscopy, and scanning electron microscopy with energy dispersive spectroscopy (SEM-EDS).

The synthesis of johnbaumite resulted in the precipitation of very fine, white powders within 2h. The SEM imaging indicated that the product was exclusively made of aggregates with individual crystals in the form of elongated rods. The particles had a maximum size of ~1 μm.

The positions of the diffraction peaks corresponded to johnbaumite (JCPDS: 33-0265). The position of an intense reflection (211) at 33.19° 2θ for johnbaumite is in very good agreement with the previous study (Puzio et al., 2018). Unfortunately, the turneaureite synthesis by wet method failed. During the synthesis no precipitate was visually observed.
Afterwards the synthesis of turneaureite was done by applying the modified flux-melt method. Unfortunately, this approach also failed. PXRD results indicated the crystallization of the intermediate phase between pure johnbaumite and turneaureite, which is possible due to the ability of apatites to form solid solutions (Hughes et al., 2016). Currently, the research group is trying to optimize the temperature and heating time to obtain a pure, synthetic analog of turneaureite. This is a key goal to start the next synthesis of Ca-mimetites with different halogen substitutions.

Acknowledgement: We would like to thank Professor M. Manecki for valuable advices regarding syntheses experiments and help in SEM - EDS analyzes. The project and B. Puzio was financed with resources of the National Science Centre of Poland, granted based on decision no. 2017/27/N/ST10/00776.

References:

Bajda, T. 2010. Solubility of mimetite $Pb_5(AsO_4)_3Cl$ at 5–55 °C. *Environmental Chemistry*, 7, 268–278.

Baker, W.E. 1966. An X-ray diffraction study of synthetic members of the pyromorphite series. *American Mineralogist*, 51, 1712–1721.

Chen, X., Wright, J.V., Conca, J.L. & Peurrung, L.M. 1997. Evaluation of heavy metal remediation using mineral apatite. *Water Air Soil Pollution*, 98, 57–78.

Cotter-Howells, J. 1996. Lead phosphate formation in soils. *Environmental Pollution*, 93, 9–16.

Flis, J., Manecki, M. & Bajda, T. 2011. Solubility of pyromorphite $Pb_5(PO_4)_3Cl$–mimetite $Pb_5(AsO_4)_3Cl$ solid solution series. *Geochimica et Cosmochimica Acta*, 75(7), 1858-1868.

Hughes, J. M., Harlov, D., Kelly, S. R., Rakovan, J. & Wilke, M. 2016. Solid solution in the apatite OH-Cl binary system: Compositional dependence of solid-solution mechanisms in calcium phosphate apatites along the Cl-OH binary. *American Mineralogist*, 101(8), 1783-1791.

Inegbenebor, A. I., Thomas, J. H. & Williams, P. A. 1989. The chemical stability of mimetite and distribution coefficients for pyromorphite–mimetite solid-solutions. *Mineralogical Magazine*, 53(371), 363-371.

Ma, Q.Y., Traina, S.J., Logan, T.J. & Ryan, J.A. 1993. In situ lead immobilization by apatite. *Environmental Science & Technology*, 27, 1803–1810.

Masaoka, M. & Kyono, A. 2006. Single crystal growth of lead vanado-chlorapatite $Pb_5(VO_4)_3Cl$ using CsCl flux method. *Materials Letters*, 60, 3922–3926.

Narasaraju, T., Lahiri, P., Yadav, P. & Rai, U. 1982. Solid solution series of hydroxyl and chlorapatites of arsenic–preparation and characterization. *Current Science*, 51, 16, 772–774.

Pan, Y. & Fleet, M.E. 2002. Compositions of the apatite-group minerals: substitution mechanisms and controlling factors. *Reviews in Mineralogy and Geochemistry*, 48, 13–49.

Puzio, B., Manecki, M. & Kwaśniak – Kominek, M. 2018. Transition from endothermic to exothermic dissolution of hydroxyapatite $Ca_5(PO_4)_3OH$ - johnbaumite $Ca_5(AsO_4)_3OH$ solid solution series at temperatures ranging from 5 to 65°C. *Minerals*, 8, 7, 281–302.

Weil, M., Đorđević, T., Lengauer, C. L. & Kolitsch, U. 2009. Investigations in the systems Sr–As–O–X (X= H, Cl): Preparation and crystal structure refinements of the anhydrous arsenates (V) $Sr_3(AsO_4)_2$, $Sr_2As_2O_7$, α-and β-$SrAs_2O_6$, and of the apatite-type phases $Sr_5(AsO_4)_3OH$ and $Sr_5(AsO_4)_3Cl$. *Solid State Sciences*, 11, 12, 2111–2117.

Polished secondary slickensides close to a major brittle fault zone in the Obir Caves (Periadriatic Fault System, Austria)

STEFANIE J. KOPPENSTEINER[1], HARALD BAUER[2], LUKAS PLAN[3] and BERNHARD GRASEMANN[1]

1 – Department of Geodynamics and Sedimentology, University of Vienna, Althanstraße 14, 1090 Vienna, Austria, s.j.koppensteiner@gmail.com
2 – Koralm Tunnel, contract section KAT3, PORR Bau GmbH, Absberggasse 47, 1100 Vienna, Austria
3 – Karst and Cave Group, Natural History Museum Vienna, Museumsplatz 1/10, 1070 Vienna, Austria

The seismogenic ESE-trending Periadriatic Fault System is the border between the Eastern and the Southern Alps (Schönlaub and Schuster, 2015). The Obir Caves are located just to the north in the Hochobir massif, which is built up of Middle Triassic Wetterstein limestone and dolostone and part of the Northern Karavanke Mountains in Austria. This study investigates polished slickensides combining microstructural observation with field data from inside and outside the cave. A special emphasis is put on detailed microstructural description of the mirror-like fault surfaces using thin section analysis, high-resolution mosaics of photomicrographs, SEM, CL and surface topography.

We observed perfectly preserved mirror-like fault surfaces on a block between two major slickensides of a left-lateral NE-SW striking strike-slip fault. The observation area at the bottom of the block covers two sides with a dimension of about five by five by four meters. Two slickensides, which both show a height of about 5 meters and a length of several meters, delimit the block.

Observations revealed distinct differences of the mirror-like fault surfaces in the cave: There is a random distribution concerning size (from a few centimeters up to one meter in length), spatial orientation and lineation where adjacent polished surfaces show different lineation directions. The polishing varies from none to highly-reflective and the surfaces can be even, bent, corrugated or rarely rough. Varying combinations of these properties occur at the outcrop. We distinguished five different colours of ultracataclasite (dark yellow, beige-coloured yellow, pale yellow, white and reddish-brown). Truncated grains along the fault surfaces differ in accumulation and size (up to a few millimeters). Some fault surfaces exhibit speleothem overgrowth, which covers parts of the polishing.

We classified the range of polishing of the fault surfaces into five different grades from none to highly-reflective. This classification of fault surfaces inside the cave compared with their spatial orientation shows that there is no relationship between the degree of polishing and fault orientation. The fault surfaces occur in the cave as a polishing of the host rock or at the boundaries to and within associated cataclastically deformed brittle fault zones, which consist of ultracataclasite with small host rock fragments up to 5 millimeters in size. Partly polished slickensides

Book of abstracts. ISBN 978-83-933330-2-8

and brittle fault zones at the cave entrance and on the eastern slope of the Hochobir massif where the fault zone localizes in shattered dolomitic rocks, show similar kinematics and spatial orientation to the faults inside the Obir Caves.

Thin section analysis classified the mirror-like fault surfaces as principal slip surfaces because of the knife-sharp localization in zones of ultracataclasites. Cataclastic grains are truncated along the principal slip surfaces and along secondary Riedel faults. Besides the undeformed host rock four different stages (I-IV) of cataclastic deformation can be distinguished: (I) Isolated fractures in the host rock with injected ultracataclastic material, (II) dilation cataclasites containing jigsaw breccia, (III) ultracataclasite with angular-to-rounded host rock fragments and jigsaw breccia and also (IV) ultracataclasite with isolated clasts and truncated grains close to the mirror surfaces. After Smith et al. (2011) the identified cataclastic deformed stages I to IV correspond to slip zones, which all contain varying amounts of cataclasites and ultracataclasites. Fondriest et al. (2013) and Smeraglia et al. (2017) described truncated clasts at mirror-like slip surfaces as results of seismic slip rates.

The microstructures including polished slickensides, injected cataclasites and truncated grains along principal slip surfaces as well as the geological position close to the seismogenic Periadriatic Fault System suggest that the investigated fault surfaces in the Obir Caves formed during seismic slip.

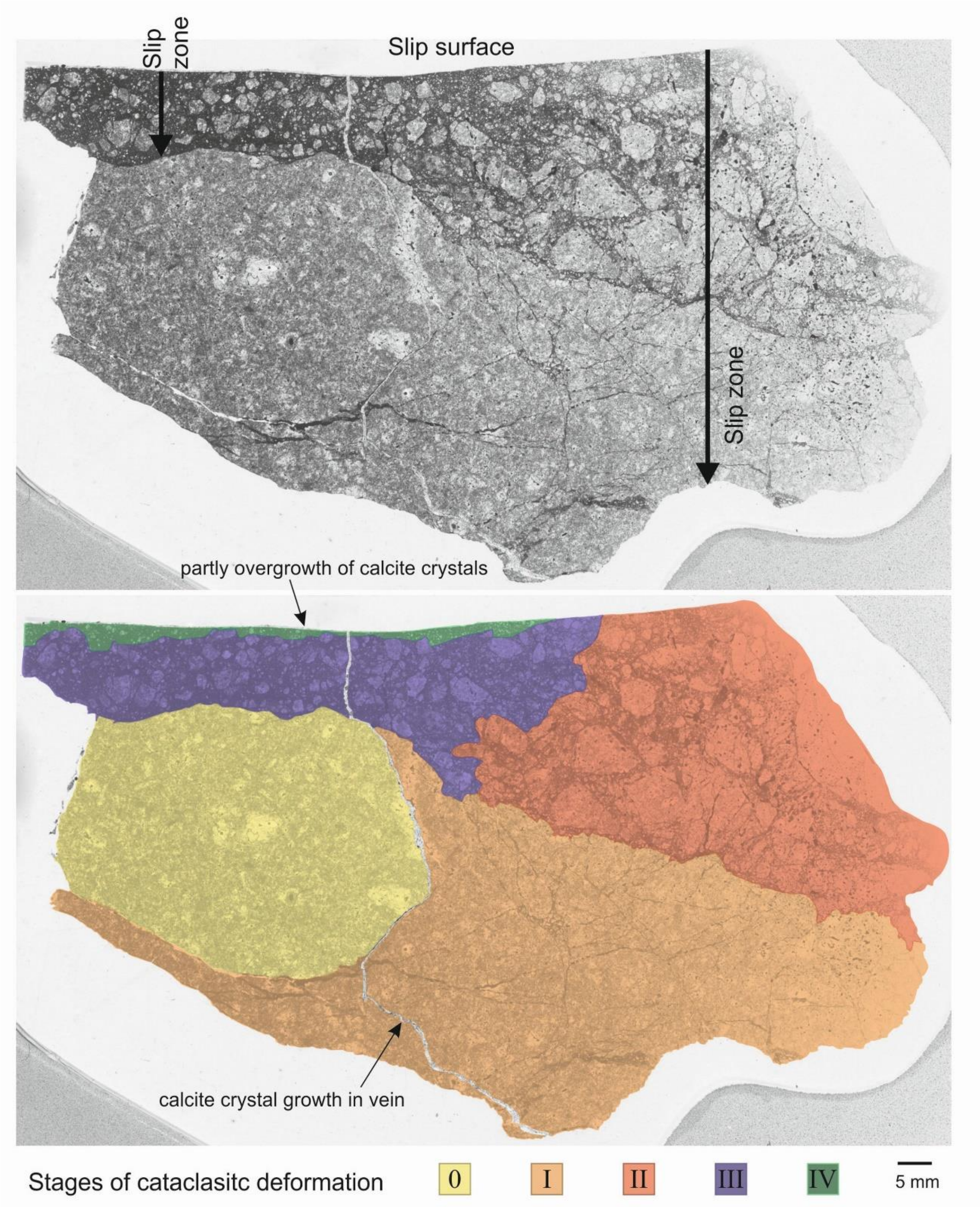

Figure 1. Thin section of a polished slickenside from the Obir Caves. Besides the undeformed host rock (0) four different stages of cataclastic deformation (I-IV) can be distinguished as described in the abstract. Calcite crystals on the slip surface as well as in the main vein are uncoloured.

References

Fondriest, M., Smith, S.A.F., Candela, T., Nielsen, S.B., Mair, K. and Di Toro, G. 2013. Mirror-like faults and power dissipation during earthquakes. *Geology*, 41, 1175–1178.

Schönlaub, H.P., Schuster, R. 2015. Die Zweiteilung der Karawanken und ihre erdgeschichtliche Entwicklung. *Geologische Bundesanstalt*, Wien.

Smeraglia, L., Bettucci, A., Billi, A., Carminati, E., Cavallo, A., Di Toro, G., Natali, M.., Passeri, D., Rossi, M. and Spagnuolo, E. 2017. Microstructural evidence for seismic and aseismic slips along clay-bearing, carbonate faults. *J. Geophys. Res. Solid Earth*, 122, 3895–3915.

Smith, S.A.F., Billi, A., Toro, D.G. & Speiss, R. 2011. Principal slip zones in Limestone: microstructural characterization and implications for the seismic cycle (Tre Monti Fault, Central Apennines, Italy). *Pure and Applied Geophysics*, 168, 12, 2365–2393.

Do lichens eat rocks?
The search for probable biomineralized metal oxalates

VIKTÓRIA KRAJANOVÁ[1]

1 – Department of Geochemistry, Faculty of Natural Sciences, Comenius University; Ilkovičova 6, 842 15, Bratislava, Slovak Republic; viktoria.krajanova@uniba.sk

Lichens are symbiotic organisms consisting of algae or cyanobacteria, and fungi in genetically fixed relationships. Lichens colonize various substrates including wood, rocks, plants, metals or plastics (Nash et al., 1996). They are considered as pioneer organisms in colonizing bare rock substrates. Despite the fact some microorganisms are acknowledged to have weathering impact on minerals and rocks (see bacteria species in mining environments or fungi species in soils; Bonneville et al., 2011), the weathering impact of other microorganisms is still under research (there are very few works done on weathering action of microscopic algae; e.g. Mustoe et al., 2018). Lichens, as symbiotic organisms consisting of multiple microorganism species, are of potential interest, yet their weathering actions are difficult to study in laboratory conditions – mainly due to their slow growth rate. There are few lichen species that show affinity to rock substrates, for instance to ultramafic rocks (Favero-Longo et al., 2004, 2018). Ultramafic rocks consist of less than 45% SiO_2, mostly in form of Mg-/Fe-silicates and they are enriched with heavy metals such as Co, Cr and Ni (Le Maitre et al., 2002). The works of authors Guttová et al. (2014, 2019) tackle the lichen species *Solenopsora liparina* that seems to show affinity to ultramafic rocks (with various levels of serpentinization). This lichen is known for its surface encrustations of biomineralized crystals that possibly contain some bonded metal ions, origin of which could be attributed to the substrate rocks. Therefore, the chemical composition of biomineralized crystals could confirm the confined relationship between this lichen species and its rock substrate. The biomineralization mechanism is based on fungi producing the oxalic acid. This acid binds with metal ions which may result in neoformation of various crystalline metal oxalates. The laboratory formation of various oxalates in reactions with minerals was confirmed in studies (Barman et al., 1992, Varadachari et al., 1994) and it is rather common in fungi (Gadd et al., 2014).

In this work we prepared one thin section sample of the lichen *Solenopsora liparina* and its substrate rock. This sample was used for electron microprobe mapping of elements and BSE imaging (EPMA). The surface encrustations of fresh lichens were manually isolated and identified by Raman spectroscopy.

The substrate rock of the lichen *Solenopsora liparina* was identified as serpentinized ultramafic rock, namely lherzolite, quite rich in Cr and Ni concentrations. In the isolated surface encrustations of lichen *Solenopsora liparina* we identified only Ca-oxalates; no other metal oxalates were detected. Based on older study (Sambo, 1937), we expected to identify at least the presence of Mg-oxalates regarding our Mg-rich lherzolite. In one study (Prieto et al., 1997), Ca-oxalates were identified in lichens growing on Ca-poor substrates (as it is in our case as well), so we rejected the hypothesis on the direct relations between the chemical composition of oxalates and mineral composition of the rock substrates. Despite this, in the future we would like to aim for more precise identification methods of unknown crystalline phases.

Acknowledgement: I want to thank to: RNDr. Štefan Méres, PhD., Mgr. Anna Bérešová, PhD., RNDr. Ľubomír Jurkovič, PhD., Mgr. Stanislava Milovská, PhD., Mgr. Rastislav Milovský, PhD. and Mgr. Tomáš Mikuš, PhD.

References:

Barman, A.K., Varadachari, C. & Ghosh, K. 1992. Weathering of silicate minerals by organic acids. I. Nature of cation solubilisation. *Geoderma*, 53, 45–63.

Bonneville, S., Morgan, D.J., Schmalenberger, A., Bray, A., Brown, A., Banwart, S.A. & Benning, L.G. 2011. Tree-mycorrhiza symbiosis accelerate mineral weathering: Evidences from nanometer-scale elemental fluxes at the hypha–mineral interface. *Geochimica et Cosmochimica Acta* 75, 6988–7005.

Favero-Longo, S.E., Isocrono, D. & Piervittori, R. 2004. Lichens and ultramafic rocks: a review. *The Lichenologist*, 36, 6, 391–404.

Favero-Longo, S.E., Matteucci, E., Giordani, P., Paukov, A.G. Rajakaruna, N. 2018. Diversity and functional traits of lichens in ultramafic areas: a literature based worldwide analysis integrated by field data at the regional scale. *Ecological Research* 33, 3, 593–608.

Gadd, G.M., Bahri-Esfahani, J., Li, Q., Rhee, Y.J., Wei, Z., Fomina, M., Liang, X. 2014. Oxalate production by fungi: significance in geomycology, biodeterioration and bioremediation. *Fungal biology reviews* 28, 36–55.

Guttová, A., Fačkovcová, Z., Martellos, S., Paoli, L., Munzi, S., Pittao, E., Ongaro, S. 2019. Ecological specialization of lichen congeners with a strong link to Mediterranean-type climate: a case study of the genus *Solenopsora* in the Apennine Peninsula. *The Lichenologist* 51, 1, 75–88.

Guttová, A., Zozomová-Lihová, J., Timdal, E., Kučera, J., Slovák, M., Piknová, K., Paoli, L. 2014. First insights into genetic diversity and relationships of European taxa of Solenopsora (Catillariaceae, Ascomycota) with implications for their delimitation. *Botanical Journal of the Linnean Society* 176, 203–223.

Le Maitre, R.W., Streckeisen, A., Zanettin, B., Le Bas, M.J., Bonin, B., Bateman, P., Bellieni, G., Dudeck, A., Efremova, S., Keller, J., Lameyre, J., Sabine, P.A., Schmid, R., Sørensen, H. & Woolley, A.R. 2002. Igneous rocks. A Classification and Glossary of Terms. Recommendations of the International Union of Geological Sciences Subcommission on the Systematics of Igneous Rocks. 2nd Edition. Cambridge. *Cambridge University Press*. 236 pp.

Mustoe, G. E. 2018. Biogenic weathering: Solubilization of iron from minerals by epilithic freshwater algae and cyanobacteria. *Microorganisms*, 6, 8.

Nash, T.H., Friedl, T., Büdel, B., Honegger, R., Elix, J.A., Fahselt, D., Galloway, D.J., Tehler, A. & Gries, C. 1996. Lichen biology. *Cambridge University Press*. 303 pp.

Prieto, B., Silva, B., Rivas, T., Wierzchos, W. & Ascaso, C. 1997. Mineralogical transformation and neoformation in granite caused by the lichens *Tephromela atra* and *Ochrolechia parella*. *International Biodeterioration & Biodegradation* 40, 2-4, 191–199.

Sambo, E. 1937. Sull'azione Vicariante del Magnesio Invece del Calcio in Licheni Calcicoli di Roccia Acalcica. *Giornale botanico italiano* 44, 2, 246–250.

Varadachari, C., Barman, A.K., Ghosh, K. 1994. Weathering of silicate minerals by organic acids. II. Nature of residual products. *Geoderma* 61, 251–268.

Preliminary study of fluid inclusions in greisens from the Saxothuringian Zone of the Bohemian Massif

MICHAELA KREJČÍ KOTLÁNOVÁ[1,2], ZDENĚK DOLNÍČEK[3], MILOŠ RENÉ[4] and VLASTIMIL MAŠEK[5]

1 – Department of Geological Sciences, Faculty of Natural Sciences, Masaryk University; Kotlarska 267/2, 611 37, Brno, Czech Republic; kotlmi@seznam.cz
2 – Research Institute of Building Materials; Hnevkovskeho 30/65, 617 00, Brno, Czech Republic
3 – Department of Mineralogy and Petrology, National Museum; Cirkusova 1740, 193 00, Prague 9, Czech Republic
4 – Institute of Rock Structure and Mechanics, Czech Academy of Sciences; V Holesovickach 41, 182 09, Prague 8, Czech Republic
5 – Institute of Molecular and Translation Medicine, Faculty of Medicine, Palacký University, Hnevotinska 5, 779 00, Olomouc, Czech Republic

Saxothuringian Zone of the Bohemian Massif is relatively rich in occurrences of Sn-W mineralization associate with greisens. Greisens are related to the Late Variscan granite bodies (Lange et al., 1972). According to the occurrence, we can distinguish two types of greisens: 1) Greisens forming the whole apical parts of granitoid intrusions, which occur e.g. in Horní Slavkov, Krupka, or Cínovec deposits. These rocks are enriched in the incompatible elements, especially Li, Rb, Cs, F and HREE. In the horizontal cross-section through the granite bodies (e.g. Huber stock and Schnőd stock), a zonal structure can be observed, when Li-mica granite passes into aplitic mica-poor albite granite, subsequently greisenized granites and Li-mica topaz greisen and then topaz-quartz greisen (Jarchovský, 2006). Hidden bodies of this type of greisen are also expected in the bedrock of Sn-W deposits near Přebuz and Rolava (Breiter, 2006). 2) Greisens associated only with brittle tectonic structures (crack-type greisens). This type of greisen occurs mainly in the Blatná granite massif. These rocks are poorer in Li, Rb, Cs, F and HREE (Breiter, 2012). Crack-type greisens are bound to fissures with orientation N-S and NNW-SSE, less also NE-SW (Heřmanská, 2013, Urban & Malina, 2014) and the thickness of greisen bands is variable, from a few centimeters to tens of decimeters. Greisens in the Blatná massif have a zonal structure, where the greisenized granite passes into muscovite-quartz greisen and then further into topaz-quartz greisen or even quartz ultragreisen (Heřmanská, 2013).
Opinions on the origin of fluids operating in highly fractionated granites and associated greisens are different. There are many supporters of magmatic (Thomas, 1994, Jarchovský, 2006) and metasomatic origin (Štemprok, 1965, Tischendorf, 1999) of these greisenizing fluids. However, recent research (Dolníček et al., 2012) has shown that also meteoric fluids may have contributed significantly to the formation of greisens.
In this study, samples of greisenized granites, greisens and hydrothermal veins from localities Krupka, Cínovec, Přebuz, Rolava and Horní Blatná were studied by means of microthermometry of fluid inclusions (Department of Geology, Palacký University in Olomouc) and Raman spectroscopy (Institute of Molecular and Translation Medicine, Palacký University in Olomouc). Some solid phases enclosed in fluid inclusions were identified by EDX (Department of Geology, Palacký University in Olomouc).
Two types of fluids enclosed in inclusions were recognized: 1) H_2O-NaCl fluids occurs in all samples and in all genetic types of inclusions. The H_2O-NaCl fluid is mainly enclosed in primary fluid inclusions. In pseudosecondary and secondary inclusions also system H_2O-NaCl-

Book of abstracts. ISBN 978-83-933330-2-8

KCl occurs. Secondary inclusions trapped in quartz from Přebuz and Krupka enclose a large number of solid phases, including quartz, topaz, micas, carbonates, sulphides and clay minerals. These phases have been identified by Raman spectroscopy and electron microprobe. Some of these phases (especially halogenides) were identified only on the basis of their behavior during microthermometric measurements. 2) Fluids consisting of H_2O-gas-NaCl was detected only in vein quartz from Cínovec, quartz from greisens from Krupka and Přebuz and quartz from greisenized granite from Horní Blatná. The gaseous component consists mostly of CO_2. In inclusions hosted by quartz from greisen sample from Krupka (KR-12), Raman spectroscopy of gaseous phase displays to 96.2 mol. % CO_2, 1.7 mol. % N_2 a 2.1 mol. % CH_4.
Preliminary results from microthermometric measurements indicate that the process of greisenization took place at temperatures between 500 and 380 °C and pressures 150 to 400 bars. This process relates to activity of low saline (0-6 wt. % NaCl eq.) F-Li rich fluids associated with crystallization of zinnwaldite, cassiterite, wolframite and other Sn-W minerals. Pseudosecondary and secondary inclusions contain two types of fluids, low saline (0-7 wt. % NaCl eq.) and high saline (17-33 wt. % NaCl eq.) fluids associated with post-greisenization processes at temperatures 270→120 °C and forming hydrothermal veins.

Acknowledgement: Thanks to Jaroslav Kapusta for EDX analyzes. This paper was elaborated with the Institutional support for long-term conceptual development of research organizations (Research Institute of Building Materials) by the Ministry of Industry and Trade of the Czech Republic.

References:

Breiter, K. 2005. *Evolution of phosphorus-rich peraluminous magma – granitic system Podlesí in Erzgebirge*, Dissertation thesis, Masaryk University, Brno. 61 p.

Breiter, K. 2012. Nearly contemporaneous evolution of the A- and S-type fractionated granites in the Krušné hory/Erzgebirge Mts., Central Europe. *Lithos*, 151, 105–121.

Dolníček, Z., René, M., Prochaska, W., Kovář, M. 2012. Fluid evolution of the Hub Stock, Horní Slavkov–Krásno Sn–W ore district, Bohemian Massif, Czech Republic. *Mineralium Deposita* 47, 821–833.

Heřmanská, M. 2013. *Mineral assemblages, alteration reactions and transport model of the greisen formation in the Horní Blatná granite pluton, Krušné hory Mts*. Master thesis, Charles University in Prague. 103 p.

Jarchovsky, T. 2006. The nature and genesis of greisen stocks at Krásno, Slavkovský les area - Western Bohemia, Czech Republic. *Journal of the Czech Geoogical Society* 51, 3–4, 201–216.

Lange, H., Tischendorf, G., Palchen, W., Klemm, I., Ossenkopf, W. 1972. Zur Petrographie ung Geochemie der Granite des Erzgebirges. *Geologie*, 21, 457–494.

Štemprok, M. 1965. Petrology and the vertical extent of mineralization in the Cinovec (Zinnwald) granite cupola. *Sborník Geologických Věd Ložisková Geologie a Mineralogie* 5, 7–106.

Thomas, R. 1994. Fluid evolution in relation to the emplacement of the Variscan granites in the Erzgebirge region: a review of the melt and fluid inclusion evidence. *In*: Seltmann R, Kämpf H., Möller P. (Eds.) *Metallogeny of collisional orogens. Czech Geological Survey, Prague,* pp. 150–158.

Tischendorf, G. 1988. Leucocratic and melanocratic crust-derived magmatism and metallogenesis. the example Erzgebirge. *Zeitschrift für Geologische Wissenschaften* 16, 199–223.

Urban, M., Malina, O. 2014. Structural position of greisen veins in the Blatenský massiv in the Erzgebirge, Czech Geological Survey, Prague.

Magnetic properties of experimental fires: implications for archaeological palaeohearths study

EKATERINA KULAKOVA[1] and IGOR DEDOV[2]

1 – Schmidt Institute of Physics of the Earth of the Russian Academy of Sciences; Bolshaya Gruzinskaya str. 10, 123242, Moscow, Russia; liverpool.town.uk@gmail.com
2 – Novosibirsk State University, Institute for the Humanities, Department of Archeology and Ethnography; Pirogova str. 1, 630090, Novosibirsk, Russia; 11.dedov.com@gmail.com

The use of fire is a key factor in human evolution and one of the most important archaeological information sources, which allows us to reconstruct the features of life and the adaptation strategies of ancient humans and paleoecological conditions. Magnetic susceptibility (MS) is a measure of the ease with which a material can be magnetized (Thompson & Oldfield, 1986). It has become a useful and powerful tool for identifying burnt layers at archaeological sites due to MS enhancement (Peters et al., 2001; Church et al., 2007). In-situ susceptibility measurements by portable susceptibility meter serve to detect heated sediments, however more precise and full methods are needed to distinguish human-controlled-fires from natural-fires and to determine circumstances and conditions of archaeological palaeohearths. We present the rock-magnetic results obtained from four experimental fires that differ in the type of fuel used. These four fuel sources are most applicable at archaeological sites of mountain regions of Central Asia.

A total four experimental fires were conducted on loess substrate and fed with a different type of fuel. We used bone, wood, winterfat (shrub variety) and dry animal dung as fuel sources. Bulk sediment samples of loess unaffected by fire (before experimental heating), ash layer and post-burn loess (after experimental heating) were collected from each fire for detailed magnetic investigations. In our study we employed methods widely used in rock-magnetic investigations such as measurements of MS at different conditions, determination of behavior remanent magnetizations and hysteresis parameters. Measurements of bulk MS were made on at two frequencies (976 Hz and 15616 Hz) with a MFK1 Agico device. Frequency dependence, χ_{fd}, is defined as follows: χ_{fd} (%) = $(\chi_{976Hz} - \chi_{15616Hz}) / \chi_{976Hz} \times 100$. Hysteresis loops and isothermal remanent magnetization (IRM) measurements were performed using a PMC MicroMag 3900Vibrating Sample Magnetometer. The backfield parameter S-ratio calculated from two reverse fields are defined as follows: S-ratio$_{100mT}$ = $-(IRM_{-100mT}/SIRM_{+1000mT})$ and S-ratio$_{300mT}$ = $-(IRM_{-300mT}/SIRM_{+1000mT})$. Anhysteretic remanent magnetization (ARM) was imparted by slowly reducing a peak AF of ±130 mT to zero and a constant DC field of 0.05 mT and measured using a 2G SQUID magnetometer.

All samples of ash layers and heated loess sediments have shown an enhancement of values of magnetic susceptibility from 1.2 to 4.2 times. The MS increase by heating is suggested to result from formation of magnetite from Fe-hydroxides (goethite or/and lepidocrocite) (Thompson & Oldfield, 1986). Hysteresis parameters measurements and high positive values (close to +1) of S-ratio$_{300mT}$ confirm main magnetic mineral being "soft" fine-grain magnetite (Table 1). A comparative analysis of magnetic data on ash layers shows an increase in the concentration of small superparamagnetic (SP) grains in ash (first described by Le Borgne, 1960) confirmed by enhancement of χ_{fd} values (Dearing et al., 1996). The difference between experimental fires using a different type of fuel consists only in the concentration of the formed SP particles, which most likely depends on the maximum temperature reached in the fires (in accordance with the caloric content of the material). A comparative analysis of magnetic data on burnt and unburnt loess substrates allows to confidently distinguish them. It is expressed in increased remanent magnetizations (as ARM and SIRM), especially in sediments heated with use of bone and wood fuel, formation of fine-grain magnetite and total MS enhancement.

Experimental approach at magnetic studies is powerful additional tool for receiving detailed information at archaeological sites. We conducted four experimental fires using different type of the fuel in order to establish more significant changes in magnetic mineralogy and properties. Results show perceptible differences at rock-magnetic parameters of burnt and unburnt sediments and some otherness between used fuel types.

Sample	Description	χ (m^3kg^{-1} x 10^{-6})	χ_{fd} (%)	SIRM (mAm^2 kg^{-1})	ARM (mAm^2 kg^{-1})	S-ratio$_{100mT}$	S-ratio$_{300mT}$
bone_ash	Ash layer of fire with bone fuel	1.20	8.8	9.0	0.09	0.863	0.970
wood_ash	Ash layer of fire with wood fuel	1.07	8.5	9.3	0.10	0.825	0.964
winterfat_ash	Ash layer of fire with winterfat fuel	1.71	9.3	14.3	0.15	0.846	0.962
dung_ash	Ash layer of fire with dry dung fuel	0.69	7.9	6.1	0.07	0.836	0.968
bone1	Unburnt loess substrate (before heating)	0.41	6.3	5.0	0.05	0.508	0.927
bone2	Heated loess substrate beneath the surface of burning	1.55	8.9	11.5	0.14	0.867	0.970
wood1	Unburnt loess substrate (before heating)	0.41	6.1	4.8	0.04	0.521	0.925
wood2	Heated loess substrate beneath the surface of burning	1.72	6.9	19.4	0.16	0.894	0.992
winterfat1	Unburnt loess substrate (before heating)	0.42	6.1	5.0	0.05	0.520	0.923
winterfat2	Heated loess substrate beneath the surface of burning	0.54	7.0	5.4	0.06	0.713	0.930
dung1	Unburnt loess substrate (before heating)	0.46	6.7	5.2	0.05	0.544	0.927
dung2	Heated loess substrate beneath the surface of burning	0.54	6.0	6.2	0.05	0.738	0.941

Table 1. Magnetic data of experimental hearth samples.

References:

Church, M.J., Peters, C., Batt, C.M. 2007. Sourcing fire ash on archaeological sites in the Western and Northern Isles of Scotland, using mineral magnetism. *Geoarchaeology* 22, 747–774.

Dearing, J.D., Dann, R.J.L., Hay, K., Lees, J.A., Loveland, P.J., Maher, B.A., O'Grady, K. 1996. Frequency-dependent susceptibility measurements of environmental materials. *Geophysical Journal International* 124, 228–240.

Le Borgne, E. 1960. Influence du feu sur les propriétés magnétiques du sol et sur celles du schiste et du granite. *Annales de Geophysique* 16, 159–195.

Peters, C., Church, M.J., Mitchel, C. 2001. Investigation of fire ash residues using mineral magnetism. *Archaeological Prospection* 8, 227–237.

Thompson, R. & Oldfield, F. 1986. *Environmental Magnetism*. Allen and Unwin:London.

Structural model of the Spišská Magura region based on multi-source data

KLAUDIA KUPČÍKOVÁ[1]

1 – Institute of Geosciences, Faculty of Mining, Ecology, Process Control and Geotechnologies, Technical University of Košice, Park Komenského 15, 042 00 Košice, Slovak Republic, klaudia.kupcikova@tuke.sk

The tectonic analysis of the Spišská Magura region has been discussed in many studies. However, a clear interpretation of the tectonic development of this area, supported by a combination of several different methods is still lacking. The aim of the research is to propose a tectonic model, based on analysis of the digital model of terrain (DMT), which is currently increasingly used in structural geology. Interpretation of the DMT depends on the monitoring of lineaments (e.g. valleys and mountain ridges) that probably indicate tectonic structures.

We complemented this method with our own structural analysis in the field and existing data from older studies. These data mainly include published articles (e.g. Jacko & Janočko, 2000, Vojtko et al., 2008) and geological maps (Fusán et al., 1964, Janočko et al., 2000, Polák et al., 2006), geophysical measurements (VES) and paleomagnetic data.

Based on the mentioned data, we assume that the most significant faults are strike-slip faults with northeast-southwest direction, which bound the Spišská Magura region from the north-west and south-east. This type of faults has been activated by transpression and we conclude that its propagation continues to adjacent areas. The part of Spišská Magura bounded by sinistral strike-slip faults is divided into blocks that rotated counterclockwise. These blocks are separated from each other by subparallel faults with E-W to NW-SE directions, which is probably the result of a dextral movement. Such a similar model situation has been described in many types of research in various localizations around the world (Ron et al., 1984, Kanaori et al., 1990; Kuhn, 1999).

The position of the strike-slip fault in the north-western edge of the Spišská Magura region was confirmed by the geological map of Czechoslovakia at a scale 1:200 000. The second significant strike-slip fault on the south-eastern edge of Spišská Magura agreed with the position of the Subtatric-Ruzbachy fault system from the geological map of Spišská Magura at a scale 1:50 000. The results of vertical electrical sounding (Májovský, 1981) are geoelectrical profiles that show gradual block subsidence along E-W subparallel faults. Tectonic structures of the same direction were verified in the area between the Belianske Tatry Mts. and the Spišská Magura region and on the border with the Pieniny Klippen Belt. These structures were described as dextral strike-slip faults (Janočko & Jacko, 2000). The rotation of separated blocks in the Spišská Magura region was documented by paleomagnetic measurements (Marton et al., 2016), indicating their rotation counterclockwise.

References:

Fusán O., Bystrický J., Kamenický L., Chmelík F., Matějka A. & Solołowski, S. 1964: Geologická mapa ČSSR 200 000, M – 34 – XXVII, list Vysoké Tatry. ÚÚG Praha.

Jacko, S. & Janočko, J., 2000. Kinematic Evolution of the Central-Carpathian Paleogene Basin in the Spišská Magura region (Slovakia). *Slovak Geological Magazine* 6, 409–418.

Janočko, J., Gross, P., Buček, S., Karoli, S., Žec, B., Rakús, M., Potfaj, M. & Halouzka, R. 2000. Geologická mapa Spišskej Magury 1:50 000. Štátny geologický ústav Dionýza Štúra, Bratislava.

Kanaori, Y., Endo, Y., Yairi, K., Kawakami, S., 1990. A nested fault system with block rotation caused by left-lateral faulting: the Neodani and Atera faults, central Japan. *Tectonophysics*, 177, 401–418.

Kuhn, D., Reuther, C.-D, 1999. Strike-slip faulting and nested block rotations: structural evidence from the Cordillera de Domeyko, northern Chile. *Tectonophysics* 313, 4, 383–398.
Májovský, J., 1981. Geofyzikálny prieskum Belianskych Tatier, Oblasť: Ždiar-Podspády. Záverečná správa. Geofyzika n.p. Brno.
Marton, E., Grabowski, Jacek, Tokarski, Antoni, Tunyi, I., 2016. Palaeomagnetic results from the fold and thrust belt of the Western Carpathians. *Geological Society of London Special Publications* 425,1, 7–36.
Polák, M., Janočko, J., Jacko, S. jr., Potfaj, M., Elečko, M., Kohút, M., Broska, I., Maglay, J., 2008. Prehľadná geologická mapa Slovenskej republiky 1:200 000, list 27 – Poprad. Štátny geologický ústav Dionýza Štúra, Bratislava.
Ron, H., Freund, R., Garfunkel, Z., Nur, A., 1984. Block rotation by strike-slip faulting: Structural and paleomagnetic evidence. Journal of Geophysical Research 89, 7, 6256–6270.
Vojtko, R., Tokárová, E., Sliva, L., Pešková, I., 2010. Reconstruction of Cenozoic paleostress fields and revised tectonic history in the northern part of the Central Western Carpathians (the Spišská Magura and Východné Tatry Mountains). *Geologica Carpathica* 61,3, 211–225.

Reconstruction of the magma flow direction in alkaline dikes from the Kotuy river valley (Siberian Traps LIP) based on AMS data

ANTON LATYSHEV[1,2], VICTOR CHMEREV[2] and VICTOR ZAITSEV[3]

1 – Institute of the Physics of the Earth RAS, 10-1 B. Gruzinskaya street, Moscow, Russia; anton.latyshev@gmail.com
2 – Lomonosov Moscow State University, Faculty of Geology; 1, Leninskie Gory, Moscow, Russia;
3 – Vernadskiy Institute of Geochemistry and Analytical Chemistry; 19, Kosygina street, Moscow, Russia

The Permian-Triassic Siberian Traps province is considered to be a classic example of Large Igneous Province (LIP). At this moment, many aspects of the evolution of the Siberian Traps are still poorly constrained, in particular, the sequence and duration of magmatic events, location of regional magma feeding zones and activity of magmatic centers. The main goal of this work was to reconstruct the magma flow directions in dike swarms from the Kotuy river valley (Maymecha-Kotuy region, the northern part of the Siberian platform) based on the detailed measurements of anisotropy of magnetic susceptibility (AMS).
Siberian Traps in the Kotuy river valley comprise two contrasting groups: 1) tholeiitic basalts, similar to the main volume of the Siberian Traps LIP; 2) alkaline-ultramafic rocks, which are scarce in other regions of the province. Alkaline lavas and tuffs in the Kotuy river valley are exposed only in a limited area (Arydzhangsky and Khardakhsky formations), however, multiphase circular plutons (Kugda, Odikhincha) and swarms of radial and parallel dikes mark the essentially wider territory of the manifestation of alkaline magmatic activity.
We performed the detailed investigation of AMS in the dike swarm of alkaline lamprophyres from the Kotuy river valley. The majority of studied dikes demonstrate I-type (intermediate) of the magnetic fabric, when the medium axis K2 of AMS ellipsoid is orthogonal to the contact of intrusion. In dikes where the minimal axis K3 is subvertical and maximal axis K1 is horizontal, we interpret the magnetic fabric as a result of cooling of the static magma column after the emplacement in the setting of horizontal extension (Park et al., 1988; Raposo and Ernesto, 1995). Also, N-type and R-type of magnetic fabric were identified as well. In some intrusions, the orientation of the axes of AMS ellipsoid changes from the contact zones to the inner part of intrusion. In this case, we used data from the contact zones for the magma flow reconstruction. Analysis of the maximal axis K1 orientation in dikes showed that in the majority of bodies it shallowly plunged to the west. This corresponds to the lateral magma flow from west to east during the emplacement. Consequently, formation of the studied dikes is not directly related to the Kugda pluton, which is located 8 km eastward. The emplacement of dikes occurred from the magmatic center located westward from the Kotuy river valley and is not associated with any known large pluton. Besides, petrographic similarity of the studied dikes to the lavas of the Arydzhangsky Formation allows us to suggest that they are coeval. This implies the wider area of magmatic activity during the Arydzhangsky magmatic stage.

Acknowledgement: This work was supported by RFBR (projects 18-35-20058, 18-05-70094, 17-05-01121 and 20-05-00573).

References:

Park, J.K., Tanczyk, E.I. & Desbarats, A. 1988. Magnetic fabric and its significance in the 1400 Ma Mealy diabase dykes of Labrador, Canada. *Journal of Geophysical Research* 93, 13,689–713.

Raposo, M.I.B. & Ernesto, M. 1995. Anisotropy of magnetic susceptibility in the Ponta Grossa dike swarm (Brazil) and its relationship with magma flow directions. *Physics of the Earth and Planetary Interiors* 102, 183–196.

Monazite-allanite relationship in Prašivá I/S granite type from the Low Tatra Mts: a record of magma mixing and metasomatic processes

MARIA MARASZEWSKA[1], IGOR BROSKA[1] and SERGYI KURYLO[2]

1 – Earth Science Institute, Slovak Academy of Sciences, Bratislava, Slovakia, geolmara@savba.sk
2 – Earth Science Institute, Slovak Academy of Sciences, Banska Bystrica, Slovakia

Monazite-(Ce) and allanite-(Ce) are predominant REE carriers in crustal rocks (Bea, 1996). The distribution of these phases in granitoids is strongly related to melt composition: monazite precipitates as an early phase in peraluminous, relatively reduced magmas with lower Ca^{2+} activities. In contrast, allanite is stable in metaluminous, higher oxidized, and Ca^{2+} rich melts. The antagonistic relation between allanite and monazite is one of the typological features distinguishing I-type granitoids from S-type in Western Carpathians (Broska et al., 2008). The coexistence of monazite and allanite is, therefore, a record of significant changes in the melt composition (Broska et al., 2000). However, the monazite-allanite transition can take place during fluid-mineral interaction (e.g. Budzyń et al., 2011).

Prašivá granitoid type is one of several local granitoid facies within the Variscan magmatic complex of Low Tatra Mts, Western Carpathians. Traditionally it is classified as the I-type granite; however, Sr-Rb and Nd-Sm isotope characteristics suggest hybrid origin (Poller et al., 2005). This study focuses on two facies of Prašivá granitoid: in area of Liptovská Lužna village (phlogopite granodiorite - LL subtype) in NW part of the body, and SE part, in the vicinity of Magurka village on the main ridge of Low Tatra Mts (annite monzogranite - Mg subtype).

Monazite-(Ce) is the main REE carrier in the Mg subtype. It forms sub- to anhedral, heterogeneous crystals up to 250µm. The central parts of many grains show concentric zonation transitional to less regular convolute or patchy zonation towards rims. The irregularly distributed lighter and darker domains differ in ThO_2, CaO, SiO_2, and REE_2O_3 content. ThO_2 content from cores, 6-7 wt%, indicates magmatic origin (Schandl and Gorton, 2004). Preliminary U-Th-Pb-total EPMA dating yielded mean age of ca. 350 Ma, which is in agreement with U-Th-Pb zircon geochronology (Maraszewska, unpublished data), however coexisting patchy domains indicate various ages (320-400 Ma).

In the LL subtype, monazite was found only in trace amounts as the inclusions (1) in apatite and (2) relicts within allanite and (3) skeletal grains in matrix. Monazite enclosed in allanite and apatite shows enrichment in ThO_2 (up to 14 wt%) and Y_2O_3 (up to 1 wt%), while skeletal grains in matrix are lower in ThO_2 (1.30-5wt%).

Allanite-(Ce) is absent in the Mg subtype. In the LL subtype, it forms relatively large sub- to euhedral crystals with locally preserved magmatic zoning overprinted by patchy, irregular zoning. In the BSE images, distinct domains with different brightness can be recognized. Margins of the grains are often overgrown by the metamictic phase enclosing Th-rich silicates. Brighter BSE areas are higher in Fe, REE, Ti and depleted in Th, Ca, Al in comparison with darker areas that suggest a transition from allanite-ferriallanite towards REE-Th-epidote/clinozoisite.

A presence of large, euhedral crystals of allanite-(Ce) in the LL subtype suggests their orthomagmatic origin. Relict monazite inclusions suggest that allanite has grown at the expense of the

Book of abstracts. ISBN 978-83-933330-2-8

former monazite due to an increase of Ca^{2+}, O^{2-} activity in the system, and reactions with surrounding aluminosilicates. Such circumstances indicate the influx of metaluminous melt into peraluminous one and destabilization of monazite in favor of allanite. In contrast, in Mg granite, monazite occurs as the only REE carrier, which suggests a lower influence of metaluminous Ca-rich magma, not sufficient for allanite stabilization. Spatial heterogeneity within the Prašivá granite body can be explained in terms of magma mixing between the upper and lower crust.
Allanite in the LL and monazite in the Mg subtypes were affected by the secondary alteration. In allanite, it resulted in local replacement by Th-REE epidote signalizing significant post-magmatic overprint (Wood and Ricketts, 2000; Poitrasson, 2002). Monazite in the Mg subtype shows an irregular modification of primary grains causing secondary Th enrichment or depletion in distinct areas, which is possibly connected with metasomatism (Poitrasson et al. 1996) or magmatic dissolution. Coexisting domains show hardly interpreted monazite ages, which suggest partial U-Th-Pb system disequilibrium in the altered areas.

Acknowledgement: This research was financed by project APVV 18-0107.

References

Bea, F. 1996. Residence of REE, Y, Th and U in granites and crustal protoliths; implications for the chemistry of crustal melts. *Journal of Petrology* 37, 521–552.

Broska, I. & Petrik, I. 2008 Genesis and stability of accessory phosphates in silicic magmatic rocks: a Western Carpathian case study Mineralogia 39 1–2, 53–65.

Broska I., Petrík I. & Williams C.T., 2000. Coexisting monazite and allanite in peraluminious granitoids of the Tribeč Mountains, Western Carpathians. *American Mineralogist* 85, 22–32.

Budzyń, B., Harlov, D.E., Williams, M.L. & Jercinovic, M.J. 2011. Experimental determination of stability relations between monazite, fluorapatite, allanite, and REE-epidote as a function of pressure, temperature, and fluid composition. *American Mineralogist* 96, 1547–1567.

Poitrasson, F. 2002. In situ investigations of allanite hydrothermal alteration: examples from calc-alkaline and anorogenic granites of Corsica (southeast France). *Contributions to Mineralogy and Petrology* 142, 4, 485–500.

Poitrasson, F., Chenery, S. & Bland, D.J. 1996. Contrasted monazite hydrothermal alteration mechanisms and their geochemical implications. *Earth and Planetary Science Letters* 145, 1–4.

Poller, U., Kohút, M., Gaab, A. & Todt, W. 2005. Pb, Sr and Nd isotope study about two co-existing Magmas in the Nízke Tatry Mountains, Western Carpathians (Slovakia). *Mineralogy and Petrology* 84, 215–231.

Schandl, E.S. & Gorton, M.P. 2004. A textural and geochemical guide to the identification of hydrothermal monazite: criteria for selection of samples for dating epigenetic hydrothermal ore deposits. *Economic Geology* 99, 1027–1035.

Wood, S.A. & Ricketts, A. 2000. Allanite-(Ce) from the Eocene Castro granite, Idaho: response to hydrothermal alteration. *The Canadian Mineralogist* 38, 81–100.

Orientation analysis and reconstruction of paleostress fields in the western part of the Orava sector of the Pieniny Klippen Belt (Western Carpathians)

MARÍNA MOLČAN MATEJOVÁ[1]

1 – Department of Geology and Palaeontology, Faculty of Natural Sciences, Comenius University, Mlynská dolina, Ilkovičova 6, 842 15 Bratislava, Slovakia; marina.matejova@uniba.sk

The area of interest is situated in the western Orava part of the Pieniny Klippen Belt (PKB), around villages Istebné, Revišné, Veličná and Beňova Lehota. Data was measured mostly in the limestone klippen of Oravic units and flysch sediments of the Central Carpathian Paleogene Basin (CCPB). Part of the study was orientation analysis, with the aim of separating structures associated with the S-dipping back-thrusts. Folds with axis oriented in the N-S direction and strike-slip faults with fault plane oriented NE-SW and NW-SE/NNW-SSE were recorded, but in the overall dataset of all measured structures, they formed a minority in comparison with normal faults and veins. However, Marko et al. (2005) and Pešková et al. (2009, 2012) documented the prevalence of south-dipping tectonic structures in other parts of the Orava sector of the PKB. The fan-like structural character of the PKB with the southern segment back-thrusted onto the sediments of the CCPB is evidenced in the studied area, by the extent of the Zuberec strata towards the N into the PKB and by a Mesozoic klippe mapped on the top of prominent elevations formed by CCPB sediments. Furthermore near Revišné, Zuberec strata was documented in a subvertical position with a slight dip at the contact with the PKB. Using paleostress analysis and by separation of structures into generations, five main deformation phases were identified. The stacking of the Oravic units was initiated by compression. The first compressional deformation phase recorded by our analysis in Mesozoic rocks and CCPB sediments took place in the Lower Miocene. Main orientation of the stress was in NW-SE direction. The rotation of the compressional stress in a clockwise direction by approximately 45° defines a second distinct deformation phase. In the Middle Miocene, there was a change to a transpressional regime (the third deformation phase), which resulted in south-inclined sharp folds, strike-slip and dip-slip faults oriented in the NW-SE and NE-SW directions. The beginning of NE-SW extension is also documented by the comparative works from other parts of PKB (Bučová, 2013; Marko et al., 1995; Mikuš, 2010; Pešková et al., 2009), but authors differ in the age determination for this tectonic event. In the presented work, the deformation phase is included in the Upper Miocene. The last documented deformation took place in the Pliocene - Quaternary? and it is divided into two subgroups. Extension in W-E direction and extension in NNW-SSE to NNW-SSW directions. The second subgroup was identified only within units of the PKB.

Acknowledgement: Financial support from the Grant Agency for Science, Slovakia (project VEGA 1-0712-11) and from the Slovak Research and Development Agency (project APVV-0212-12) is gratefully appreciated.

References:

Bučová, J. 2013: *Geologická stavba a štruktúrny vývoj západnej časti pieninského bradlového pásma.* Dizertačná práca, 160 s.

Marko, F., Plašienka, D. A Fodor, L. 1995: Meso-cenozoic tectonic stress fields within the Alpine-Carpathian transition zone: A review. *Geologica Carpathica*, 46, 1, 19 – 27.
Marko, F., Vojtko, R., Plašienka, D., Sliva, Ľ., Jablonský, J., Reichwalder, P. & Starek, D. 2005: A contribution to the tectonics of the periklippen zone near Zázrivá (Western Carpathians). *Slovak Geological Magazine*, 11, 1, 37 – 43.
Mikuš, V. 2010: *Tektonika pieninského úseku bradlového pásma medzi Jarabinou a Litmanovou na východnom Slovensku*. Dizertačná práca, 130 s.
Pešková, I., Vojtko, R., Starek, D. & Sliva, Ľ. 2009: Late Eocene and Quaternary deformation and stress field evolution of the Orava region (Western Carpathians). *Acta Geologica Polonica*, 59, 1, 73 – 91.
Pešková, I., Hók, J., Potfaj, M. & Votko, R. 2012. Štruktúrna interpretácia varínskeho a oravského úseku bradlového pásma. *Geologické práce, Správy* 120, 51 – 64.

Experimental weathering of regolith from the forefield of a retreating Arctic glacier

JUSTYNA NOSEK[1] and GRZEGORZ RZEPA[1]

1 – AGH - University of Science and Technology, Faculty of Geology, Geophysics and Environmental Protection, Department of Mineralogy, Petrography and Geochemistry, Al. Mickiewicza 30, 30-059 Kraków, Poland; e-mail: justyna.nosek12@gmail.com, gprzepa@cyf-kr.edu.pl

One of the effects of global warming is the rapid retreat of glaciers, especially in the Arctic, where the expected average temperature increase is higher than elsewhere. Freshly exposed regolith is very reactive and susceptible to chemical weathering. The weathering processes, in turn, are among the most important factors that regulate the global carbon cycle and, thus, the Earth's climate.

The aim of this study was to assess the influence of the ambient temperature on the course and rate of weathering processes in the initial soil collected from the proglacial zone of the Arctic glacier. This research was inspired by a classic work by Brown et al. (1996) on experimental weathering of rocks from the forefield zone of the Alpine glacier.

Three samples of regoliths were used in this study, collected in the increasing distance from the terminus of the Werenskioldbreen glacier (SW Spitsbergen, Svalbard). The geological and geographical settings, as well as details of sampling and characteristics, are presented in Czerny et al. (1992) and Kwaśniak-Kominek et al. (2016). Briefly, the original samples are coarse-grained regoliths composed of glacially reworked rock-forming minerals from the common (mainly metamorphic) rocks in the area. These minerals include quartz, Na-plagioclase, amphibole, epidote, various phyllosilicates as well as carbonates (calcite, dolomite, siderite) and ore minerals (mainly Fe, Cu, Zn and Pb sulphides). The air-dried and gently crushed samples were homogenized and reacted with double distilled water (liquid-to-solid ratio 250:1) for several months. During the experiment, suspension aliquots were collected and after filtration using 0.22 µm syringe filters, pH, electrolytic conductivity (EC) and chemical composition (ICP-EAS and AAS) were analysed. Mineralogy of the fine fraction (<2 µm) was examined before and after experiments using X-ray diffractometry (XRD) and scanning electron microscopy (SEM-EDS). Two experimental sets were used. In the first experiment, carried out at room temperature (RT), three samples collected at a distance of about 20 m (close, C), 950 m (middle, M) and 1700 m (far, F) from the glacier terminus, were mixed with water using a magnetic stirrer for six months. In the second set, two samples (C and F) were kept stirred for approximately four months (i) at room temperature (RT) and (ii) in a fridge, at ca. 4°C (LT).

The results showed that the rate of chemical alterations depends on "age" of regolith (i.e. the distance from the glacier front) as evidenced by the faster increase in EC of samples M and F compared to sample C. This is probably due to differences in available mineral surface since the youngest regolith (C) is coarser-grained than the older ones. The increase in electrolytic conductivity is associated with the continuous release of the major cations as well as bicarbonates and sulphates. Chemical analyses showed that all the waters were dominated by calcium and bicarbonate (up to ca. 40 and ca. 140 mg/L, respectively). Silica concentration was also quite high, reaching ca. 90 mg/L at the end of the experiments. On the other hand, the concentration of chlorides was very low and did not follow any clear trend.

After several months of reaction, the EC values of both LT samples are surprisingly higher than those measured at RT, despite the initial more pronounced increase in EC of the latter samples. This can be partially explained by the higher solubility of carbonates at low temperature – both LT samples contained more Ca^{2+} and HCO^{-}_{3} while the concentrations of the remaining major ions were often lower compared to RT samples. Despite some slight fluctuations, pH values were similar in all cases and were about 8.

Mineralogical analyses did not show any distinct changes in the composition of altered solids, which is probably associated with low sensitivity of the methods used and morphological and chemical similarity of the primary and potential secondary phases.

The results suggest that the main processes of chemical weathering are carbonate dissolution and (alumino)silicate hydrolysis. Oxidation of sulphides seems to be of minor importance, which is somewhat contradictory to field observations but may be caused by the lack of micro-organisms in laboratory conditions as well as the relatively short duration of the experiment.

References:

Brown G.H., Tranter, M. & Sharp, M.J., 1996. Experimental investigations of the weathering of suspended sediment by Alpine glacial meltwater. *Hydrological Processes* 10, 579–597.

Czerny, J., Lipień, G., Manecki, A. & Piestrzyński, A., 1992. Geology and ore-mineralization of the Hecla Hoek succession (Precambrian) in front of the Werenskioldbreen, South Spitsbergen. *Studia Geologica Polonica* 99, 67–115.

Kwaśniak–Kominek, M., Manecki, M., Rzepa, G., Płonka, A.M. & Górniak, D. 2016. Weathering in a regolith on the Werenskioldbreen forefield (SW Spitsbergen): Modelling of pore water chemistry. *Annales Societatis Geologorum Poloniae* 86, 249–264.

Paleomagnetic and Geochronological data from Mesoproterozoic rocks of Northern Siberia

ALEKSANDR PASENKO[1]

1 – The Schmidt Institute of Physics of the Earth of the Russian Academy of Sciences (B.Gruzinskaya str. 10-1, 123242, Moscow, Russia Address); pasenkoal@ya.ru

The Udzha structure is located between the Anabar Shield and the Olenek uplift in the northern part of the Siberian Craton, and is considered as a north-south elongated paleo-rift (Gladkochub et al., 2009). Mesoproterozoic volcano-sedimentary rocks cut by mafic intrusions are exposed inside the Udzha paleo-rift. Phanerozoic sedimentary rocks with an unconformity cover the Precambrian succession. The pre-Vendian sequence is divided into the following locally recognized units: limey-shales with tuff interbeds of the Ulahan-Kurung and Ungoakhtah Formations, carbonates of the Khapchanyr Formation, and terrigenous sedimentary rocks of the Udzha Formation, which overall reaches a thickness of ~1500 m. For a long time, the Udzha Basin has been considered as a long-lived basin with at least 500 Ma of evolution. Gladkochub et al. (2009) have criticized this model, and obtained a new Ar-Ar age 1074±11 Ma from dyke which cuts the Ungoakhtah Formation. Also, some of the dykes of the Udzha Complex cut the Udzha Formation, which allows us to establish the end of sedimentation at 1074±11 Ma. However, we would not consider this age as accurate for the intrusion, as the age spectra did not give a plateau. For the first time, we used the U-Pb method for dating the Great Udzha Dyke, which cuts the full pre-Vendian sedimentary succession and can constrain the age of sedimentation. Also, we employed paleomagnetic analysis for correlation of this dyke with the others inside the Udzha paleo-rift. Furthermore, we present new paleomagnetic data from sedimentary rocks of Mesoproterozoic Udzha Uplift, and apparent polar wander of the Siberian Craton during the Mesoproterozoic.

The Great Udzha Dyke (GUD) is a medium-grained dolerite with ophitic and coarse-grained textures, being composed of plagioclase, clinopyroxene, quartz and hornblende. Zircon or baddeleyite were not found, but apatite was separated. Apatite was used therefore for U-Pb dating performed by the LA-ICP-MS method at the University of Tasmania (Hobart, Australia, Chew et al., 2011; Thompson et al., 2016). On a Tera-Wasserburg diagram, the analyzed apatite grains are discordant, but they form a distinct regression line. At zero values of $^{238}U/^{206}Pb$, this regression line is anchored by the isotope composition of common lead obtained from calcite from the same dyke, and a lower intercept of the concordia the regression line creates an age of 1386 ± 30 Ma (Malyshev et al., 2018).

Paleomagnetic studies were carried out to correlate the GUD with other intrusive bodies. From each intrusive body, we collected 10-15 oriented block samples, from which oriented cubic samples were later prepared for further laboratory studies. Paleomagnetic and rock magnetic studies were carried out on equipment in the paleomagnetic laboratory of the IPE RAS.

Great Udzha Dyke. As a result of stepwise thermal demagnetization, two components of magnetization were isolated in samples of the Great Udzha Dyke. The average direction of the HT (high temperature) magnetization component in the rocks of the Great Udzha Dyke has a north-eastern declination and a moderate negative inclination: n = 8; Dec = 37°; Inc = -30°; K = 30; $\alpha 95 = 10°$ (hereinafter all directions are given for the stratigraphic coordinate system).

Sill at Udzha and Hapchanyr river junction. As a result of the thermal demagnetization and principal component analysis, two components of the magnetization were isolated. The HT-vectors have northeastern declinations and moderately negative inclinations: n = 13; Dec = 32°; Inc = −23°; K = 50; α95 = 6.

Dyke on the right bank of the Udzha. According to the results of thermal demagnetization, in all samples only one stable HT component of magnetization was present. We noted the proximity of high-temperature directions, which with a high probability indicates that the intrusive bodies under consideration are of the same age. They were formed at the same time, and we could calculate the average direction of magnetization.

The U-Pb age of the Great Udzha Dyke is 1386 ± 30 Ma, obtained in the present study, is coeval with the age of the Chieress Dyke (Anbar Shield, 1384 ± 2 Ma, Ernst et al., 2000). This fact can be considered as an indication of the widespread occurrence of magmatism of this given age in the northern Siberian Craton. The virtual geomagnetic pole obtained from the samples of the Chieress Dyke, taking into account the accuracy of its determination, virtually does not differ from the paleomagnetic pole of the Udzha intrusions. Paleomagnetic and geochronological data thus mutually confirm each other, significantly increasing the reliability of both paleomagnetic and geochronological results obtained for the Great Udzha and the Chieress dykes.

Based on the information presented, we calculated the VGP for the Siberian Craton for the time of ca. 1.38 Ga, and used these poles for reconstruction of the paleogeographic position of the Siberian platform.

According to this reconstruction, ~1380 Ma, the northern (in modern coordinates) areas of the Siberian Craton occupied the equatorial latitudes, and the paleo-meridian passed through these territories at an angle of 20-30˚ relative to the present day.

References:

Chew, D.M., Sylvester, P.J. & Tubrett, M.N. 2011. U-Pb and Th-Pb dating of apatite by LA-ICPMS. *Chemical Geology* 280, 1–2, 200–216.

Ernst, R.E., Buchan, K.L., Hamilton, M.A., Okrugin, A.V. & Tomshin, M. 2000. Integrated paleomagnetism and U–Pb geochronology of mafic dikes of the eastern Anabar Shield region, Siberia: Implications for Mesoproterozoic paleolatitude of Siberia and comparison with Laurentia. *Journal of Geology* 180, 381–401.

Gladkochub, D.P., Stanevich, A.M., Travin, A.V., Mazukabzov, A.M., Konstantinov, K.M., Yudin, D.S. & Kornilova, T.A. 2009. The Mesoproterozoic Udzha paleorift (Northern Siberian Craton): New data on age of basites, straigraphy, and microphytology. *Doklady Earth Sciences 425*, 2, 371–377.

Konstantinov, K.M., Pavlov, V.E. & Petukhova, E.P. 2007. The results of reconnaissance paleomagnetic studies of the rocks of the Udja uplift (north of the Siberian platform). *In*: *Paleomagnetism and Magnetism of Rocks; Theory, Practice, Experiment. Workshop Materials Borok*, pp. 69–71.

Malyshev, S. V., Pasenko, A. M., Ivanov, A. V., Gladkochub, D. P., Savatenkov, V. M., Meffre, S., Abersteiner, A., Kamenetsky, V. S., and Shcherbakov, V. D. Geodynamic significance of the mesoproterozoic magmatism of the udzha paleo-rift (northern siberian craton) based on u-pb geochronology and paleomagnetic data. *Minerals 8, 12 (2018)*

Thompson, J., Meffre, S., Maas, R., Kamenetsky, V., Kamenetsky, M., Goemann, K. & Danyushevsky, L. 2016. Matrix effects in Pb/U measurements during LA-ICP-MS analysis of the mineral apatite. *Journal of Analytical Atomic Spectrometry* 31, 1206–1215.

Book of abstracts. ISBN 978-83-933330-2-8

Tectonometamorphic history of the Veporic-Gemeric contiguous zone (Central Western Carpathians, Slovakia)

TOMÁŠ POTOČNÝ[1], ŠTEFAN MÉRES[2] and DUŠAN PLAŠIENKA[1]

1 – Department of Geology and Palaeontology, Faculty of Natural Sciences, Comenius University, Mlynská dolina, Ilkovičova 6, 842 15 Bratislava, Slovakia; potocny9@uniba.sk; dusan.plasienka@uniba.sk
2 – Department of Geochemistry, Faculty of Natural Sciences, Comenius University, Mlynská dolina, Ilkovičova 6, 842 15 Bratislava, Slovakia; stefan.meres@uniba.sk

During deformation and metamorphism rocks adapt to different temperature and pressure conditions that leave signs in the fabric of the rock, mainly structural elements and new mineral paragenesis. We tried to connect these two main components in order to understand the tectonometamorphic processes. We focused on the part of the contact zone of two basement-involved tectonic superunits of Central Western Carpathians – Veporic and Gemeric. The contact is represented by Lubeník fault zone, which was originally the thrust plane, later affected by significant movements. The investigated area between Čierna Lehota and Honce villages in central Slovakia include three superposed major Western Carpathians units. In the lowermost structural position is the Veporic Superunit, composed of the pre-Alpine crystalline basement (Kráľova hoľa Complex and Hladomorná valley Complex - Klinec 1966, 1971) and the post-Variscan Upper Paleozoic-Triassic sedimentary cover represented by Permian Rimava Formation in this area. Along the SW-NE trending Lubeník fault zone, rocks of the Veporic Rimava Formation are juxtaposed to the Mississippian Ochtiná Group and Pennsylvanian Dobšiná Group (e.g., Vozárová 1996). These North Gemeric Paleozoic complexes are overthrust by the main Gemeric basement and cover thrust sheets (Gelnica and Gočaltovo Group). The rocks of the Gemeric Unit are overridden by the Meliatic Superunit, which is formed by Permian to Jurassic high-pressure/low-temperature volcano-sedimentary complex - Bôrka Nappe (Mello et al. 1998, Plašienka et al. 2019) and very low-grade Jurassic syn-orogenic sedimentary formations with olistostrome bodies Meliata Unit s.s. (Mock et al. 1998). The Meliatic forms a combined accretionary complex with the overlying Turňa Unit (Lačný et al. 2016). Complicated geological setting in this area resulted in deformation processes connected with superposition of several units, which show common tectonic and metamorphic relationships. We investigated ca. 100 samples (also oriented) from all these units. In the field we measured different structural elements, but we focused on metamorphic foliation. Metamorphic foliation is dipping mainly to SE, what correlates with the main Alpine tectonic stage. On the other hand, foliations in complexes of the Veporic crystalline basement are dipping to SW or S, what is probably a sign of the pre-Alpine period. We also study our samples using the polarized microscope and electron probe microanalyzer (EMPA). Samples that contain metamorphic monazites were dated by the Th-U-total Pb method. Based on age and position in fabric with metamorphic foliation, we divide the tectonometamorphic history of this area into three main stages. The oldest monazites (ca. 360 Ma) from Skarnoid body within granitoides of the Veporic indicate the Variscan regional metamorphism related to the intrusion of granitoids into the Hladomorná valley Complex. The second age group of monazites ca. 150-145 Ma is from chlorite-sericite phyllite of the Meliatic Bôrka Nappe. This age is probably connected to the exhumation and metamorphic retrogression after the subduction of the Meliata Ocean and during the origin of the Meliatic accretionary wedge. The youngest monazite age group (90-100 Ma) from all complexes presents the Alpine overprint during the main phase of the Western Carpathian nappe stacking.

Acknowledgement: Financial support from the Grant Agency for Science, Slovakia (project VEGA 1/0085/17) and from the Slovak Research and Development Agency (project APVV-17-0170) is gratefully appreciated.

References:

Klinec A. 1966: Zum Bau und Bildung des Veporiden-Kristallin. Sbor. Geol. vied, rad ZK, 6, 7–28.

Klinec A. 1971: The main tectonic elements in the eastern Veporides. Geol. práce, Správy, 57, 105–109.

Vozárová A. 1996: Tectono-sedimentary evolution of late Paleozoic basins based on interpretation of lithostratigraphic data (Western Carpathians, Slovakia). Slovak Geol. Mag., 3–4/96, 251–271.

Mello J., Reichwalder P. & Vozárová A. 1998: Bôrka nappe: high-pressure relic from the subduction-accretion prism of the Meliata ocean (Inner Western Carpathians, Slovakia). Slovak Geol. Mag., 4, 261–273.

Mock R., Sýkora M., Aubrecht R., Ožvoldová L., Kronome B., Reichwalder P. & Jablonský J. 1998: Petrology and stratigraphy of the Meliaticum near the Meliata and Jaklovce Villages, Slovakia. Slovak Geol. Mag., 4, 223–260.

Plašienka D., Méres Š., Ivan P., Sýkora M., Soták J., Lačný A., Aubrecht R., Bellová S. & Potočný T. 2019: Meliatic blueschists and their detritus in Cretaceous sediments: New data constraining tectonic evolution of the West Carpathians. Swiss J. Geosci., 112, 55–81.

Lačný A., Plašienka D. & Vojtko R. 2016: Structural evolution of the Turňa Unit constrained by fold and cleavage analyses and its consequences for the regional tectonic models of the Western Carpathians. Geol. Carpath., 67, 177–193.

Thermodynamics of mimetites

BARTOSZ PUZIO[1], JULIA SORDYL[1] and MACIEJ MANECKI[1]

1 – Department of Mineralogy, Petrography and Geochemistry, Faculty of Geology, Geophysics and Environmental Protection, AGH University of Science and Technology, al. Mickiewicza 20, 30-059 Krakow, Poland; bpuzio@agh.edu.pl; sordyljulia@gmail.com.pl; gpmmanec@cyf-kr.edu.pl

Mimetite $Pb_5(AsO_4)_3Cl$, apatite supergroup member, is a mineral of very low solubility. A very flexible structure of apatite allows for substitution of Cl by F, OH, Br, I or even CO_3. Halogenated mimetites are probably also quite insoluble. Due to lack of solubility constants K_{sp} at temperature ranging from 5 up to 75°C, and other thermodynamic parameters (enthalpy of formation ΔH^o_f, specific heat capacity C^o_p entropy of formation ΔS^o_f, Gibbs free energy of formation ΔG^o_f), it is unclear which of the investigated phases is the most soluble? Which is the most stable in given experimental conditions? Answers on these questions have multiple mineralogical, environmental and technological consequences.

Hence, the objective of this study was to run dissolution experiments of synthetic halogenated analogs of mimetite: $Pb_5(AsO_4)_3F$, $Pb_5(AsO_4)_3OH_{0.87}(CO_3)_{0.04}$, $Pb_5(AsO_4)_3Cl_{0.80}(CO_3)_{0.05}$, $Pb_5(AsO_4)_3Br_{0.80}(CO_3)_{0.05}$, and $Pb_5(AsO_4)_3OH_{0.62}I_{0.46}$., and calculation their thermodynamic functions of state.

Phases have been successfully synthesized by precipitation from aqueous solutions (in normal atmosphere) and analyzed via pXRD, SEM-EDS, FTIR, Raman spcectroscopy, thermal analysis with gas analysis and synchrotron pXRD (Sordyl et al. 2020). Afterwards, batch dissolution and dissolution–recrystallization experiments of five synthesized precipitates were conducted in triplicates at 5, 15, 25, 35, 45, 55, 65 and 75 °C, pH = 3.5 (to avoid crystallization of secondary phases during dissolution) and in a 0.05 M NH_4NO_3 background electrolyte. The experiments were carried out for a period of 6 (dissolution) and 9 (dissolution–recrystallization) months. A plateau in the [Pb] evolution patterns was used to determine equilibrium because of nonstoichiometric behavior of As and X ions in the solution. The ionic activity products (IAP) of the mimetites series were calculated based on the dissolution reaction:

$$Pb_5(AsO_4)_3X \;<=>\; 5\{Pb^{2+}\} + 3\{AsO_4^{3-}\} + \{X^-\}$$

where X denotes activity of F^-, OH^-, Cl^-, Br^-,I^- and CO_3^{2-}.

The new, experimentally determined values of $logK_{sp}$ at 25 °C for mimetites are: -76.16±0.72; -76.47±0.35; -76.17±0.35; -75.42±0.21 and -75.84±0.48 respectively. The $logK_{sp}$ of $Pb_5(AsO_4)_3Cl$ determined here is in good agreement with the $logK_{sp}$ determined by Bajda, 2010. The discrepancy equals to 0.24%. The nonlinear regression of $logK_{sp}$ versus temperature and thermodynamic data of specific ions allowed for calculation of ΔH^o_f, C^o_p, S^o_f and ΔG^o_f. The calculated ΔG^o_f for mimetites increases linearly with increase of ionic radius of X^-. Thus, the most stable phase is F-mimetite while the least stable, in terms of Gibbs free energy of formation, is probably pure (OH and CO_3 free) I-mimetite. The thermodynamic data from dissolution experiment and calorimetric measurements (high-temperature oxide melt calorimetry) were also compared. The thermodynamic data reported in this study supplement existing databases used in geochemical modeling.

Acknowledgement: Financial support for the research was provided to B.P. by the Polish National Science Centre (NCN) grant No. 2017/27/N/ST10/00776.

References:

Bajda T. 2010: Solubility of mimetite $Pb_5(AsO_4)_3Cl$ at 5–55 °C. Environ. Chem. 7, 268–278.

Sordyl, J., Puzio, B., Manecki, M., Borkiewicz, O., Topolska, J., and Zelek-Pogudz, S. 2020: Structural Assessment of Fluorine, Chlorine, Bromine, Iodine, and Hydroxide Substitutions in Lead Arsenate Apatites (Mimetites)–$Pb_5(AsO_4)_3X$. Minerals, 10, 494.

Paleomagnetic "cross-bedding" test on the Ediacaran Lopata Fm. redbeds of the Yenisei Ridge: verifying the hypothesis of hyperactivity of the geomagnetic field at the boundary of the Precambrian and Phanerozoic.

DMITRIY RUDKO[1], SERGEY RUDKO[2], ANDREY SHATSILLO[2], NIKOLAY KUZNETSOV[2]

1 – Schmidt Institute of Physics of the Earth of the Russian Academy of Sciences; Bolshaya Gruzinskaya str., 10-1,Moscow 123242,Russia; dvrudko@gmail.com
2 – Geological Institute, Russian Academy of Sciences; 119017, Pyzhevsky lane, 7- 1. Moscow, Russia; svrudko@gmail.com

Paleomagnetic data on the late Ediacaran has accumulated in recent decades and has led to the hypothesis of hyperactivity of the geomagnetic field at the boundary of the Precambrian and Phanerozoic (Bazhenov et al. 2016). The starting point for the hypothesis was the discovery of an anommalous magnetostratigraphic record in some sections of the late Ediacaran in the Baltica. In these sections, an unusually large number of magnetic polarity zones was found through a relatively low stratigraphic thickness — 27 reversals per 90 m of a section in the Erga Fm. of the Winter Coast of the White Sea (Popov et al. 2005) and more than 30 reversals per 110 m in the Zigan Fm. of the Southern Urals (Bazhenov et al. 2016). A similar phenomenon was recorded in a typical section of the late Precambrian Lopata Fm. in the northeastern part of the Yenisei Ridge (Siberian Platform) (Shatsillo et al. 2015) – here in a section of 60 m thickness, reveals 60 reversals. Moreover, the actual number of reversals recorded in the Lopata Fm. may be even greater, and possibly significantly greater, which is determined by the current detalization of paleomagnetic sampling of the section. In particular, when attempting a layer-by-layer study of the supposed reversal transition zone in a lithologically homogeneous member of siltstones (~ 40 cm thick), eight magnetic polarity zones were detected, while no signs of “transitional” paleomagnetic directions were found in the section.

The Lopata Fm. is composed of red-colored continental sedimentary deposits, the nature of the remanent magnetization of which has not yet been established. This is due to the well known problem of the nature of remanent magnetization in redbeds - the abundance of mineral phases that can carry remanence and the uncertain relationships of their formation over time create difficult interpretations. We show herein a “cross-bedding” paleomagnetic field-test (CB-test) aimed to detect superimposed (secondary) chemical magnetization. Based on existing ideas about (1) the duration of the reversal process and (2) the almost instantaneous (on a geological time scale) accumulation of cross-bedded laminae, we believe that the presence of boundaries in magnetic zones inside a single cross-bedded unit should clearly indicate the superimposed process of magnetization formation (a positive CB-test result). The coincidence of boundaries in magnetic zones with erosional surfaces bounding the section fragments, with internal cross-bedded structures (a negative CB-test result), gives strong arguments in favor of the close temporal link between the formation of natural remanent magnetization and sedimentation processes, i.e., may indicate the primary nature of magnetization in the studied rocks.

At the base of a studied section of the Lopata Fm, above the pack of basal conglomerates, lies a pack of sandstones and siltstones, forming several cross-bedded layers separated by erosional boundaries. According to the results of our paleomagnetic studies, at least two zones of magnetic polarity were identified inside this unit. We sampled a continuous profile with a thickness of 60 cm from the cross-bedded member, inside which at least 3 erosional boundaries were confidently established (Fig.1). In the lower part of the selected profile, there are several thin cross-bedded layers with poorly set boundaries. Sixty one oriented samples were made from a complete profile, which was subsequently subjected to temperature demagnetization. In most of the samples (58 samples), a characteristic component of remanence with blocking temperatures of 650–680 °C is confidently established. The component is represented by directions of both polarities, while the boundaries of the magnetic zones coincide within a centimeter with erosional boundaries that are reliably identified. This allows us to conclude that the CB- test shows negative result. Thus, there are serious reasons to believe that the magnetostratigraphic record in the rocks of a typical section of the Lopata Fm. is not related to chemical magnetization, separated in time from sediment accumulation, but has a synsedimentational age. That is, the anomalous magnetostratigraphic record contained in the Lopata Fm. probably reflects the behavior of the geomagnetic field at the termination of the Precambrian.

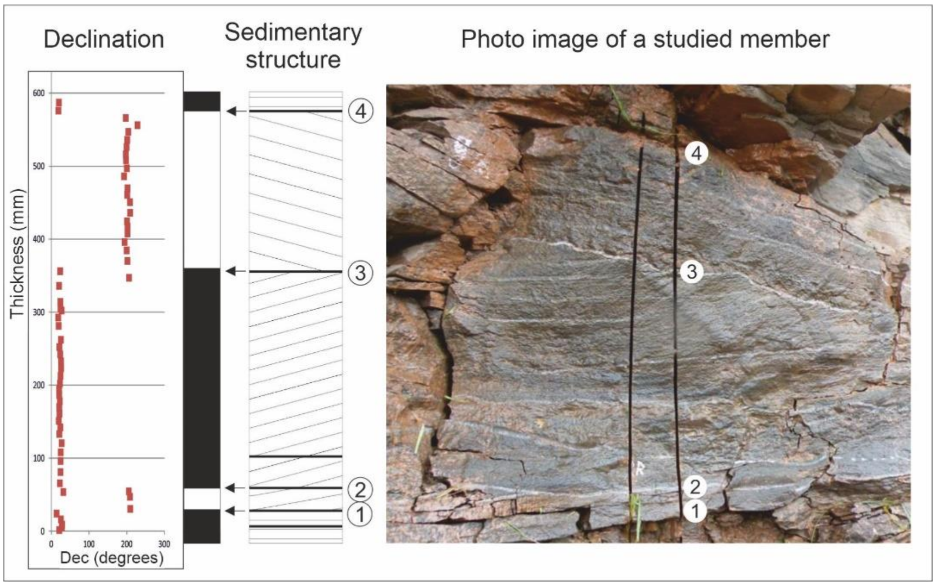

Figure 1. Magnetostratigraphy through a cross-bedded member at the base level of a typical section of the Lopata Fm on the Teya River (4 km upstream the Teya village).

Acknowledgement: The research was partially supported by RFBR (project No. 19-05-00794).

References:

Bazhenov, M. L., Levashova, N. M., Meert, J. G., Golovanova, I. V., Danukalov, K. N., & Fedorova, N. M. (2016). Late Ediacaran magnetostratigraphy of Baltica: evidence for magnetic field hyperactivity?. Earth and Planetary Science Letters, 435, 124-135.

Popov, V. V., Khramov, A. N., & Bachtadse, V. (2005). Palaeomagnetism, magnetic stratigraphy, and petromagnetism of the Upper Vendian sedimentary rocks in the sections of the Zolotitsa River and in the Verkhotina Hole, Winter Coast of the White Sea, Russia. Russian Journal of Earth Sciences, 7(2).

Shatsillo, A. V., Kuznetsov, N. B., Pavlov, V. E., Fedonkin, M. A., Priyatkina, N. S., Serov, S. G., & Rudko, S. V. (2015, December). The first magnetostratigraphic data on the stratotype of the Lopata Formation, northeastern Yenisei Ridge: problems of its age and paleogeography of the Siberian Platform at the Proterozoic–Phanerozoic boundary. In Doklady Earth Sciences (Vol. 465, No. 2, pp. 1211-1214). Pleiades Publishing.

Efficiency of selected anions removal by Mg/Al and Mg/Fe LDH obtained with different sources of Mg

KAROLINA RYBKA[1] and JAKUB MATUSIK[1]

1 – Department of Mineralogy, Petrography and Geochemistry, Faculty of Geology, Geophysics and Environmental Protection, AGH University of Science and Technology, al. Mickiewicza 20, 30-059 Krakow, Poland; krybka@agh.edu.pl; jmatusik@agh.edu.pl

The number of methods used for wastewater treatment is constantly growing and includes numerous studies on different materials. With a rapidly growing amount of wastewaters, there is a high demand for low-cost and efficient materials dedicated for specific industrial wastewaters. Adsorption is considered to be a rapid, efficient and relatively cheap wastewater treatment process, therefore adsorption efficiency of different types of adsorbents is studied. However, a minority of them are appropriate for the removal of anions. Layered Double Hydroxides (LDH) are a large group of crystalline non-silicates with general formula: $[Me^{II}_{1-x} Me^{III}_{x} (OH)_2]^{x+} [A^{n-}]_{x/n} \cdot y H_2O$, where Me^{II} and Me^{III} are divalent- and trivalent metals, respectively. Their structure comprises of positively charged layers of metal hydroxides with weakly bonded anions counterbalancing the positive charge. As a result LDH have excellent anion-exchange properties. They are rare in nature, but can be easily synthesized in the laboratory, where their structural features and therefore adsorption properties can be controlled. Usually LDH are synthesized with the excessive use of chemical reagents, which generates a high cost of the final material. This study focused on the synthesis of Mg-Al and Mg-Fe LDH, which are the two most common LDH groups, where Mg precursor was replaced with abundant and cheap magnesite (M) (Grochów deposit, Poland). The materials were obtained via a simple co-precipitation method, with 2 h ageing instead of typically used 24 h. The adsorption affinity of the products towards As(V), P(V) and Cr(VI) was studied and compared to the adsorption efficiency of reference samples of Mg/Al and Mg/Fe LDH obtained from chemical reagents.

For the synthesis of the reference samples, $MgCl_2 \cdot 6H_2O$, instead of M, was used as a source of Mg(II). For all materials, $AlCl_3 \cdot 6H_2O$ or $FeCl_3 \cdot 6H_2O$ were used as a source of Al(III) or Fe(III) respectively. Prior to the synthesis, chemical reagents were dissolved in water and the M was dissolved in pure HCl to obtain Me^{II} and Me^{III} solutions. Then, appropriate solutions were dropwise added to the 2 M NaCl, with constantly controlled pH=10 with NaOH aqueous solution. The obtained precipitates were aged for 2 h, washed and dried at 60˚C overnight. For the adsorption experiments, aqueous solution of $Na_2HAsO_4 \cdot 7H_2O$, KH_2PO_4 and $K_2Cr_2O_7$ were used as sources of As(V), P(V) and Cr(VI) respectively, with initial pH set to 5 and concentration range of 2 - 25 mmol/L. The anion concentrations were determined using colorimetric methods: molybdenum blue for As(V) and P(V) and 1,5-diphenylcarbazide for Cr(VI). All the solids before and after adsorption experiments were characterized by XRD and FTIR.

The XRD confirmed the presence of Mg/Al and Mg/Fe LDH as compared to their natural analogues: hydrotalcite (ICDD #14-191) and pyroaurite (ICDD #14-293) standards, respectively. For the M/Al sample, an admixture of gibbsite was also present. Therefore, despite the short ageing time, all materials were successfully synthesized. The FTIR spectra exhibited bands attributed to the presence of water at ~3450 cm^{-1}, Me-O vibrations below 1000 cm^{-1} and bands related to the presence of carbonates in the LDH interlayer space in the 1510-1360 cm^{-1} region. Adsorption isotherms indicate that the materials exhibited high adsorption capacity depending on the studied anionic adsorbate. For the M/Al and M/Fe LDH, adsorption efficiency towards As(V) and Cr(VI) was lower than for the reference samples and did not exceed 600 mmol/kg. However, these materials were equally efficient scavengers of P(V), where adsorption efficiency of the materials derived from magnesite was as high as their analogues derived from chemical reagents and reached ~15 000 mmol/kg.

The XRD patterns after adsorption experiments showed, that the structure of treated LDH did not change significantly. In the case of Mg/Fe and M/Fe materials the LDH peaks intensity decreased as a result of partial dissolution. The diffractograms of Mg/Al after As adsorption and Mg/Fe and M/Fe after P adsorption showed peaks attributed to Mg and Al-As and M-P bearing phases, respectively, suggesting precipitation as an additional mechanism of As and P removal. In turn, the Mg/Al pattern after Cr adsorption exhibited reflections characteristic for $Al(OH)_3$ and $MgCl_2$. The FTIR spectra in all cases showed appropriate bands related to the studied elements. Moreover, the bands attributed to carbonates in the spectra of Mg/Fe and M/Fe were of lower intensity, which may indicate either partial dissolution of LDH or anion exchange with adsorbate.

LDH materials were successfully derived via transformation of magnesite. M/Al and M/Fe were less effective than their reference analogues in the removal of As(V) and Cr(VI). However, no significant difference was noticed in the case of P(V) adsorption. In general, all materials showed a good affinity towards As(V), Cr(VI) and P(V).

Acknowledgement: This research was supported by the National Science Centre, Poland under the project no. 2017/27/B/ST10/00898.

Cockroaches as early pollinators

HEMEN SENDI[1]

1 – Institute of Zoology, Slovak Academy of Sciences, Dúbravská cesta 9, 845 06 Bratislava, Slovakia
hemen.sendi@savba.sk

The global turnover from abiotic to biotic pollination in the Mesozoic, firstly accomplished by nectarivores in gymnosperms, and later, by modern pollinators in angiosperms had a significant impact on past and extant ecosystems since modern flowering plants (the most diverse group of terrestrial plants) are mostly insect-pollinated (Ren et al., 2009; Khramov and Lukashevich, 2019; Hu et al., 2008). Nevertheless, direct fossil evidence for Mesozoic flower pollination is scarce. Our research provides four new species of cockroaches from the families Umenocoleidae, Alienopteridae, and Liberiblattinidae from Baremian Lebanese amber and Cenomian Myanmar amber. The specimens have pollen grains attached to the body, and together with unique morphological adaptations, they provide evidence for flower and gymnosperm pollination and cockroach nectarivory during the Early Cretaceous. The forewing surface of a newly described cockroach is also unique, with photonic crystal structures within the scales, similar to those of butterflies and curculionid beetles (Vukusic and Sambles, 2003). Earlier, Hinkelman (2020) described a new cockroach, *Formicamendax vrsanskyi*, with attached pollen grains, and together with the newly described species, they refine our understanding of early pollinators and indicate well established insect-plant associations in the Cretaceous. In addition, they further emphasize high specialization and huge species diversity of cockroaches from (sub)tropical Lebanese and Myanmar Kauri forests. The dynamic period of modern pollinators across the K/Pg boundary does not seem associated with the interactions of cockroaches with plants, as in the Maastrichtian, when no significant change occurred among plants, all Cretaceous lineages of pollinating cockroaches with an externally protruding ovipositor went extinct (Vršanský et al., 2017).

References:

Hinkelman, J. 2020. Earliest behavioral mimicry and possible food begging in a Mesozoic alienopterid pollinator. Biologia, 75(1), 83-92.

Hu, S., Dilcher, D.L., Jarzen, D.M. & Taylor, D.W. 2008. Early steps of angiosperm–pollinator coevolution. Proceedings of the National Academy of Sciences of the United States of America 105(1), 240–245.

Khramov, A.V. & Lukashevich, E.D. 2019. A Jurassic dipteran pollinator with an extremely long proboscis. Gondwana Research, 71, 210–215.

Ren, D., Labandeira, C.C., Santiago-Blay, J.A., Rasnitsyn, A., Shih, C., Bashkuev, A., Logan, M.A.V., Hotton & L., Dilcher, D. 2009. A probable pollination mode before angiosperms: Eurasian, long-proboscid scorpionflies. Science, 326(5954), 840–847.

Vršanský, P., Oružinský, R., Aristov, D., Wei, D.D., Vidlička, Ľ., & Ren, D. 2017. Temporary deleterious mass mutations relate to originations of cockroach families. Biologia, 72(8), 886-912.

Vukusic, P. & Sambles, J.R. 2003. Photonic structures in biology. Nature, 424(6950), 852.

Lower Oligocene mixed siliciclastic-carbonate turbidites – results of macro- and microscopic observations (Szczawa Tectonic Window, Polish Outer Carpathians)

PIOTR SIWEK[1] and MAREK WENDORFF[1]

1 – Faculty of Geology, Geophysics and Environmental Protection, AGH University of Science and Technology, A. Mickiewicza 30 av., 30-059 Kraków, Poland, petersiwek18@gmail.com, wendorff@agh.edu.pl

Mixed deposits are composed of mixtures of siliciclastic grains, carbonate grains (mainly bioclasts and intraclasts) and a mixture of silt, clay, carbonate mud and micrite (Mount, 1985; Chiarella et al., 2017) According to Chiarella et al. (2017), there are two main types of mixing: strata mixing, which results from interbedding of siliciclastic and carbonate beds, and compositional mixing which occurs when siliciclastic and carbonate particles are mixed and deposited contemporaneously in time and space to form millimetre- to metre-scale beds. Szczawa Tectonic Window is located in Polish Outer Western Carpathians, 60 km south of Cracow, Poland. The studied section is a 165 m thick fragment of a succession comprising lower Oligocene strata described as the Grybów Beds, and Cergowa Beds of the Grybów Unit (Oszczypko-Clowes & Oszczypko, 2004). The studied succession was chosen for detailed centimetre-by-centimetre logging, photographic documentation and sampling. Microscopic observations including carbonates content estimations were performed on 28 thin sections; moreover, 55 samples obtained from different lithological types were prepared to measure carbonates content using the Scheibler's method.

The succession is composed of turbiditic Bouma-type sequences, which form very thin to very thick beds intercalated with marls, and thick and very thick massive sandstones described as Cergowa-type arenites. Turbiditic Bouma-type sequences constitute about 73% of studied succession. They form beds 5–315 cm thick. The lowermost parts of these beds are developed as parallel-laminated sandstones (Tb), ripple cross-laminated sandstones and coarse siltstones (Tc) and parallel-laminated siltstones (Td). Tbcd, Tcd, Td sequences can attain 30 cm in thickness. They pass into calcareous mudstones, or into massive marls (Te). Thickness of Te subdivisions vary from some centimetres to more than 150 cm (up to 275 cm). Within turbidite beds, there occur depositional rhythms composed of very thin and thin beds of marls alternating with very thin mudstone intercalations, which together form packets up to 50 cm thick. The whole succession contains solitary extremely thick beds: sandstone- marlstone couplets, up to 9.4 m thick. Sandstones are very thick, medium to fine-grained, with massive lower parts and uppermost parts which exhibit signs of soft-sediment deformation and laminated structures. These are followed by normally-graded calcareous mudstones and grading into massive marlstones.

Compositional mixing is the major type of mixing observed in the Szczawa section. Almost the entire succession contains carbonates as: 1) skeletal grains (lithoclasts and bioclasts) and matrix/cements or 2) almost only matrix/cements with minor fraction of carbonate grains. The first case corresponds to classical definition of compositional mixing, and it is applicable to sandstones and siltstones. The second case generally refers only to mudstones and marlstones.

Sandstones and siltstones developed as divisions of Bouma-type sequences contain relatively high proportion of carbonates, varying from 15% to more than 50%. The proportion of carbonate grains in total grain population changes from less than 1–2% of bulk volume of framework grains to more than 30% in some laminated siltstones and sandstones. Carbonate grains occur mostly as abraded lithoclasts of micrite/sparry texture, and bioclasts – foraminifera tests and other microplanktonic skeletal remains. Microscopic observations of laminated intervals reveal two regularities: 1) segregation of components in ripple cross-laminations within single cross lamina; 2) alternating of silt laminae enriched in carbonates and laminae depleted of carbonates. Massive sandstones which constitute the lower part of extremely thick beds are usually lacking significant amount of carbonate grains in the total grain number. These are mainly coarse and very coarse sand-sized bioclasts.

In the studied succession, there are different patterns of change of carbonates content in vertical profiles of individual beds. In the case of turbidite beds composed of Bouma-type sequence, carbonates content: 1) increases towards bed top – Tbcd, Tcd, Tc, Td intervals usually contain relatively high proportion of carbonates (20–35% of total weight) and grades into marlstones which contain more than 40% of carbonates; 2) is highest in laminated intervals (some ripple cross-laminated intervals contain more than 50% of carbonates in rock total weight) and decreases upward. The highest content of carbonates is recorded from depositional rhythms composed of thin-bedded marlstones, up to 60%.

In the studied section, only characteristic depositional rhythms composed of thin-bedded marlstones (carbonate beds), which interbed turbidite beds (mixed ones) fit the definition of strata mixing used by Chiarella et al. (2017). Moreover, it is the example of coexistence of compositional and strata mixing.

The structures and textures of laminated intervals, especially segregation of components, were formed due to hydraulic separation of fractions of different physical properties. Hydraulic sorting is most effective in some cross laminae: heavy siliciclastic grains are separated from lighter and coarser bioclasts. Changes of carbonate content in vertical profiles of beds may be owing to segregation of carbonate grains and pelitic carbonate matrix within sediment gravity flows. Mixing of marlstone rhythms with turbidite beds, classified as strata mixing of bed-scale, can be interpreted, according to Chiarella et al. (2017), as the result of: 1) short-term sea level changes and deposition of marlstone rhythms during relative sea level rise; 2) short-term climate changes from arid (marlstones) to humid (turbidite beds) conditions or 3) tectonic control on the sediment supply from the continent. Moreover, the occurrences of extremely thick sandstone-marlstone beds may indicate catastrophic events, e.g. floods or large-volume submarine slumps triggered by seismic shocks or tsunamis.

References:

Chiarella D., Longhitano S. G. & Tropeano M. 2017. Types of mixing and heterogeneities in siliciclastic-carbonate sediments. *Marine and Petroleum Geology* 88, 617–627.

Mount J.F. 1985. Mixed siliciclastic and carbonate sediments: a proposed first-order textural and compositional classification. *Sedimentology* 32, 435–442.

Oszczypko-Clowes M. & Oszczypko N. 2004. The position and age of the youngest deposits in the Mszana Dolna and Szczawa tectonic windows (Magura Nappe, Western Carpathians, Poland). *Acta Geologica Polonica* 54, 339–367.

Application of emerging contaminants analysis to determine the impact of river infiltration on groundwater quality

KINGA ŚLÓSARCZYK[1]

1 – Institute of Earth Sciences, Faculty of Natural Sciences, University of Silesia in Katowice, Będzińska 60 St., 41-200, Sosnowiec, Poland; kinga.slosarczyk@us.edu.pl

Over the last decades water pollution has become a serious problem in many countries of the world. This issue involves important supplies of drinking water, which include aquifers. Among the contamination sources that may contribute to deterioration of groundwater quality, there are polluted rivers and infiltration of surface water into the ground. In this way, a wide range of contaminants can reach not only shallow aquifers, but, in some cases, deeper groundwater reservoirs may also be vulnerable. Currently, different methods are applied to determine the hydrologic connection between surface and groundwater, including environmental tracers, geochemical modeling and isotopic studies. The two latter methods were used in the study on groundwater chemistry in the Gliwice-Łabędy well-field area (southern Poland) and the findings suggested the negative influence of the Kłodnica River infiltration on groundwater quality of a Triassic carbonate aquifer. It was especially noticeable in the groundwater abstracted from the S2Cz well, located in the vicinity of the river (Ślósarczyk, Jakóbczyk-Karpierz, 2018). However, having regard to growing concern on emerging contaminants (ECs) in water and high persistence of some compounds, ECs could be also used as environmental tracers to confirm the connection between polluted river and groundwater quality, especially since the Kłodnica River receives sewage discharges from Wastewater Treatment Plants (WWTP), which are the main source of ECs.

In order to confirm the negative impact of river infiltration on the aquifer in the area of the Gliwice-Łabędy well-field, four water samples were collected: 1 sample of untreated sewage and 1 sample of treated sewage from the WWTP "Gliwice" as well as 1 sample of surface water from the Kłodnica River and 1 sample of groundwater from the S2Cz well. The analyses of 82 compounds qualified as emerging contaminants (incl. pharmaceuticals and personal care products) were performed with the use of the liquid chromatography tandem mass spectrometry method (LC-MS/MS).

The analysis reavealed the presence of emerging contaminants in all the collected samples. Most of the studied compounds were detected in both untreated sewage (65) and treated sewage (59) with the total concentrations exceeding 64 μg/L and 61 μg/L, respectively. The slight difference in ECs concentrations in sewage before and after treatment processes implies lower efficiency of applied treatment methods and persistence of some ECs. Therefore, wastewater discharges to the river resulted in the presence of 53 ECs in the water sample from the Kłodnica River, where the sum concentrations of ECs was nearly 50 μg/L. Furthermore, some of ECs (10) were detected in the groundwater sample as well. In this case, the total ECs concentration did not exceed 1 μg/L, nevertheless, it is highly probable that their occurrence in the aquifer is associated with river infiltration, since ECs observed in groundwater from the S2Cz well are the same compounds as in the surface water sample. Thus, ECs analysis, along with geochemical modeling and isotopic studies, may be assumed as another method useful in determination of the impact of river infiltration on groundwater quality. It may also serve as a supportive method in identification of pollution sources.

Acknowledgement: This study was supported by the Ministry of Sciences and Higher Education of Poland.

References:

Ślósarczyk, K., Jakóbczyk-Karpierz, S. 2018. Application of sulfate isotope studies and geochemical modeling in determining processes affecting groundwater chemistry in the Gliwice-Łabędy well-field area. *Przegląd Geologiczny*, 66, 8, 495-502.

Cockroach fauna of mid-Cretaceous Myanmar amber as valuable insight into the phylogeny of the group

LUCIA ŠMÍDOVÁ[1]

1 – Institute of Geology and Paleontology, Charles University, Albertov 6, 12800, Prague, Czech Republic; smidovaluc@natur.cuni.cz

The order Blattodea comprises of approximately 4 500 living species of cockroaches and 2 700 species of termites (Isoptera) (Beccaloni and Eggleton, 2011) which makes it the eighth largest order of insects (Stork, 2018). However, its diversity peaked during previous geological eras. This research is focused mainly on one of the crown groups, the family Blattidae. Up to date, we have recognized the following species of this family from the Myanmar amber: *Balatronis cretacea* Šmídová et Lei, 2017, *Bimodala ohmkuhnlei* Šmídová, 2018, *Bubosa poinari* Šmídová, 2020, *Cretaperiplaneta kaonashi* Qiu, Che et Wang, 2020, *Spinka fussa* Vršanský, Šmídová and Barna, 2018.

Each one of them is somehow connected to bark cohort, some of them even specialized to myrmecophilous lifestyle. This coincides with ecological interpretations of the forest's character which gave origin to the amber (Grimaldi et al., 2002; Smith and Ross, 2017). The family Blattidae differs from related families, among other traits, by having two symmetrical valves on the subgenital plate of the female and not-derived laying of the ootheca, the hardened case of cockroach eggs. This is a key element in distinguishing between families in the complex of Mesoblattinidae-Blattidae-Ectobiidae (Šmídová, 2018). The family Mesoblattinidae is represented in Myanmar amber with genus *Spinaeblattina* Hinkelman, 2019 carrying pollen (Hinkelman, 2020). Representatives of this family possess multisegmented styli, contrary to family Blattidae, which has from one to several segments.

The exceptional state of preservation of the inclusions from mid-Cretaceous Myanmar amber allows us to correlate traits on the level of anatomical structures as it was done for above mentioned species with behavior such as oviposition.

Acknowledgement: I would like to give thanks to the anonymous reviewer and Dr. Peter Vršanský for his guidance.

References:

Beccaloni, G. W., Eggleton, P. 2011. Order Blattodea Brunner von Wattenwyl, 1882. In: Zhang, Z.-Q. (Ed.) *Animal biodiversity: An outline of higher-level classification and survey of taxonomic richness. Magnolia Press, Auckland*, pp. 199–200.

Grimaldi, D., Engel, M. S., Nascimbene, P. C. 2002. Fossiliferous Cretaceous Amber from Myanmar (Burma): Its Rediscovery, Biotic Diversity, and Paleontological Significance. *American Museum Novitates* 3361, 1–71.

Hinkelman J., Vršanská, L., 2020. A Myanmar amber cockroach with protruding feces contains pollen and a rich microcenosis. *The Science of Nature*, (in press).

Stork, N. E. 2018. How Many Species of Insects and Other Terrestrial Arthropods Are There on Earth? *Annual Review of Entomology* 63, 31–45.

Šmídová, L., 2018. Unusual cockroaches (Blattidae) from Cenomanian Myanmar amber. *Univerzita Karlova v Praze, Přírodovědecká fakulta,* p. 70, (Master thesis).

Temperature stability of chemically synthesized alginate-based aerogel during metal ions removal

MACIEJ SOBCZYK[1], AKINNYI AKINSUNMADE[2] and TOMASZ BAJDA[1]

1 – Department of Mineralogy, Petrography and Geochemistry, Faculty of Geology, Geophysics and Environmental Protection, AGH University of Science and Technology, al. Mickiewicza 30, 30-059, Kraków, Poland; macieksobczykswim@gmail.com
2- Department of Geophysics, Faculty of Geology, Geophysics and Environmental Protection, AGH University of Science and Technology, al. Mickiewicza 30, 30-059, Kraków, Poland; aniyi200@yahoo.com

The effectiveness of alginate-based aerogel is multifaceted and dependent on many factors. One of the key parameters is temperature variation, since deviations from the appropriate range render its inefficiency.
In this study we attempt to analyze effective sorption capability of alginate-based aerogel and its thermal stability based on TG-DTA measurements.
Aerogel was synthesized via sol-gel process (Maleki, *et al*., 2016) which involves gelation of sodium alginate solution with Ca^{2+} cation followed by freeze-drying in liquid nitrogen and liophylisation.
In order to assess the phase structure of an aerogel, XRD (X-ray Diffraction) analysis was carried out on the synthesized sample and subsequently followed by TG-DTA (Thermogravimetric - Differential Thermal Analysis) measurements to determine a thermal stability of the aerogel. Moreover, functional groups on the surface of studied material were determined utilizing FT-IR (Fourier Transform - Infrared) methods and the analysis of the structure was carried out with SEM-EDS (Scanning Electron Microscope with Energy Dispersive Spectroscopy).
Sequel to the analyses of the synthesized materials, a batch sorption experiment of two metal ions, namely Pb^{2+} and Cd^{2+}, were performed and the responses of the synthesized material were evaluated as a function of the temperature increase. It was delineated that optimum range of temperature at which the material is the most effective as a sorbent for removal of studied metal ions is in a range between 550^{o} and 650^{o} Celsius (Choi *et al*., 2009).
The results of the research suggests that alginate-aerogel is thermally stable within a temperature up to 650^{o}C. Its affinity toward sorption of undesired pollutants is high at this temperature compared to zeolites, metal organic frameworks (MOFs) and activated carbons.

References:

Maleki H., Duraes L., Portugal A., (2014). An overview on silica aerogels synthesis and different mechanical reinforcing strategies. *Non-crystalline Solids*, 385, 55-74.
Choi S., Drese J.H., Jones C.W., (2009). Adsorbent materials for carbon dioxide (CO_2) capture from large anthropogenic point sources. *Sustainable Chemistry*, 2(9), 796-854.

The structural evolution of the enigmatic Jørgenfjellet Nappe from Spitsbergen

EWA STĘPIEŃ[1], ALEKSANDRA WARZECHA[1] and GRZEGORZ ZIEMNIAK[1]

1 – AGH - University of Science and Technology, Faculty of Geology, Geophysics and Environmental Protection, al. Mickiewicza 30, 30-059 Kraków, Poland; estepien12@interia.pl

The metamorphic basement of the Svalbard Archipelago has a complicated internal structure and is traditionally divided into three provinces: the Eastern, Northwestern and Southwestern Basement Province (e.g. Gee & Teben'kov 2004). The Southwestern Basement Province exposed in western Oscar II Land (Spitsbergen) represents a basement that is poorly recognized and lacks detailed mapping and structural framework. The examined metamorphic rocks crop out on the peak and slopes of Jørgenfjellet mountain separated by horizontal tectonic boundary from underlying rocks and represent lithologies that do not correspond with the units presented in geological maps (e.g. Ohta, 1984; Dallmann, 2015). According to the geological map of Oscar II Land, the samples were taken from the St. Jonsfjorden Group which is dated to late Mesoproterozoic – early Neoproterozoic age and is characterized by the pelites and quartzites overlying volcanic and pyroclastic rocks. However, the occurrence of a sequence of metamorphosed marbles, dolomites and pyroclastics suggest that this affiliation can be ruled out. The inconsistencies associated with the lithostratigraphy and tectonics require clarification, therefore the microstructural observations were performed on the metapyroclastic rocks as they were deemed most suitable for deciphering the genesis of this rock unit. The protolith of the rock in question was probably a mudstone with the addition of pyroclastic material, which underwent metamorphism under greenschist facies conditions. The mineral assemblage, dominated by calcite, white mica, biotite, chlorite and dispersed epidote. The occurrence of epidote and titanite suggests a pyroclastic origin of the rock. Rare bands of quartz and feldspar of pyroclastic or detrital origin are less common. The observed opaque minerals are mainly pyrite, chalcopyrite and goethite. The structural observations reveal that the studied sample was subjected to two events of deformation. Ductile to semi-ductile deformation (D1) was followed by a brittle event (D2), which together show complicated intersecting structural relationships. D1 resulted in the formation of a metamorphic foliation emphasized by phyllosilicates. This foliation dips moderately to the ESE. Pressure shadows form asymmetrical patterns around rigid feldspar and quartz porphyroclasts. More flexible minerals, such as micas, are sheared and elongated, creating mica fishes. Carbonate uniaxial veins were rotated about their axis, and calcite has deformed edges. These kinematic indicators show top to the west sense of shear during ductile to semi-ductile D1 deformation. D2 brittle deformation is manifested by traces of porphyroclastic fractures and offsets of their constituent parts. The uniaxial veins were fragmented by E-W trending horizontal fault planes and their offset shows top to the E sense of shear. Brittle microstructures occur parallel to the tectonic boundary that is observed in the outcrop scale.

Petrographic and structural observations suggest that the rocks in question form an approximately 1 km long nappe on the top of the Jørgenfjellet mountain and are exotic concerning the underlying rocks of the St. Jonsfjorden Group. The sequence of pyroclastics, dolomites and marbles were transported to the E-ENE during D2 deformation. It is probably related to the Eurekan (Paleogene) event (e.g. Bergh et al. 1997). The Jørgenfjellet Nappe can be correlated with the Vestgötabreen Complex on Oscar II Land (Kanat and Morris, 1988) or the Peachflya Group of Prins Karls Foreland. The Vestgötabreen Complex crops out to the east of Jørgenfjellet and as the nappe was transported eastward, it is less likely to be its correlative. The Peachflya Group is exposed to the west of Jørgenfjellet and besides containing similar lithological sequence, it is also characterized by top to the west Caledonian structures (Manby, 1986). Therefore, the Jørgenfjellet Nappe may represent fragments of Prins Karls Foreland basement that was transported eastwards during the Eurekan Orogeny.

References:

Gee, D. G., & Teben'kov, A. M. 2004. Svalbard: a fragment of the Laurentian margin. Geological Society, London, Memoirs, 30(1), 191-206.

Ohta, Y. 1985. Geochemistry of Precambrian basic igneous rocks between St. Jonsfjorden and Isfjorden, central western Spitsbergen, Svalbard. Polar Research, 3(1), 49-67.

Dallmann, Winfried K. (2015) Geoscience atlas of Svalbard

Kanat, L. & Morris, A. 1988. A working stratigraphy for central western Oscar Il Land, Spitsbergen

Bergh, S. G., Braathen, A., & Andresen, A. 1997. Interaction of basement-involved and thin-skinned tectonism in the Tertiary fold-thrust belt of central Spitsbergen, Svalbard. AAPG bulletin, 81(4), 637-661.

Manby, G. M. 1986. Mid-Palaeozoic metamorphism and polyphase deformation of the Forland Complex, Svalbard

Finding alternative natural entrances to the Krčahovo-Červené-massif cave system

IVAN ŠULEK[1]

1 – Faculty of Natural Sciences, Comenius University in Bratislava, Mlynská dolina, Ilkovičova 6, 842 15 Bratislava, Slovakia; ivansulek99@gmail.com

The aim of the study is to find new elements of the cave system in the Krčahovo-Červené massif, located in Nizke Tatry in Slovakia. Krčahovo is the west ridge of the Krakova hola mountain and Červené is Krčahovo´s side ridge.Our exploration was focused only up to an altitude of 1209 m above sea level, where there is an entrance to the highest cave explored (Cave on Krčahovo), which can potentially lead to an unknown cave system. This cave is formed in gutenstein limestone of the Fatrikum Unit. On the walls of the cave can be recognised many signs of freatic activity of the river Demänovka. Currently, the river flows over 300 m below the entrance of the cave. The watercourse is mostly formed in allochtone sediments accumulated by river Demänovka and in the glacial moraine from the last Pleistocene glaciation(Bella et al., 2014). These sediments do not allow us to find a natural entrance. However, we have located five to six swallow holes. The number of sinkholes is changing according to river conditions. (Herich, 2017). In the selected swallow holes, we measured the temperature and humidity and we participated in the tracing tests (Auxt et al., 2012). Reconnaissance in the sinkholes allowed us to conclude that the sinkhole in Červené is probably the only one that is related to the cave system. In the underground, we focused mainly on exploring the southernmost parts of Demänová cave system, in the Pustá cave. During our exploration over the years, we have selected three sites that are currently under investigation. The first is The Siphon of Respect, which is located along the erosion base level. The siphon is the southernmost known place where Demänovka reappears from swallow holes from Lúčky. In 2011 we managed to pass the siphon with the help of cave divers. Behind the siphon there is a breakdown, which, according to divers, could be overcome if cavers who are not divers could get there. Further south and 70 m above the siphon there is a second prospective site. It is located in the Corridor of Happiness, which is predisposed by huge tectonic fault that can also be observed on the surface. Overcoming this place would lead to a bypass behind another breakdown currently being explored, where there is a local air draught (Dzúr, 2004). We suspect that the cave continues further south beneath Machnatá valley into the Zapač massif and then into the Krčahovo-Červené massif. The above mentioned tectonic fault appears on the surface in the Zapač massif as a 15-30 cm wide crack (Ventarola). The appearance of air draught is one of the signs of the upper entrance to the cave. The Ventarola is located 110 m above the erosion level of the Demänovka River and is on the same line as the Corridor of Luck and the sinkhole in Červené.

Based on facts gathered over the years we are convinced that the system of caves in the Krčahovo-Červené massif exists, but we are not able to predict when and where the natural entrance will open.

Acknowledgement: We thank to members of Demänovská Valley Cave Club, especially P. Herich ml. for help with surveying and expert assistance.

References:

Bella, P., Haviarová, D., Kováč, L., Lalkovič, M., Sabol, M., Soják M., Struhár, V., Višňovská, Z., Zelinka, J. 2014. Jaskyne Demänovskej doliny, *Správa slovenských jaskýň, Liptovský Mikuláš*, 191.

Auxt, A., Malík, P., Klačanová, Z., Pristaš, P., Filo, J., Šuchová, M., Gretch, J., Gregor, M., Bottlík, F., Mikita, S., Pažická, A., Buček, S., Černák, R., Nagy, A., Michalko, J., Maglay, J., Máša, B., Švasta, J., Danko, D. 2012. Doplnkový prieskum a monitoring ramsarskej lokality - jaskyne Demänovskej doliny. Záverečná správa, *archív SSJ, Liptovský Mikuláš*, 181.

Dzúr, J., 2004. Objav Žikešovho dómu v Pustej jaskyni. Archív Jaskyniarskeho klubu Demänovkská dolina. Published 21.12.2004 [cited 4.3.2019]. Available on www.speleodd.sk/ main.php?pageid=11&novinka=1

Herich ml., P. 2017. O veľkej povodni v Demänovskej doline. Archív Jaskyniarskeho klubu Demänovská dolina. Published 23.8..2018. [cited 15.2.2019]. Available on speleodd.sk/main.php?pageid=11&novinka=565

New data on sedimentology and tafonomy of the Late Miocene locality Polevoe 1 (Northwest Caucasus, Republic of Adygea)

KONSTANTIN TARASENKO[1]

1 – Borissiak Paleontology Institute; Profsoyznaya str.123, Moscow; tarasenkokk@gmail.com

The Late Miocene marine mammals' locality Polevoe was discovered in 2005 (Volkodav, 2007; Tarasenko and Titov, 2009). The locality is situated on the left bank of the Kurdzhips river near its mouth and extends north on the port side of the White River. From this location, the complete skeleton of the *Cetotherium*-like whale *Zygiocetus nartorum* is known (Tarasenko, 2014).

During the work of the research group of the PIN RAS in November 2019, new materials were collected from this locality. The new data make it possible to judge the presence at this location of a significant accumulation of skeletal elements of several individuals, *Z. nartorum* buried in the thickness of the bryozoans-reef. The reef buildings here are confined to the Krasnooktyabr'sk Formation, which reaches up to 5 m in thickness and lies on the Krasnooktyabr'sk Formation (Volkodav, 2007; Beluzhenko et al., 2007; Tarasenko, 2014). The thickness of the bioherm reef is up to 0.7-1 m.

The position of the skeletons in the bone-bearing stratum allows us to judge the absence of a long transfer and to attribute this taphocoenosis to the "ejection fields". The phenomenon of ejection of whales-shore for fossil whales has been studied extremely poorly, primarily because of the lack of detailed taphonomic material that could help restore paleobiocenoses and especially the conditions of the existence of ancient cetaceans. Of the well-known examples of the most ancient natural burial sites of cetaceans, it is necessary to note a representative of Archaeocete from deep-water sediments of the Middle Eocene (Hulbert et al., 1998). Also, several finds are found from deep-water deposits of the Oligocene on the Olympic Peninsula (Washington, USA) (Goedert et al., 1995), in Louisiana (Lancaster, 1986) and several cetaceans from the Espiritu Santo locality, in southern Spain (Sendra, De Renzi, 1999). The remains of a whale from the Middle Miocene of the El Camp basin in Tarragona (northeast of Spain) are represented by an incomplete skeleton of a juvenile individual without articulation of individual skeleton bones (Belaústegui et al., 2011). These remains were buried on a hill; apparently, the burial conditions represented the beginning of shallowing and low sedimentation rates within the carcass. Such conditions cause the natural decomposition and exarticulation of the carcass. The interpretation of this paleo-environment is based on various data: taphonomic data of bone remains, paleoecological and taphonomic information provided by the fauna associated with bones, as well as theriological and sedimentary interpretation of sediments, including the remains of whales. This finding demonstrates the case of the cetacean burial on land in the absence of a fast carcass burial.

The new findings, represented by numerous fragments of the skeletons of *Z. nartorum*, the nature of the location in the bone-bearing lens, the absence of traces of transfer, and also the relatively young ontogenetic age of the individuals, make it possible to suggest massive ejection of these whales on the sandbank formed by bioherm reefs (Fig. 1). This is a rare case when the whales that have washed ashore very quickly undergo a burial process.

One important feature should be noted: if the skeletons are located on the ventral side in the taphocoenoses of "natural death", which is associated with the peculiarities of the carcass burial during its long movement in the open sea, such as the remains of a whale lying on the seabed

Book of abstracts. ISBN 978-83-933330-2-8

in the Santa Catalina basin, coast of California (Bennett et al., 1994; Smith et al., 1998; Allison et al., 1999), the skeleton is usually located "on its side" in taphocoenoses of "ejection fields". The author observed a similar example in modern cases of ejection of cetaceans. The whales thrown ashore lie on their side (usually on the right), and one of the forelimbs is lost in most cases during burial (for example, a thrown blue whale on the Canadian coast near Port Hawkesbury; a high-necked bottlenose near Lopshenga and others). The remains of a whale from Santa Catalina are surrounded by numerous representatives of invertebrate scavengers. Naganuma et al. (1996) describe a similar case in Torishima (western Pacific). In both cases, whale carcasses act as biological oases existing in oxygen-free deep-sea basins. The remains of *Z. nartorum* apparently acted as oases of invertebrate tidal plots of the reef and the wetted water zone.

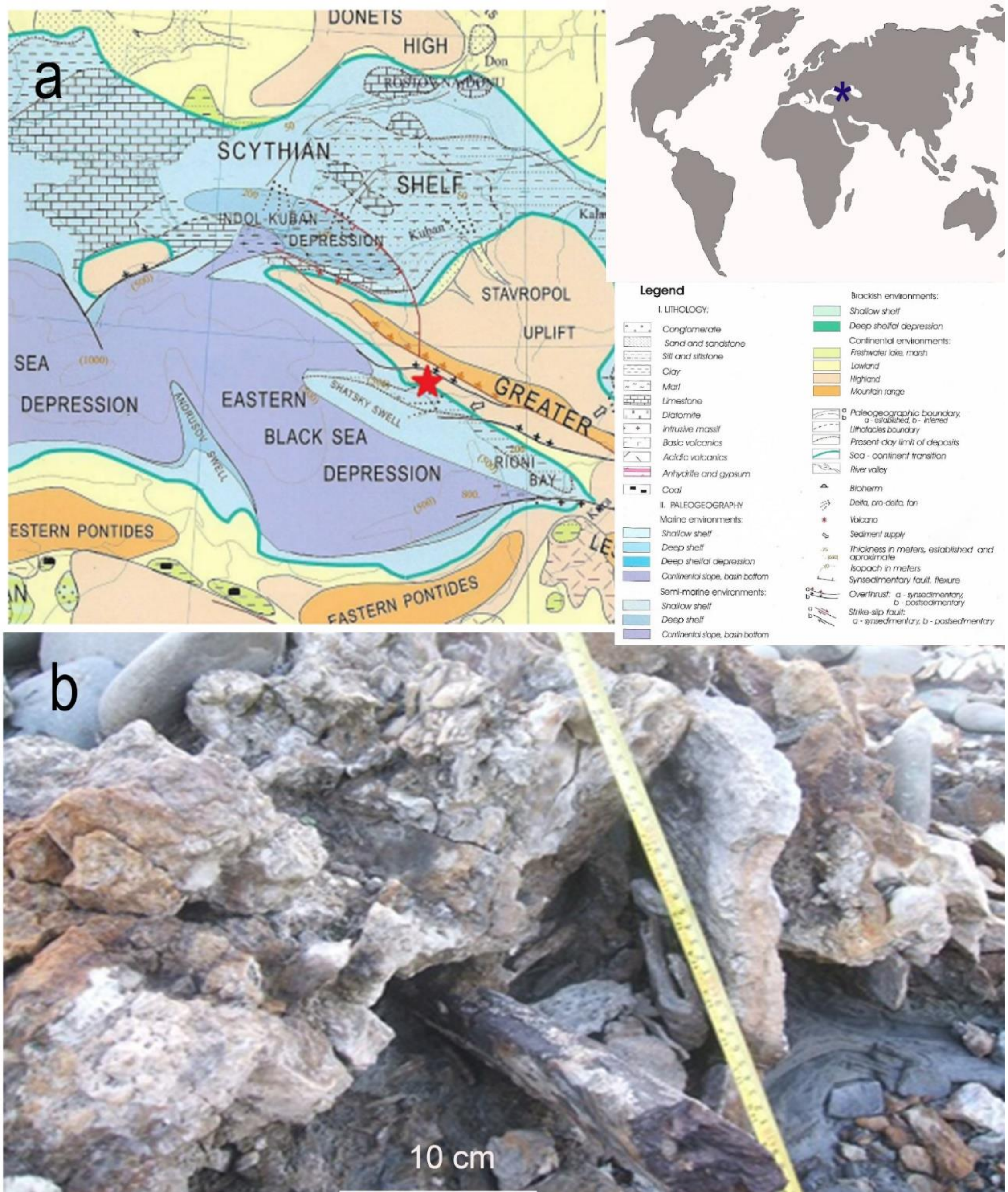

Figure 1. a- Position of the Polevoe Locality on the Paratethys map (red and dark blue stars indicate locality). b- Fragments of the upper jaw of *Cetotherium*-like whale in bioherm reef.

Acknowledgment: I would like to express our gratitude to all those who took part in the excavation in the 2019 season. This study was supported by the Russian Foundation for Basic Research, project no. 18-35-00206

References:

Allison P. A., Smith C. R., Kukert R., Deming J. W, Bennett B. A. 1999. Deep-water taphonomy of vertebrate carcasses: a whale skeleton in the bathyal Santa Catalina Basin. // Paleobiology. 17. P. 78-89.

Belaústegui Z., Gibert J.M. de, Domènech R., Muñiz F., Martinell J. 2011. Taphonomy and paleoenvironmental setting of cetacean remains from the Middle Miocene of Tarragona (NE Spain). Geobios 44, 19-31.

Beluzhenko, E.V., Volkodav, I.G., Derkacheva, M.V., et al., 2007. Oligotsenovye i neogenovye otlozheniya doliny reki Beloi (Adygea) (Oligocene and Neogene Deposits of the Belaya River Valley, Adygea), Maikop: AGU, 109.

Bennet B. A., Smith C. R., Glaser B., Maybaum H. L. 1994. Faunal community structure of a chemoautotrophic assemblage on whale bones in the deep northeast Pacific Ocean. Marine Ecology Progress Series, 108, 205-223.

Goedert J. L., Squires R. L., Barnes L. G. 1995. Paleoecology of whale-fall habitats from deepwater Oligocene rocks, Olympic Peninsula, Washington State. Palaeogeography, Palaeoclimatology, Palaeoecology, 118, 151-158.

Hulbert R. Jr., Petkewich R. M., Bishop G. A., Bukry D. Aleshire D. P. 1998. A new Middle Eocene protocetid whale (Mammalia: Cetacea: Archaeoceti) and associated biota from Georgia. Journal of Paleontology, № 72.V.5, 907-927.

Lancaster W. C. 1986. The taphonomy of an Archaeocete skeleton and its associated fauna. In: Schiebout, J. A., van den Bold, W. (eds.), Montogomery Landing Site, marine Eocene (Jackson) of central Louisiana. Proc. Gulf Coast Assoc. Geol. Soc. Symposium, Baton Rouge, Louisiana, 119-131.

Naganuma T., Wada H., Fujioka K. 1996. Biological community and sediment fatty associated with the deep-sea whale skeleton at the Torishima Seamount. Journal of Oceanography, 52, 1-15.

Sendra J., De Renzi M. 1999. A taphonomical study of marine mammals from the Almeria region, SE Spain. In: BSRG / BGRG SE Spain Field Meeting Guide Book (edited by Mather, A. E. & Stokes, M.), University of Plymouth, England, 169-176.

Smith C. R., Maybaum H. L., Baco A. R., Pope R. H., Carpenter S. D., Yager P. L., Macko S.A., Deming J. W. 1998. Sediment structure around a whale skeleton in the deep Northeast Pacific: macrofaunal, microbial and bioturbation effects. Deep-Sea Research II, 45, 335-364.

Tarasenko, K.K. 2014. New genera of baleen whales (Cetacea, Mammalia) from the Miocene of the Northern Caucasus and Ciscaucasia: 3. Zygiocetus gen. nov. (Middle Sarmatian, Adygea), Paleontol. Zh. 5, 99–109.

Tarasenko, K.K. and Titov, V.V. 2007. Records of *Cetotherium* sp. (Cetacea, Mammalia) in the Middle Sarmatian of Adygea, in Sovremennaya paleontologiya: klassicheskie i noveishie metody. Tezisy IV Vserossiiskoi nauchnoi shkoly molodykh uchenykh–paleontologov (IV AllRussia Scientific School of Young Scientists Paleontologists on Modern Paleontology: Classical and New Methods), Moscow: Paleontol. Inst. Ross. Akad. Nauk, 50–51.

Volkodav, I.G. 2007. Geologiya Adygei (Geology of Adygea), Maikop: AGU, 251.

Raman spectroscopic study of monazite and xenotime – signatures and features from experimental products

Fabian TRAMM[1], Bartosz BUDZYŃ[1], Grzegorz RZEPA[2]

1 – *Institute of Geological Sciences, Polish Academy of Sciences (ING PAN), Research Centre in Kraków, Senacka 1, PL–31002 Kraków, Poland; ndtramm@cyf-kr.edu.pl*

2 – *AGH University of Science and Technology, Faculty of Geology, Geophysics and Environmental Protection, al. Mickiewicza 30, PL–30059 Kraków, Poland*

Monazite and xenotime are REE-orthophosphates with the stoichiometric formula APO_4 incorporating significant amounts of U and Th in their structure. A high closure temperatures (>850 °C for monazite, Cherniak et al., 2004; >900 °C for xenotime, Cherniak, 2006) makes them a robust U(-Th)-Pb geochronometers for dating igneous and metamorphic processes as well as deformation history (Williams et al., 2017). The experimental works have shown vulnerability to alkaline fluids which alter monazite and xenotime via coupled dissolution-reprecipitation reactions during metasomatic processes leading to depletion of REEs, Pb and other elements (Hetherington et al., 2010; Budzyń et al., 2017). Fluid-induced removal of Pb in monazite and xenotime results in the partial or complete resetting of the geological clock, offering an opportunity to date metasomatic processes under temperatures way below closure temperature (Williams et al., 2011; Budzyń et al., 2018). However, due to the complex nature of the fluid-induced alteration, discordant data are often difficult to interpret.

In order to understand these complex metasomatic processes, several previous structural studies with Raman spectroscopy have been done on monazite and xenotime. However, most of these studies focused either on full range Raman spectra of synthesized endmember composition (LREE-phosphate, HREE-phosphate); or on natural monazite delimited to the primary Raman features (symmetric PO_4^{3-} stretching, REE bending modes; Begun et al., 1981; Ruschel et al., 2012).

This contribution evaluates experimentally altered Burnet monazite and NWFP (North-West Frontier Province) xenotime (selected samples from experiments by Budzyń and Kozub-Budzyń, 2015; Budzyń et al., 2015, 2017) with micro-Raman spectroscopy using a 532 nm laser at 5 mW power, 100–3500 cm^{-1} range. Single point and line measurements proceeding from unaltered center to altered rims demonstrate new features at higher Raman shift (1500–2500 cm^{-1}) for monazite. These features appear as four broad peaks at approximately 1750, 1900, 2030 and 2330 cm^{-1} possibly caused by photoluminescence effects. The Raman spectra reflect the natural signature of the Burnet monazite with the described photoluminescence effects present in all investigated samples from experimental P-T conditions of 200–1000 MPa and 350–750 °C.

The Raman spectra of the NWFP xenotime are overwhelmed with fluorescence effects. However, distinct features are present at 1500–3000 cm^{-1}. Previously such features were reported in natural Brazil xenotime by Lenz et al. (2015). They deciphered the photoluminescence effects at Raman shift of 1500–3000 cm^{-1} with Raman spectra of synthetic endmember HREE phosphates, and identified Er, Eu, Sm and Ho as the effect inducing elements. This suggests the possibility of using photoluminescence effects within a Raman spectrum as indices for these elements. In our work, a similar approach is conducted to decipher the photoluminescence effects in the observed broad peaks at 1500–2500 cm^{-1} of the experimentally altered monazite by comparing with Raman spectra of the synthetic REE phosphates.

Furthermore, a transition between monazite and secondary fluorcalciobritholite formed during experiment was documented for the Raman spectra. Line measurements through a monazite – fluorcalciobritholite phase intersection demonstrate that all Raman features characteristic for monazite (i.e., REE bending modes at 100–700 cm^{-1} and PO_4 symmetric stretching at ~970 cm^{-1}) decrease, while the four broad peaks at 1500–2500 cm^{-1} shift and increase drastically overwhelming the spectrum completely.

Further investigation of monazite and xenotime using Raman spectroscopy with various laser wavelengths, together with quantitative EMPA measurements, are expected to provide new data important for additional interpretation. These will contribute to a vast Raman spectra database and will describe a new approach for evaluation of these minerals in metasomatically altered rocks.

Acknowledgement: This work was funded by the National Science Centre of Poland, grant no. 2017/27/B/ST10/00813.

References:

Begun, G. M., Beall, G. W., Boatner, L. A. & Gregor, W. J. 1981. Raman spectra of the rare earth orthophosphates. *Journal of Raman Spectroscopy*, 11, 273–278.

Budzyń, B., Konečný, P. & Kozub-Budzyń, G. A. 2015. Stability of monazite and disturbance of the Th-U-Pb system under experimental conditions of 250–350 °C and 200–400 MPa. *Annales Societatis Geologorum Poloniae*, 85, 405–424.

Budzyń, B. & Kozub-Budzyń, G. A. 2015. The stability of xenotime in high Ca and Ca-Na systems under experimental conditions of 250–350°C and 200–400 MPa: the implications for fluid-mediated low-temperature processes in granitic rocks. *Geological Quarterly*, 59, 316–324.

Budzyń, B., Harlov, D. E., Kozub-Budzyń, G. A. & Majka, J. 2017. Experimental constraints on the relative stabilities of the two systems monazite-(Ce) – allanite-(Ce) – fluorapatite and xenotime-(Y) – (Y,HREE)-rich epidote – (Y,HREE)-rich fluorapatite, in high Ca and Na-Ca environments under P-T conditions of 200–1000 MPa and 450–750 °C. *Mineralogy and Petrology*, 111, 183–217.

Budzyń, B., Sláma, J., Kozub-Budzyń, G. A., Konečný, P., Holický, I., Rzepa, G. & Jastrzębski, M. 2018. Constraints on the timing of multiple thermal events and re-equilibration recorded by high-U zircon and xenotime: case study of pegmatite from Piława Górna (Góry Sowie Block, SW Poland). *Lithos*, 310–311, 65–85.

Cherniak, D. J. 2006. Pb and rare earth elements diffusion in xenotime. *Lithos*, 88, 1–14.

Cherniak, D. J., Watson, E. B., Grove, M. & Harrison, T. M. 2004. Pb diffusion in monazite: A combined RBS/SIMS study. *Geochimica Cosmochimica Acta*, 68, 829–840.

Hetherington, C. J., Harlov, D. E. & Budzyń, B. 2010. Experimental metasomatism of monazite and xenotime: mineral stability, REE mobility and fluid composition. *Mineralogy and Petrology*, 99, 165–184.

Lenz, C., Nasdala, L., Talla, D., Hauzenberger, C., Seitz, R. & Kolitsch, U. 2015. Laser-induced REE^{3+} photoluminescence of selected accessory minerals – An “advantageous artefact” in Raman spectroscopy. *Chemical Geology*, 415, 1–16.

Ruschel, K., Nasdala, L., Kronz, A., Hanchar, J. M., Többens, D. M., Škoda, R., Finger, F. & Möller, A. 2012. A Raman spectroscopic study on structural disorder of monazite-(Ce). *Mineralogy and Petrology*, 105, 41–55.

Williams, M. L., Jercinovic M. J., Harlov D. E., Budzyń B. & Hetherington C. J. 2011. Resetting monazite ages during fluid-related alteration. *Chemical Geology*, 283, 218–225.

Williams, M. L., Jercinovic M. J., Mahan K. H. & Dumond G. 2017. Electron Microprobe Petrochronology. *Reviews in Mineralogy and Geochemistry*, 83, 1, 153–182.

Mole roach indicates absence of hierarchy and structure in origin of true sociality

PETER VRŠANSKÝ[1]

1 – Institute of Zoology, Slovak Academy of Sciences, Dúbravská cesta 9, 845 06 Bratislava, Slovakia, geolvrsa@savba.sk

Spectacular fossils from the dinosaur-aged Myanmar amber might have just revealed general pattern of evolution. New wood-boring mole roaches belong to a new, most primitive, termite family Pabuonqedidae. At the same time it has numerous cockroach symplesiomorphies. The earliest eusociality of cockroaches conserved in termites is indicated by 6 larvae preserved together (with 960 feces), a larva amber-embedded inside a wood tunnel and nuptial-flight-related wing shedding sutures of adult females (one dealate). Nineteen syninclusions include a true termite, an archaeognathan bristletail, a wood boring caterpillar, 9 mites - one attached parasitic. Mesozoic all-termite phylogeny reveals a basal (explosively-appearing) diversification ring resulting from general fluid Bauplan tunings to simple reductions from a single transitional taxon.

Groundwater Inflows and Surface Runoff to the Salza in the Region of the Zeller Staritzen, Austria

SABINE WÖHRER[1]

1 – Department of Geodynamics and Sedimentology, University of Vienna, Althanstraße 14, 1090 Vienna; woehrer.sabine@gmx.at

This study presents a budget of the surface and groundwater runoff to the Salza River in the region of the Zeller Staritzen, which was established for two different hydrological situations. The Zeller Staritzen is part of the Hochschwab group situated in the Northeast of Styria, Austria. The Hochschwab, including the investigated area, consists mainly of the Mürzalpen nappe of the Northern Calcareous Alps with distinctive fold architecture (Mandl et al. 2002). Some of the most important springs for Vienna's water supply are located in the region under study. Quantified surface and groundwater runoff improve the understanding of hydrological conditions in this crucial catchment area.

During mean-flow conditions and high water, the surface runoff was measured using salt dilution gauging. The groundwater inflow remains relatively stable between 2.686 m^3/s and 2.817m^3/s during hydrological changes, while the surface runoff changes from 1.898 m^3/s to 9.893 m^3/s. During mean-flow conditions, the Salza had a discharge of 10.797 m^3/s, whereof 25 % were groundwater inflow, during high water the discharge was 26.31 m^3/s with 10 % groundwater. The surface runoff can be divided into orographically left and right, whereof the left side represents the Zeller Staritzen. Orographically left the surface runoff changed from 0.235 m^3/s to 0.92 m^3/s, orographically right from 1.663 m^3/s to 8.973 m^3/s. Around 10 % of the surface runoff originates from the Zeller Staritzen; the ratio between left and right does not change significantly with hydrological changes. The Zeller Staritzen mainly consists of karstified lime- and dolostone, where water infiltrates rapidly into the thick fractured and karstified aquifer (Fabiani et al. 1980). On the orographically right side, impermeable rocks such as shale, siltstone, and sandstone cover significant areas of the catchments of the tributary streams leading to higher surface runoff values than those observed in the karstified Zeller Staritzen. The groundwater exfiltrating directly into the Salza River is expected to originate primarily from the Zeller Staritzen.

Acknowledgement: I thank Dr. Kurt Decker for his supervision of this project, as well as Dr. Martin Kralik for his expertise regarding the used measurement method and his helping hand in the field. Furthermore, I want to thank Franziska Pezzei and Sophie Decker for working with me in the field to make the measurements possible.

References:

Fabiani, E., Weissensteiner, V. & Wakonigg, H. (1980). Grund- und Karstwasseruntersuchungen im Hochschwabgebiet Teil I: Naturräumliche Grundlagen, Geologie - Morphologie - Klimatologie. *Berichtsbände der wasserwirtschaftlichen Rahmenplanung Band 44*, 16.

Mandl, G.W., Bryda, G., Kreuss, O. (2002). Erstellung moderner geologischer Karten als Grundlage für karsthydrogeologische Spezialuntersuchungen im Hochschwabgebiet. *Geologische Bundesanstalt*

Thickness of Quaternary fluvial sediments and the substratum subsidence in the Seewinkel area (Austria)

PAUL ZEMANN[1] and ERICH DRAGANITS[1]

1 – University of Vienna, Department for Geodynamics and Sedimentology, Althanstraße 14, A-1090, Vienna, Austria; paul.zemann@univie.ac.at

The Seewinkel area is located east of Lake Neusiedl, Austria's largest lake, in the western part of the Little Hungarian Plain. The landscape is characterized by extremely low relief and abundant shallow lakes and pans. Geologically, the Quaternary fluvial strata covered with minor occurrences of aeolian sediments overlie the Pannonian (Miocene, Tortonian) fine-grained limnic sediments. Recent seismic data shows the existence of numerous brittle faults in the subsurface, related to the formation of the Pannonian Basin. (Loisl *et al*., 2018)
In this study we model the thickness of the Quaternary fluvial sediments, to gain more insight into their deposition and the relation with the still ongoing subsidence of the Little Hungarian Plain (Joó, 1992), as well as the influence of pre- and post-tectonic structures. This study combines existing borehole data with high-resolution airborne laser scanning (ALS) topographic data and statistical methods to model the thickness of the Quaternary fluvial sediments in a geographic information systems (GIS) environment.
A clear lithological contrast to the finer-grained Pannonian sediments (Zámolyi *et al*., 2017) can be observed in many logs and was applied to define the lower edge of the Quaternary strata. While the used data varies in quality and accuracy, different statistical methods provide various results. For this work it was crucial to compare these models and find one that considers the regional geological setting best. In this case the choice was a natural neighbor interpolation. It shows that the Quaternary fluvial sediments pinch out towards the northwest, becoming virtually absent close to the eastern shore of Lake Neusiedl, and increase in thickness eastwards, reaching almost 30m at the Austrian/Hungarian border. This trend mimics a similar lateral change in thickness of the underlying Pannonian sediments, and is most likely related to the still ongoing regional subsidence in the area of the Little Hungarian Plain.

Acknowledgement: The borehole data for this project was provided by OMV, Geological Survey of Austria, Gruppe Wasser Ziviltechnikergesellschaft für Wasserwirtschaft GmbH and Amt der Burgenländischen Landesregierung.

References:

Joó, I. 1992. Recent vertical surface movements in the Carpathian Basin. *Tectonophysics* 202, 2-4, 129-134.

Loisl, J., Tari, G., Draganits, E., Zámolyi, A. & Gjerazi, I. 2018. High-resolution seismic reflection data acquisition and interpretation, Lake Neusiedl, Austria, NW Pannonian Basin. *In:* Németh, B., Tari, G., Radivojević, D., Tomljenovic, B. & Krézsek, C. (Eds.), *Special section: Characterization of hydrocarbon and geothermal resource potential and carbon sequestration opportunities of the Pannonian Basin*.

Zámolyi, A., Salcher, B., Draganits, E., Exner, U., Wagreich, M., Gier, S., Fiebig, M., Lomax, J., Surányi, G., Diel, M., Zámolyi, F. 2017. Latest Pannonian and Quaternary evolution at the transition between Eastern Alps and Pannonian Basin: New insights from geophysical, sedimentological and geochronological data. *International Journal of Earth Science* 106, 1695-1721.

Attendees of jubilee XXth International Conference of Young Geologists, Herl'any, 3-5.04.2019, Slovakia.

Book of abstracts. ISBN 978-83-933330-2-8

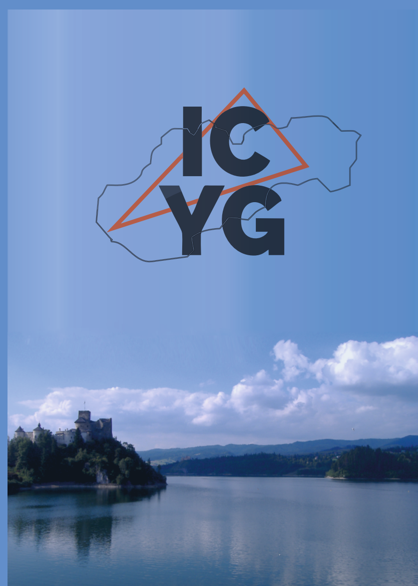

ISBN 978-83-933330-2-8
www.mineralpress.com.pl